Universität Rostock Traditio et Innovatio

Differentiation and Survival of Human Neural Progenitor Cells in 3D Scaffolds of Self-Assembling Peptide Hydrogels

Dissertation

zur

Erlangung des akademischen Grades

doctor rerum naturalium (Dr. rer. nat.)

der Mathematisch-Naturwissenschaftlichen Fakultät

der Universität Rostock

vorgelegt von

Andrea Liedmann

Rostock, 02.01.2013

verteidigt am 17.06.2013

https://doi.org/10.18453/rosdok_id00002503

Gutachter:

Arndt Rolfs, MD
Albrecht-Kossel-Institute for Neuroregeneration (AKos)
Zentrum für Nervenheilkunde
University of Rostock

PD Dr. Sergei A. Kuznetsov
Lichtmikroskopiezentrum
Institut für Zellbiologie und Biosystemtechnik
Fachbereich Biowissenschaften

Prof. Dr. med. A. Wree
Universitätsmedizin Rostock
rechtskräftige Teilkörperschaft der Universität Rostock
Institut für Anatomie

Content

1. Introduction

1.1. Biomaterials

Biomaterials are biocompatible materials and consist of synthetic or natural material. They are used to replace part of a living system and to function in intimate contact with living tissue. They are used for different medical devices like wound dressing, implants, tissue engineering and drug delivery. Biometric materials are synthetic but their composition and properties are similar to materials of living organisms. Coupling of protein layers to the surface provide the basis for materials called bioactive materials.

The rapidly developing field of regenerative medicine will require rational molecular and supramolecular design of temporary scaffold materials for cells to control their bioactivity and physical properties (Green et al., 2002; Fields et al., 1998; Liu et al., 2004). Tissue engineers develop three-dimensional (3D) scaffolds because they are attractive candidates for repair of injured tissues and organs to be used in transplantation therapies (Weaver et al., 1997; Hayman et al., 2004; Willerth et al., 2006). Tissue engineering is an interdisciplinary field that applies the principles of engineering and biomedical sciences toward the development of biological substitutes that restore, maintain, or improve tissue or organ function (Ratner et al., 2004; Cheung et al., 2007). A tissue engineered implant is a biologic-biomaterial combination in which cells are transplanted to penetrate and proliferate in all directions to populate all regions of the implant (Akdemir et al., 2008).

The ideal material in neuroscience is biocompatible with low immunogenicity, biodegradable with chemically and mechanically stable and non-toxic to neurons or other cellular components of brain tissue. Most biomaterials are reproducibly, structurally stable for long enough to allow repaired or regenerated tissues to organize into a desired three-dimensional structure. The material should ideally degrade without any foreign residues remaining. The microstructure and porosity of the material should be controllable, so that the biomaterials can be used to provide structural support to the surrounding brain or to encourage local neurite and axonal regrowth. This can be accomplished with techniques that include modifying the material's pore structure, surface topography or charge, or functionalising the material surface with extracellular-matrix-like molecules or therapeutic proteins. Ideally, a given biomaterial can be formed or processed into a variety of shapes such as tubes, sheets, meshes, sponges, foams, etc. In cases in which local delivery of potentially therapeutic molecules is desirable,

the materials should provide a controlled and sustained delivery of that molecule for the required duration (Orive, 2009). Three groups of materials are used: 1) synthetic materials; 2) natural materials; and 3) biosynthetic materials (Table 1).

Synthetic Polymers	**Natural Polymers**	**Biosynthetic materials**
Hydroxyapatite Poly(glycolic acid) (PGA), Poly(lactic acid) (PLA), Poly(lactic-co-glycolic acid) (PLGA), Poly(e-carpolactone) (PCL), Poly(ethylene glycol) (PEG), Poly(vinylalcohol) (PVA), Poly(N-vinyl 2-pyrrolidone) (PNVP), Poly(propylene fumarate) (PPF), Poly(acrylic acid) (PAA), Poly(ß-hydroxybutyrate) (PHB), Polypyrrole polymers (Ppy) Polydioxanone (PDS), Poly(acrylonitrile-co-methylacrylate) (PAN-MA), Hydroxyethyl methacrylate (HEMA), Poly(2-hydroxylethyl methacrylate) (pHEMA), self-assembling peptide hydrogels, Peptide, DNA (artificially prepared natural polymers)	Collagen, Gelatin, Hyaluronate, Glycosaminoglycan, Chitosan, Alginate, Silk, Fibrin, Dextran, Matrigel, etc.	combine the pros of both synthetic and natural materials

Table 1: Overview of existing Biomaterials. Table 1 shows existing materials, which can be used as biomaterials. Biomaterials could divide in three groups of materials, completely synthetic materials, natural derived materials and the combination of both.

1.1.1. Natural derived biomaterials

Natural materials are desirable to be biodegradable, non-toxic/non-inflammatory, mechanically similar to the tissue to be replaced, highly porous, encouraging of cell attachment and growth, easy and cheap to manufacture, and capable of attachment with other molecules. Natural materials include collagen, chitosan, agarose/alginate, hyaluronic acid and fibronectin. Various cells have been used to seed and culture onto different 3D matrices, such as collagen (O'Connor et al., 2000; Ma et al., 2004) and fibrin (Woerly et al., 1996; Sakiyama et al., 1999; Willerth et al., 2006). Collagen for example as the major component of the

extracellular matrix ECM, contains many chemo-attractant binding domains, provides support to connective tissue such as skin, tendons, bones, cartilage, blood vessels, and ligaments in its native environment, and also interacts with cells in connective tissues, and transduces essential signals for the regulation of cell anchorage, migration, proliferation, differentiation, and survival (Tabesh et al., 2009). Collagen gel can used as a carrier for cell transplantation (Weinand et al., 2007) and a cell infiltration matrix to induce regeneration and remodelling *in vivo* (Patino et al., 2002), as coating in a guidance conduit to induce neurite extension from dissociated dorsal root ganglia (Schnell et al., 2007) or on implants which is more successful than the bare ones (Munisamy et al., 2008). NPC culture in 3D collagen gels is well documented (O'Connor et al., 2000; Ma et al., 2004). Various matrices of collagen in combination with neural induction factors allow the development of experimental transplantation therapies (Marchand and Woerly, 1990; Houwelling et al., 1998).

Hyaluronic (HA) acid-based hydrogel has been shown to inhibit scar formation and promote angiogenesis, which is also very beneficial for wound healing (Peattie et al., 2004; Cencetti et al., 2011). HA is a major constituent of the natural ECM and is biocompatible, biodegradable, water soluble, and immunoneutral. The great hydrophilicity of HA hydrogels provides a good environment for cell growth, and the cavernous structure provides significant space to cells, which enhances nutrient exchange, ability to stretch their prominences, and ability to build up their intercellular connections. The HA material possesses excellent biocompatibility, which supports the attachment and the survival of the neurons and axonal growth (Hou et al., 2005 & 2006).

Chitosan, as a natural polysaccharide in the shell of crustacean, cuticles of insects and cell walls of fungi (Khor & Lim, 2003), can be used for wound dressing, drug delivery, and tissue engineering (cartilage, nerve and liver tissue) applications (Tabesh et al., 2009).

Agarose and alginate are linear polysaccharides obtained from seaweed and algae and encapsulation of certain cell types enhances cell survival and growth and has been explored for use in liver, nerve, heart, and cartilage tissue engineering. Incorporation of BDNF protein into agarose nerve guidance scaffold significantly increased the quantity of axons growing into scaffolds (Stokols et al., 2006). Prang et al. (2006) show in an entorhino-hippocampal slice culture model that alginate-based scaffolds elicit highly oriented linear axon regrowth in the injured mammalian CNS and appropriate target neuron reinnervation. Therefore alginate hydrogels can be used as bridging materials for both spinal cord (Bunge, 2002; Suzuki et al., 1999) and peripheral nerve repair (Suzuki et al., 2000; Labrador et al., 1998). But extensive

purification is needed to prevent immune responses after transplantation (Willerth & Sakiyama-Elbert, 2007).

Fibronectin is a glycoprotein, which exists outside of cells and on the cell surface, in blood and in the other body fluids. It is associates with other proteins of the extra cellular matrix like fibrinogen, collagen, glycosamineglycans and with suitable receptors, which are in the cell membrane (Tabesh et al., 2009). Functional fibrous fibronectin biomaterials take the form of mats or cables, which have been developed for use in the repair of peripheral nerves or injured spinal cord. Combination of SCs with alginate-fibronectin and resorbable scaffold has been shown to support axonal regeneration in adult rodents after spinal cord and peripheral nerve injury (Novikov et al., 2002; Mosahebi et al., 2003). Such material also have been used as a depot for the supply of soluble factors such as NGF, NT3 and antibodies, slowly releasing the content to sites of nervous system repair (Tabesh et al., 2009).

The natural derived biomaterials include matrigel, which is a soluble basal membrane extract of the Engelbreth-Holm-Swarm tumour cell line that gels at room temperature forming a genuine reconstituted basal membrane (Kleinman et al., 1986). The major components of matrigel are laminin, collagen IV, entactin and heparan sulphate proteoglycan, and it also includes growth factors such as FGF-2, EGF, IGF-1, PDGF, NGF, and TGF-ß (manufacturer's data). It has been widely used in cell culture applications and enhances growth and migration of different cell types (Lelièvre et al., 1998). It induced significant sprouting of DRG neurits (Novikova et al., 2006) and can been used experimentally as bridging materials for both spinal cord (Bunge, 2002; Suzuki et al., 1999) and peripheral nerve repair (Suzuki et al., 2000; Labrador et al., 1998). *In vitro* it is used as alternative feeder-free cell culture environments effective for long-term embryonic stem-cell culture (Blow, 2008).

Natural materials such as collagen, alginate, gelatine, laminin, chitosan, and fibrin share similar properties with soft tissues, like mechanical strength, physical properties and biomolecular recognition. On the other hand they display disadvantages like high cost, possible immunogenicity and batch-to-batch variability. Naturally derived polymers can face various challenges like inflammatory response, pathogen transfer and purity. The abundant presence of growth factors in matrigel can masked any simultaneous neurotrophic or neurotropic effects of the scaffold structure itself (Novikova et al., 2006). Its future clinical use as cell carrier is somewhat problematic, because for *in vivo* and *in vitro* studies as well main initial components must be, biocompatible and well defined. Therefore many synthetic materials have been developed to avoid this challenge.

1.1.2. Synthetic biomaterials

Synthetic hydrogels are devoid of animal derived material and pathogens and therefore are important to form defined *in vitro* systems to conduct a completely controlled study. Regardless of their purity or chemical tailorability, the biocompatibility of the biodegradation products and host responses upon transplantation supposed their use *in vivo*.

As synthetic tree-dimensional scaffold materials bioceramics, microfiber scale polymers, or nanofiber hydrogels can be used. Synthetic polymers have been widely used as surgical structures, with long established clinical success and many are approved for human use by the Food and Drug Administration (FDA). They also represent a more reliable source of raw materials with the ability to provoke an immune response in the body. These materials exist: hydroxyapatite (Shikinami et al., 1999); polyesters such as *polylactic* (PLA) and *polyglycolic acids* (PGA), *poly(e-carpolactone)* PCL, *poly(ß-hydroxybutyrate)* PHB and their copolymers (Tab.1); and self-assembling peptide hydrogels (Holmes, 2000).

Hydroxyapatite has a sufficient rigidity and is used as artificial bone matrix. Surface functionalisation of artificial hips with calcium hydroxylapatite is used in bone replacement and induces attachment of the implant to the living bone. Along with biocompatibility requirements, these synthetic materials need to resemble biological extracellular matrices and interact with cells at molecular level in order to effectively control the processes of tissue regeneration.

Polymer scaffolds could be divided into macroporous scaffolds, microporous scaffolds and nanofiber scaffolds. Scaffolds with pores bigger than cell size are called macroporous or with pores smaller than cell size microporous. Nanofiber scaffolds are composed of a network of overlapping nanofibers (Fig. 1I). Macroporous scaffolds like PLA or PGA polymers are less rigid and provide a pseudo 3D microenvironment. Whereas peptide hydrogels often form nanofiber scaffolds and therefore provides a truly 3D microenvironment similar to natural tissue.

Polyesters can be degraded by hydrolysis of ester bond leading and degradation products can be desorbed through metabolic pathways. PLA for example is biodegradable polyester attainable by poly-condensation of lactic acid. L-lactic acid occurs in the metabolism of all animals and microorganism and is a non-toxic degradation product of polylactides (Kricheldorf, 2001). The implantation of a macroporous PLA tubular scaffold or a PLA single channel tubular scaffold containing Schwann cells in the transected rat spinal cord elicited a modest axonal regeneration (Oudega et al., 2001; Patist et al., 2004).

PGA is highly crystalline, has a high melting point and low solubility. Co-polymers with the more soluble PLA increase the hydration, hydration rate and the degradation (Tabesh et al., 2009). The microbially produced *poly-ß-hydroxybutyrate* (PHB) degrades after implantation slowly at body temperature and forms a non-toxic metabolite that is secreted in urine (Tabesh et al., 2009). PHB has been previously used as a wound scaffolding device, designed to support and protect wounds against further damage, while promoting healing by encouraging cellular growth on and within the device from the wound surface. Ljungberg et al. (1999) used PHB as a wrap-around implant to guide axonal growth after peripheral nerve injury. The aliphatic polyester *poly-e-caprolactone* (PCL) is used in pharmaceutical products and wound dressings with his bioresorbable and biocompatible properties (Venugopal et al., 2005a, b). Owing to its slower degradation than PLA, it is interesting for the preparation of long-term implantable devices. *Polypyrrole polymers* (Ppy) for example can be molded into a variety of shapes, allows cell adhesion and is therefore convenient for use in neural prosthetic applications (Tabesh et al., 2009). Other synthetic polymers such as PDS, PAN-MA has been shown to induce nerve growth (Sangsanoh et al., 2007). The most commercially important polymer *poly ethylene glycol* (PEG) resists protein adsorption and cell adhesion, minimizing the immune response after implantation and to seal cell membranes after injury, making it useful for limiting cell death. The widely in medicine used *hydroxyethyl methacrylate* (HEMA) can be prepared to various hydrogels, to immobilize proteins or cells. Attractive for biomedical engineering applications is *poly(2-hydroxylethyl methacrylate)* (pHEMA), because of its physical properties and high biocompatibility. This polymer can be easily manipulated through formulation chemistry and it has been extensively used in medical applications, e.g. contact lenses, kerato prostheses and as orbital implants. Longitudinally oriented channels within pHEMA hydrogels have the potential to enhance nerve regeneration after transection injuries of the spinal cord by increasing the available surface area and providing guidance to extending axons and invading cells (Flynn et al., 2003).

1.1.3. Hydrogels

Hydrogels are also good candidates for tissue-engineered implants because of their hydrophilic structure, which gives them physical characteristics similar to tissue (Shin et al., 2003). Hydrogels are water swollen crosslinked polymers. The crosslinks may occur by reaction of one or more monomers, hydrogen bonds and van der Waals interactions. Highly

swollen hydrogels like cellulose derivatives, *poly(vinyl alcohol)* PVA, *poly(N-vinyl 2-pyrrolidone)* PNVP, PEG and moderately or poorly swollen hydrogels like pHEMA and derivatives are described. Hydrogel scaffolds are shown to promote neurogenesis (Martin et al., 2008) and are used in the field of stem cell research (Brännvall et al., 2007; Gerecht et al., 2007; Uemura et al., 2010; Pan et al., 2009) and neural engineering applications (Novikova et al., 2006; Prang et al., 2006) to promote differentiation of cells into different cell types. Hydrogels with additional functions, like swelling, shrinking, bending, or degradation, are often called smart hydrogels, responding to changes of environmental conditions (Geever et al., 2008). These types of stimuli-responsive polymers can undergo relatively large and abrupt, physical or chemical changes in response to small external changes in the environmental conditions. Jongpaiboonkit et al. (2008) demonstrated that the hydrogel network chemistry (both natural and synthetic), cell type, cell density, cell adhesion ligand density, and degradability can be systematically varied to screen for environments that promote cell viability in a 3D context.

1.1.4. Biosynthetic materials

Biosynthetic materials combine the pros of both synthetic and natural materials (Ahmed et al, 2003). Composites of synthetic and natural biological polymers such as alginate, collagen alone or with bioactive motifs, substances or proteins, can be designed to yield materials for tissue engineering (Langer & Tirrell, 2004; Cha et al., 2011; Hrynyk et al., 2012; Reichert et al., 2009; Yu et al., 2012). For example, current difficulties using chitosan as a polymer scaffold in tissue engineering, like low strength and inconsistent behaviour (Madihally and Matthew, 1999), could be avoid by using mixtures with synthetic polymers (Tabesh et al., 2009). The coupling of protein layers to the surface provides the basis for bioactive materials. The combination of bioactive scaffolds and cell culture techniques is a rapid and useful way to study cell viability and the delivery of bioactive molecules for possible transplantation into tissue and organs (O'Connor et al., 2000; Ma et al., 2004; Silva et al., 2004). PHB conduits coated with alginate hydrogel and fibronectin and seeded with SCs reduce spinal cord cavitation as well as retrograde degeneration of injured spinal tract neurons (Novikov et al., 2002). Furthermore, chemistry is used to modify PEG hydrogels to add sites for cell adhesion or extracellular matrix molecules to allow cells to infiltrate the scaffolds, extending their potential applications (Willerth & Sakiyama-Elbert, 2007).

1.1.5. Fabrication of biomaterials

The field of materials chemistry (Green et al., 2002; Fields et al., 1998; Hartgerink et al., 2001 & 2002; Silva et al., 2004) offer strategies synthesize biometric materials meeting the challenges of designing artificial extracellular matrices. Synthetic polymers can be tailored to produce a wide range of mechanical properties and degradation rates. Several techniques are used to create nanostructured scaffolds (Fig. 1). Polymers can be combined to benefit from their unique properties (Willerth & Sakiyama-Elbert, 2007). Using nanotechnology, biomaterial scaffolds can be manipulated at atomic-molecular and macromolecular levels and constructed into specific geometrical and topological structures ranging from 1-100 nm scales. New properties of the materials occur such as mechanical (stronger), physical (lighter), more porous (tunable), optical (colour emission), chemical reactivity (more active and less corrosive), electronic properties (more electrically conductive), and magnetic properties (super paramagnetic). Several techniques have been developed to process synthetic and natural scaffold materials into porous structures. Existing conventional scaffold fabrication techniques are solvent-casting, particulate-leaching, gas foaming, fibre meshes/fibre bonding, phase separation, melt molding, emulsion freeze drying, solution casting, and freeze drying (Tabesh et al., 2009) (Fig. 1F, G, H). One common way for fabrication of nanofibrous scaffold is electrospinning. Polymers can be spun to nanofibers with diameters in the nano- to micrometer range (Fig. 1C, D, E, I). Such small diameter fibres with a defined volume, even approach densities of axons found in peripheral nerve (Schnell et al., 2007). Nanofibrous scaffolds can be utilized to provide a better environment for neural cell attachment, migration, proliferation and differentiation (Martins et al., 2007). Electrospinning is additionally used to create thin films of different coating designs, applied on prosthetic devices aimed to be implanted in the central nervous system (Buchko et al., 1999). Many of the fabrication technologies for polymers are based on harsh operating conditions, such as particulate leaching, heat compression and extrusion, lading to limited incorporation of bioactive proteins and cells. An alternative method for producing porous scaffolds is freeze-dry processing (Fig. 1F). Stokols et al. (2004) developed a novel procedure for using freeze-dry processing to create nerve guidance scaffolds made from agarose, with uniaxial linear pores. An elegant way to produce nanofibrous scaffolds existing of *poly (L-lactic acid)* (PLLA) is a liquid phase separation method, which supporting the neural stem cell differentiation and neurite outgrowth (Yang et al., 2004). For nerve regeneration two fibre-fabrication methods are possible: electrospinning (fibres with diameters from several micrometers to hundreds of

nanometre) and self-assembly (fibres have diameters of tens of nanometres) (Cao et al., 2009).

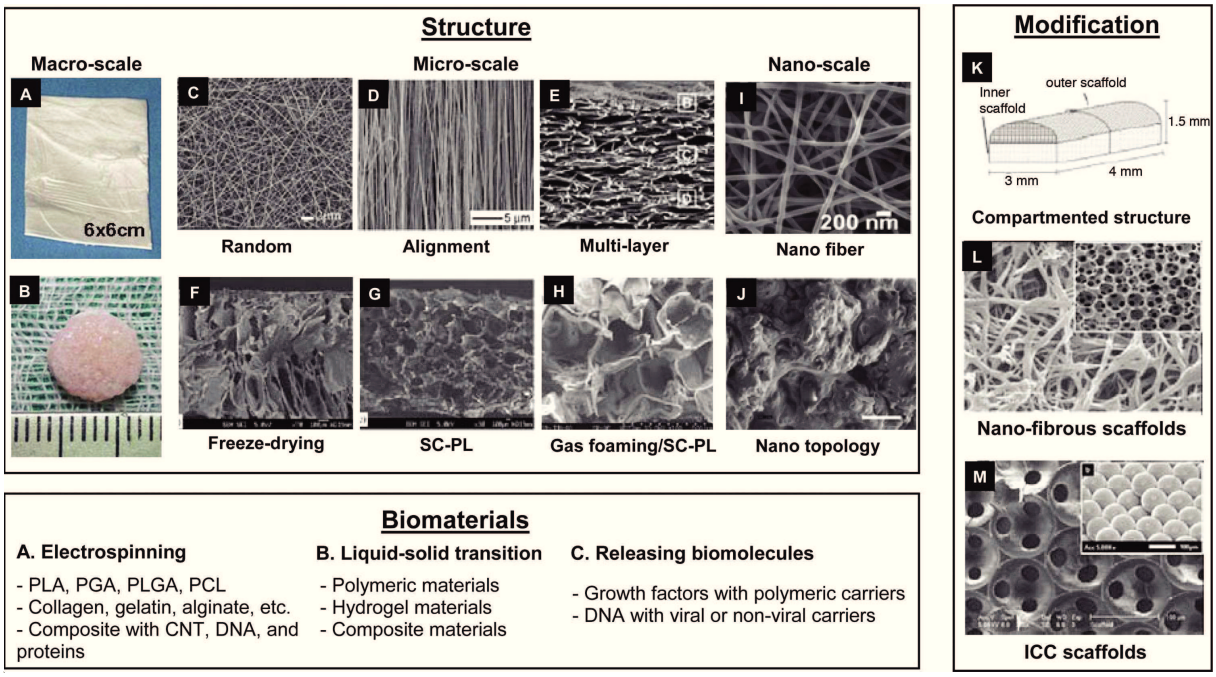

Fig. 1: Different biomaterial structures formed by using different fabrication methods for polymers (Lee et al., 2008)**. A, C, D, E, I:** Different structures can produce for individual usage, ranging from several cm (macro scale) to nm size (Nano scale). Electrospinning can be used for a wide field of polymers and with liquid-solid transition polymeric materials, hydrogels and composites can produced. Biomaterial scaffolds should provide more than temporary architectural structure. They can be produced to release biomolecules, to surround tissue or cells and can be modified by filling or coating with other polymers or peptides to increase attachment, migration and differentiation of cells (K, L, M).

1.1.6. Self-assembling peptide hydrogels

One group of novel materials for tissue engineering applications are peptide-based self-assembling fibrous networks (Hartgerink et al., 2001 & 2002; Silva et al., 2004; Zhang, 2003; Petka et al., 1998). Several self-assembling peptide hydrogels are described EAK16-II, KFE8, KLD12 and different types of RADA16 (for further study, review Zhang, 2002). *Peptide amphiphile* (PA) molecules are composed of peptide segments, containing 6-12 amino acids, which are coupled via an amide bond to fatty acid chains, with lengths of 10 to 22 carbon atoms (Hartgerink et al., 2001 & 2002; Silva et al., 2004). These peptide molecules are able to self-assemble, where the reaction is triggered by metal ions (Beniash et al., 2005), a change of salt concentrations (Holmes et al., 2000, Semino et al., 2004), pH (Ye et al., 2008) or temperature (Ye et al., 2008). The process of supramolecular self-assembly includes three phases, namely transitions, intermolecular hydrogen bonds, and a combination of attractive or

repulsive electrostatic interactions (Zhao et al., 2008). The gels are formed by a network of overlapping cylindrical nanofibers, ranging from 5 to 8 nm in diameter. They have a weak mechanical strength, a pore size between 50-100 nm, are permeable to gases, metabolites, and macromolecules and have a very low signalling capacity. Peptide hydrogel scaffolds are proved to be an effective environment for neural cells (Holmes et al., 2000; Semino et al., 2004; Wang et al., 2010; Xu et al., 2010) in spinal cord replacement (Tysseling et al., 2010) and tissue engineering (Beniash et al., 2005). They are used for studies to promote signalling pathways, influencing critical cell functions such as proliferation, differentiation and migration of cells in well-defined 3D culture systems (Mooney et al., 1994; Friedl et al., 1998, Silva et al., 2004; Semino et al., 2004).

A great advantage of self-assembling peptides, used to build nanostructures in a bottom-up approach, is their amenability to easy functionalisation. Because of their consistent composition and predictable manipulation of properties, they can be used to combine with synthetic materials containing biometric cues, to induce cell attachment, differentiation and migration. Specific features can be incorporated and the peptides can be modified and functionalized to create microenvironments suited for culturing cells (Silva et al., 2004; Gelain et al., 2006), triggering tissue regeneration (Zhang et al., 2004; Ellis-Behnke et al., 2006) and other applications. Hartgerink et al. (2001) have reported that peptide amphiphile nanofiber networks can be mineralized with hydroxyapatite to recreate the nanoscale structure of bone. Silva et al. (2004) reported on the use of bioactive peptide amphiphile nanofibers to promote rapid and selective differentiation of neural progenitor cells into neurons. With modern synthetic biomaterials it is possible to control the distribution of biological signals and their presentation in a well-defined manner.

Simplified growth scaffolds such as peptide-derived hydrogels should be seen as highly advantageous and will likely become more commonplace in cell culture methodology (Liebmann et al., 2007).

1.1.6.1. Self-assembling peptide hydrogel RADA16-I

Soluble hydrogels like the RADA-16-I (BD PuraMatrix^{TM}) are advantageous, because they are injectable and able to fill any shape or defect *in vivo* and they can easily formulate with cells by simple mixing (Ellis-Behnke et al., 2006; Wang et al., 2010). The hydrogel is formed rapidly after injection, to prevent the undesirable diffusion of the gel precursors and cells to

the surrounding tissue (Wang et al., 2010). The self-assembling peptide hydrogel RADA16-I (BD PuraMatrix™), which is used in this study, is a synthetic biocompatible matrix that is used to create defined three-dimensional (3D) microenvironments for a variety of cell culture experiments.

The hydrogel consists of the repeated amino acid sequence RADA, arginine (R), alanine (A), aspartic acid (D), and alanine (A) (Ac-RADARADARADARADA-COHN2, 1% w/v) and 99% water. The motif RAD is similar to the ubiquitous *integrin receptor-binding site* RGD (Zhang et al., 2004). The peptide component self-assembles under physiological conditions due to altered salt concentration, with a transition from a viscous solution into an elastic 3D hydrogel. The hydrogel exhibits a nanometre scale fibrous structure with an average pore size of 50-200 nm. The RADA16-I hydrogel is biocompatible, resorbable, and devoid of animal derived material and pathogens. Experiments in mammals showed that inoculation of Scrapie with the RADA-16-I peptide disrupt prion accumulation and extends survival (Hnasko & Bruederle, 2009). The treatment with RADA-16-I solution enables reconnection of brain tissue after acute injury, which resulted in functional behavioural recovery (Ellis-Behnke et al., 2006).

In recent *in vitro* studies RADA-16-I matrices were used to elucidate the influence of the 3D environment on the development of muria and human neural progenitor cells (Holmes et al., 2000; Thonhoff et al., 2008; Semino, 2008; Ortinau et al., 2010). Holmes et al. (2000) showed extensive neurite outgrowth and active synapse formation of primary rat neurons on the self-assembling peptide scaffolds. Semino et al. (2004) developed a simple method to entrap migrating neural cells from postnatal hippocampal organotypic cultures in the 3D peptide nanofiber scaffold. RADA-16-I showed low toxicity and retain several crucial properties of hNPCs, including migration and neuronal differentiation (Thonhoff et al., 2008). It can be utilised for regenerative medicine applications and for delivering cytokines. Drugs can be released slowly and sustained; therefore they are confined in scaffold hollow cavities or interact weakly with the net surface charges of the self-assembled nanostructures (Gelain et al., 2010). The release of epidermal growth factor from the RADA-16-I nanofiber scaffold can accelerate wound healing by being well suited for the treatment of cutaneous wounds including wound coverage, localized growth factor release and activation of wound repair (Schneider et al., 2008).

The in our lab established *in vitro* protocol of RADA16-I peptide hydrogel supplemented with laminin was used in this study to describe the behaviour of hNPCs encapsulated into 3D scaffolds on the differentiation potential and survival (Ortinau et al., 2010).

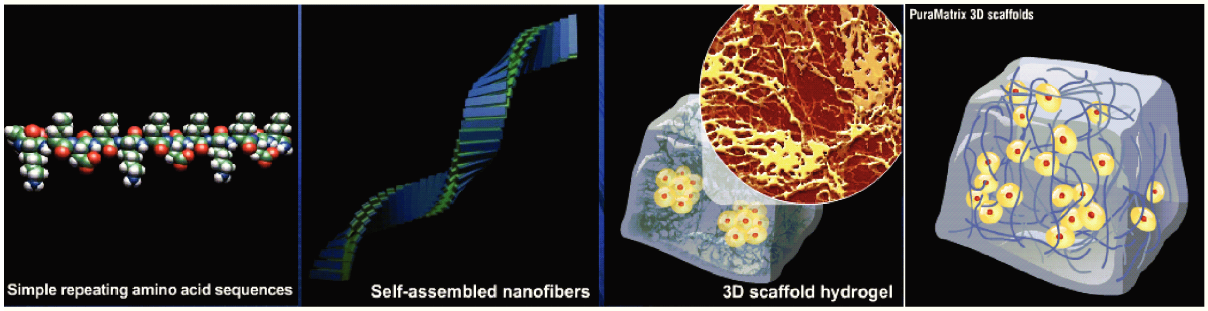

Fig. 2: Schematic demonstration of the self-assembling process. This picture shows steps of self-assembling, ranging from the single RADA-16-I peptide to assembled nanofibers and finally the formed 3D scaffold hydrogel. This 3D scaffold can be supplemented with extracellular components like laminin (right). **Left to right**: Structure of RADA-16 peptide (blue = arginine, white = alanine, red = aspartic acid), self-assembled nanofibers, 3D scaffold with spheroid like cell aggregates, 3D scaffold supplemented with laminin and distributed cell growth (www.nanosprint.com).

1.1.6.2. Next generation of self-assembling peptides

The next generation of self-assembling peptides consist of self-assembling backbone sequences, which are functionalised with specific biological motifs at the C-terminal of the RADA16-I peptide. They were tailored to be regenerate specific tissues (Gelain et al., 2006, Chau et al., 2008, Taraballi et al., 2010, Gelain et al., 2011). Zhang et al. (2009) showed that RADA-16-I with incorporated RGD sequence stimulates mouse pre-osteoblast attachment, spreading and proliferation. Enhanced neural differentiation directed by functional epitopes is described for surface modulation (Kam et al., 2002; Tong & Shoichet, 2001; Li & Chau, 2010) and 3-dimensional cultivation (Silva et al., 2004; Gunn et al., 2005; Gelain et al., 2006; Wei et al., 2007; Salinas et al., 2008; Tysseling et al., 2010). Further studies showed that an increased number of amino acids, acting as linkers between the self-assembling peptides and the motifs, can increase the effect because the bioactive motifs are more exposed to the solvent (Taraballi et al., 2010).

Modified RADA16-I with functionally modified peptide, composed of two domains, self-assembling domain RADA16-I and functional biological motifs at the C-terminal of RADA16-I, which functionalize 3-dimentional scaffolds to suit user needs. The used functionally modified RADA16-I is supposed to promote more cell adhesion and differentiation than standard RADA16-I. The focus in the study was on the SDP-peptide a cell adhesion motif in laminin (SDPGYIGSR), which is due to promote cell adhesion and extensibility of neural cells and the PFS-peptide a motif of the bone marrow homing factor

(GGPFSSTKT) is due to stimulate NSC adhesion and differentiation *in vitro* (Gelain et al., 2006) and stabilize the ß-sheet structures of the scaffold (Taraballi et al., 2010).

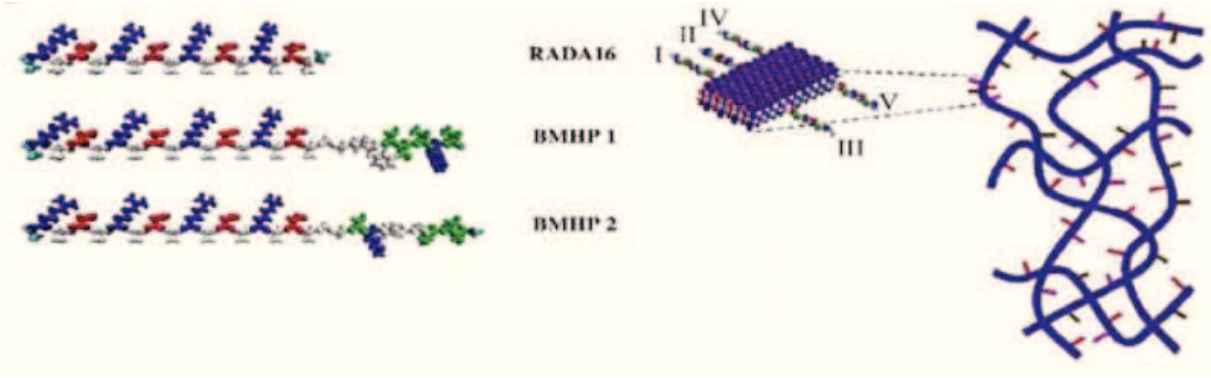

Fig. 3: Molecular and schematic models of designer peptides and of the scaffold. Modifications of standard RADA-16 modified in means of an elongation by biologic active peptide sequences BMHP 1 and 2 (left). (Gelain et al., 2006). Schematic model of a self-assembling nanofiber scaffold with combinatorial motifs (I, II, III, IV, V).

1.2. Advantages of the 3D culture

Conventional cell culture studies have been performed on 2D surfaces, resulting in flat, extended cell growth. As research has already shown that cells forming 3D structures often resemble their *in vivo* counterparts more closely in comparison to two dimensional systems, 3D culture allows defined microenvironments recapitulating the *in vivo* milieu in a better way. Biomaterials provide an attractive strategy because these materials exhibit several desirable characteristics. Hydrogels have been commonly used as model systems for 3D cell biology. Natural and synthetic hydrogels have been used to gain fundamental insights into virtually all aspects of cell behaviour, including cell adhesion, migration, and differentiated function. The material should be able to control cell functions such as migration, attachment and differentiation. In cases of transplantation with cells (such as stem cells) it will be advisable to use ’biomimetic materials’ to encourage the cells to survive and functionally integrate into the host tissue.

1.3. Stem cells

The isolation of human embryonic stem cells in 1998 was a milestone in stem-cell research while the availability of cell lines dramatically increased. Since 1998, about 200 embryonic stem-cell lines have been derived (Blow, 2008). Stem cells can be found in all multicellular organisms and possess two unique properties namely potency and self-renewal. Potency is the capacity to differentiate into specialized cell types. Self-renewal is the ability to go through numerous cycles of cell division while maintaining the undifferentiated state. In an embryo, stem cells start out in the yolk sac, then translocate to the aortic arch, to the liver and finally to the bone marrow. They being modificated at each of the stages during this way that the degree of specification gradually increases. There are three main categories of stem cells: totipotent, pluripotent and multipotent stem cells (Schöler, 2007).

Totipotent stem cells are only cells from an earlier stage of the embryo, the first diploidic basic cell and the daughter cells from 3 to 4 cell divisions, known as the morula. They are able to become all tissues in the body and the extraembryonic placenta (Mitalipov & Wolf, 2009). The first differentiation step of totipotent cells during mammalian development is the formation of the blastocyst in an early stage of embryogenesis.

Pluripotent stem cells are embryonic cells. They have the potential to generate all kind of adult and embryonic cell types. Embryonic stem cells are isolated from the inner cell mass of blastocysts. During development embryonic stem cells build all derivatives of the three primary germ layers: ectoderm, endoderm and mesoderm (Loebel et al., 2003). They can develop into each of the more than 200 cell types of the adult body when given sufficient and necessary stimulation. The endoderm gives rise to the entire gut tube and the lungs, the ectoderm to the nervous system and skin, and the mesoderm gives rise to muscle, bone-, and blood (Loebel et al., 2003).

Whereas embryonic stem cells are pluripotent, adult stem cells are multipotent. Adult stem cells are found in various tissues and can only develop into specific adult cell types in the body. In adult organisms, the system of multipotent stem cells is exploited for regeneration purposes, replenishing adult tissues (Schöler, 2007).

The two main characteristics of stem cells self-renewal and potency are essential for growth and development of organisms (ontogeny). They are especially crucial in the early stage of development, known as embryogenesis. The capacity of the stem cells to differentiate into specialized cell types allows for their use in medicine. They are used for cell replacement therapies in the treatment of spinal cord injuries (Olson et al., 2009), traumatic brain injury

(Harting et al., 2008) or neurological diseases like Parkinson's and Huntington's disease (Bosch et al., 2004). The embryonic stem cells often cultured on mouse embryonic fibroblast cells as 'feeder' cells in different media formulations containing serum. The containing animal products of this culture could limit the potential of stem-cell lines for therapeutic applications (Blow, 2008). Therefore many researchers are trying to identify biomaterials like Matrigel scaffolds, which could be alternative feeder-free cell culture environments for long-term human embryonic stem-cell culture (Blow, 2008).

1.3.1. Neural progenitor cells

Neural precursor cells (NPCs) are multipotent cells that contain both neural stem cells and neural progenitor cells (Gage, 2000). Multipotent neural progenitor cells (NPCs) divide in the ventricular zones to give rise to neurons and glial cells during central nervous system (CNS) development (Hirabayashi & Gotoh, 2005). Neural precursor cells divide symmetrically resulting in an increased NPC population, this begins in mice at 7.5 days pc (post coitum). Asymmetric cell divisions follow in the neurogenic phase around stage 13 pc resulting mainly in an increased number of neurons. Asymmetric cell divisions at stage 18 pc and early postnatal stages lead to the generation of mainly glial cells (Hirabayashi & Gotoh, 2005). Progenitor cells have a tendency to differentiate into a specific type of cell, but are already more specific than stem cells and can divide only a limited number of times (Fischer, 1997). Progenitor cells are said to be in a further stage of cell differentiation and are a developing state between stem cells and fully differentiated cells.

Mammalian CNS progenitor cells are not only present during developing stages. Neural progenitor cells have been found in different brain regions, the hypothalamus, the dentate gyrus of the hippocampus and the forebrain, the subgranular zone of the dentate gyrus and the structure of the subventricular zones of the lateral ventricle (Arsenijevic et al., 2001), within the olfactory bulb (Temple & Alvarez-Byulla, 1999), the neocortex (Gould et al., 1999) and the substantia nigra (Zhao et al., 2003). They are able to differentiate into neurons and glial cells (Donato et al., 2007). It is shown in rat striatal progenitor cell line ST14A, that self-renewal, migration and differentiation of neural progenitor cells are controlled by a variety of pleiotropic signal molecules. Members of the morphogen family of Wnt molecules play a crucial role for developmental and repair mechanisms in the embryonic and adult nervous system (Lange et al., 2006).

NPCs can be directly isolated from fetal or adult tissue (Ling et al., 1998; Arsenijevic et al., 2001) or generated from ES cells (Kim et al., 2007; Stacpoole et al., 2011). Neural stem cells (NSC) / NPC can be propagated as free-floating aggregates *in vitro*, so called neurospheres, by addition of epidermal growth factor or fibroblast growth factor (Reynolds & Weiss, 1992; McKay, 1997). These neurospheres are heterogeneous and contain NPCs and NSCs.

1.3.2. Neural progenitor cell line ReNcell VM cells

The neural progenitor cell line ReNcell VM, which is used in this study, was provided by ReNeuron (Guildford, UK). Human NPCs are derived from the ventral midbrain of a 10-week-old fetus and immortalized by retroviral v-Myc transduction (Donato et al., 2007; Hoffrogge et al., 2006). This cell line is able to proliferate without morphological and molecular changes for 40 passages with supplemented growth factors and shift to differentiation under growth factor withdrawal. The cells are known to differentiate mostly into astrocytes, some neuronal cells and only few dopaminergic neurons (Donato et al., 2007). These neuronal progenitor cells differentiate faster into neurons than reported for other neuronal progenitor cells or stem cell lines such as N-tera2 (Schwartz et al., 2005) or PC12 cells (Greene & Tischler, 1976), which need several weeks to differentiate. The ReNcell VM cells were used as model for profiling and functional proteome studies of neuronal differentiation processes to describe the protein inventory as well as protein activity and interactions, subcellular localization and posttranslational modifications (Hoffrogge et al., 2006). Results displayed the large rearrangement of the proteome during this process. Morgan et al. (2009) describe a protection of developing dopaminergic neurons, derived from these human neural progenitor cells, by Na^+ channel agonist veratridine treatment, most likely based on voltage-dependent mechanisms reducing premature death amongst developing neurons.

Furthermore ReNcell VM cells are shown to be a suitable tool to study Wnt/ß-catenin signalling during neurogenesis, because the Wnt/β-catenin pathway is known to be involved in ReNcell VM differentiation. Components of the Wnt/β-catenin pathway are shown to be strongly activated and regulated in ReNcell VM cells, which is shown by mRNA up-regulation of Wnt ligands (Wnt5a and Wnt7a), receptors including Frizzled-2, -3, -6, -7, and -9, and co-receptors, as well target genes including Axin2 (Mazemondet et al., 2011). The

over-expression of Wnt-3a increases neurogenesis during the differentiation of ReNcell VM cells and the activation of Wnt/β-catenin signalling increases TCF-mediated transcription and the expression of the Wnt target genes Axin2, LEF1 and CyclinD1 in ReNcell VM cells (Hübner et al., 2010). They suggest that neurogenesis induced by Wnt-3a is independent of the transcriptional activity of Wnt/β-catenin pathway in ReNcell VM cells. The aim to increase the neurogenesis in ReNcell VM cells is of great interest in many studies. GSK-3beta inhibitors, like kenpaullone, SB-216763 and the synthesized non-symmetrically substituted indolylmaleimide IM-12, acting via the canonical Wnt signalling pathway by inhibition of the key enzyme GSK-3beta and resulted in an increase of neuronal cells of ReNcell cell VM cells (Schmöle et al., 2010, Lange et al., 2011). As well the proliferation and differentiation of this hNPCs under hypoxic conditions results in an increased neurogenesis and it is shown that erythropoietin partially mimicked these hypoxic effects by an increase of the metabolic activity during differentiation and protection of differentiated cells from apoptosis (Giese et al., 2010). But the increase in neuronal cells is low, the shift to more physiological conditions by using biomaterials to create a 3D structure for the cells enforces the neurogenesis of this cells (Ortinau et al., 2010). However, the neurons obtained are not functional. In an approach to obtain fully functional neurons, ReNcell VM was plated on top of rat hippocampal slices. Patch clamp recordings revealed that the transplanted progenitor cells could express neuronal-type voltage-gated currents and rapidly receive synaptic input from hippocampal brain slice cultures (Morgan et al., 2011). These results highlight the utility of this cell line for the present study.

1.4. Apoptosis

An important parameter in biomaterial research is the survival of the encapsulated cells, if either the material enhances or decreases the survival of the cells. The 3D culture by the use of different biomaterials was shown to enhance survival of stem cells (Mahoney & Anseth, 2006; Orive et al., 2009; Ortinau et al., 2010). Therefore it was of interest if apoptotic processes are decreased by the 3D scaffold.

1.4.1. Definition of apoptosis

Apoptosis is the process of *programmed cell death* (PCD) and is a normal physiologic process and also a part of the neurogenesis. Apoptosis occurs during embryonic development as well as in maintenance of tissue homeostasis (Zakeri & Lockshin, 2002). A clutch of biochemical events leads to characteristic morphologic cell changes and death. The apoptotic program is characterized by certain morphologic features, including blebbing (formation spherical cellular protrusions), loss of plasma membrane asymmetry and attachment, cell shrinkage, condensation of the cytoplasm and nucleus, and internucleosomal cleavage of DNA. The process of apoptosis is controlled by a diverse range of cell signals, which may originate either by extrinsic inducers (extracellular) or intrinsic inducers (intracellular). Extracellular signals can include cytokines, growth factors, hormones, nitric oxide or toxins (Popov et al., 2002; Brüne, 2003). These signals may initiate apoptosis (positive induction) or repress / inhibit apoptosis (negative induction). A cell initiates intracellular apoptotic signalling in response to distress. The release of intracellular apoptotic signals by a damaged cell can be triggered through the binding of nuclear receptors by glucocorticoids, heat, hypoxia, nutrient deprivation, radiation, viral infection and increased intracellular calcium concentration after damage to the membrane (Mattson & Chan, 2003). Regulatory proteins initiate the apoptosis pathway before enzymes precipitate the actual process of cell death (Zahir & Weaver, 2004).

1.4.2. Regulation of apoptosis

Two main methods of regulation play a decisive role, targeting mitochondria functionality, or directly transducing the signal via adaptor proteins to the apoptotic mechanisms. This allows apoptotic signals to initiate cell death, or to stop the process. There are two main regulation pathways of the apoptosis, the extrinsic pathway mediated by the *tumour necrosis factor* (TNF) and the intrinsic pathway mediated by the *Fas ligand* FasL (Wajant, 2002).

At the **extrinsic regulation**, the caspase activation via the intermediate membrane proteins *TNF*, *receptor-associated death domain* (TRADD) and *Fas-associated death domain protein* (FADD) is initiated after binding of TNF to *TNF-receptor* TNF-R1 (Chen & Goeddel, 2002). Via autocatalysis activated caspase-8 initiates a downstream cascade of events, the caspase cascade, whereat a positive feedback enforces this process (Tamm et al., 1998). Furthermore the activation of transcription factors involved in cell survival and inflammatory responses is indirectly activated (Goeddel, 1999) (Fig. 4).

The **intrinsic pathway** is characterized by the formation of the *death-inducing signalling complex* (DISC), the increase of pro-apoptotic factors from mitochondria, the amplified activation of caspase-8 and the release of Cytocrome c. Released Cytocrome c serves a regulatory function as it precedes morphological change after it binds to the *apoptotic protease activating factor - 1* (Apaf-1) and ATP. Thereby the protein binding domain CARD (*caspase recruiting domain*) von Apaf-1 become amenable to the CARD domain of pro-caspase-9 and create with pro-caspase-9 a protein complex known as an apotosome, which cleaves the pro-caspase to its active form of caspase-9. The caspase-9 in turn activates the effector Caspase-3. The activation of the initiator caspases then initiates a downstream cascade of events, the caspase cascade, that results in the induction of effector caspases that function in apoptosis (Gewies, 2003) (Fig. 4).
There also exists a **caspase-independent** apoptotic pathway that is mediated by *apoptosis-inducing-factor* AIF (Susin et al., 1999).

The mitochondrial regulation is one of the main methods in the regulation of apoptosis. Apoptotic proteins can lead to mitochondrial swelling through the formation of membrane pores or they increase the permeability of the mitochondrial membrane for apoptotic effectors. After the increase in permeability, *second mitochondria-derived activator of caspases* (SMACs) is released into the cytosol. SMAC binds to *inhibitor of apoptosis proteins* (IAPs) and deactivates them (Gewies, 2003) (Fig. 4). IAPs like XIAP and Survivin suppress the activity of caspases, which implement the degradation of the cell (Fesik & Shi, 2001). The *Mitochondrial Apoptosis-Induced Channel* (MAC) mediates the release of Cytocrome c to the cytosol based on the formation of MAC on the outer mitochondrial membrane in response to certain apoptotic stimuli (Dejean et al., 2006b). Consequently MAC triggers the commitment step of the mitochondrial apoptotic cascade.

Next page

Fig. 4: Schematic representation of some major apoptotic signalling pathways. The **extrinsic pathway** is mediated by cytokine TNF. After binding of TNF to the TNF-R1, the death domain of TRADD binds to FADD that initiates the caspase activation by binding of the *death effector domain* (DED) of pro-caspase-8 to the DED of FADD. In consequence of the local high concentration of procaspase-8 it becomes active via autocatalysis and initiates the caspase cascade. **Intrinsic pathway:** The formation of the *death-inducing signalling complex* (DISC) results after FasL binding, which results in the release of Cytocrome c. Cytocrome c acts as a regulator by binding to the *apoptotic protease activating factor - 1* (Apaf-1) and dATP. Apaf-1 binds to pro-caspase-9 to create the apotosome. The apotosome cleaves the pro-caspase to its active form of caspase-9, which activates the effector Caspase-3 via proteolytic cleavage, and the degenerative stage of apoptosis begins. A positive feedback is mediated by caspase-7. IAPs inhibit apoptosis by physically binding to and inhibiting proper caspase function (Gewies, 2003).

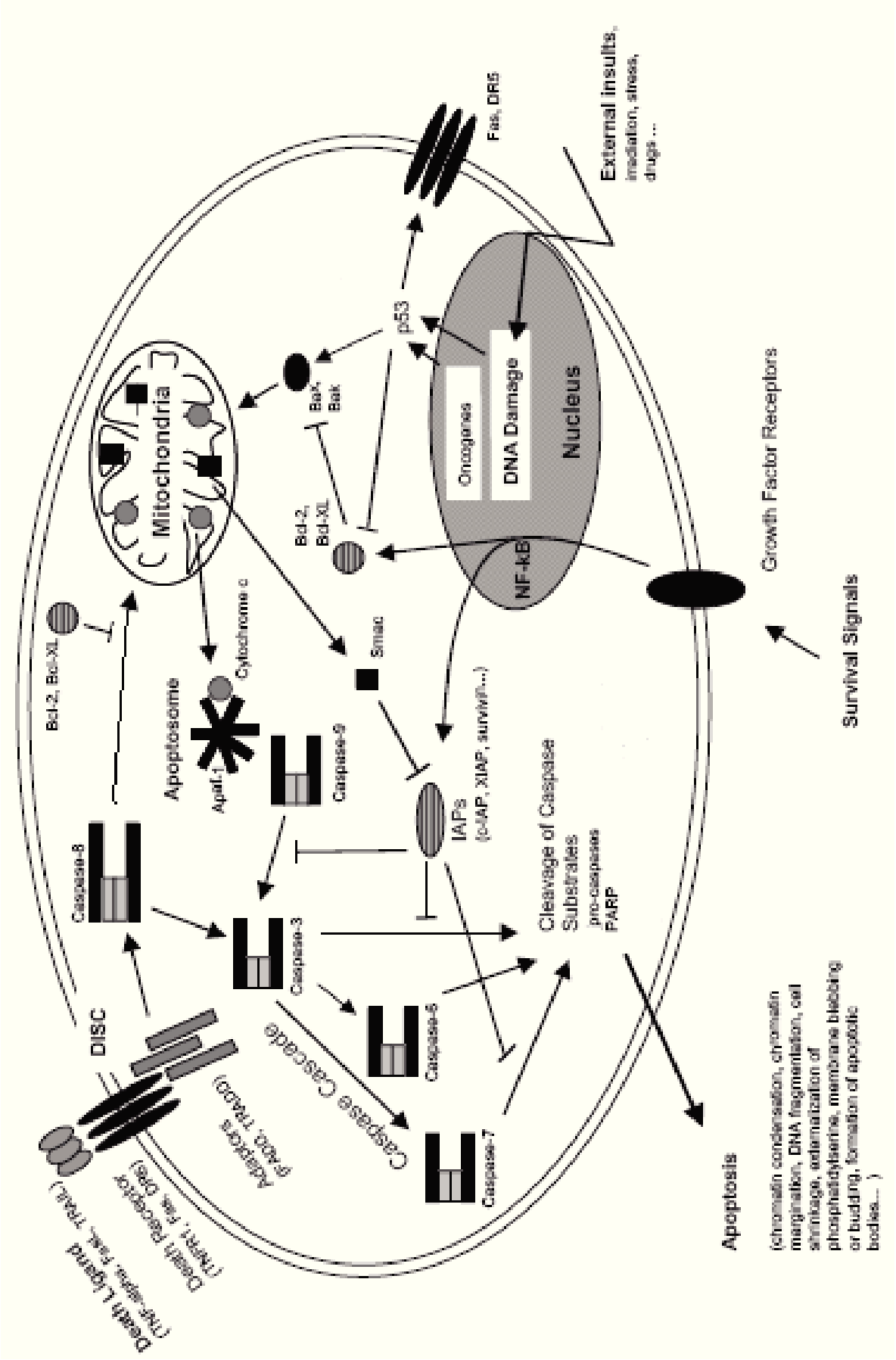

Fig. 4: Apoptotic signalling pathways (http://www.celldeath.de/encyclo/aporev/aporev.htm).

1.4.3. Execution and removal of dead cells (efferocytosis)

A cell undergoing apoptosis shows a characteristic morphology: Because of the breakdown of the proteinaceous cytoskeleton by caspases, cell shrinkage and rounding are shown and the cytoplasm appears dense with tightly packed organelles. The chromatin undergoes condensation into compact patches against the perinuclear envelope, a process called pyknosis (Susin et al., 2000; Kihlmark et al., 2001). During karyorrhexis the nuclear envelope becomes discontinuous and the DNA inside is fragmented by endonuclease activity. Based on the degradation of DNA the nucleus breaks into several discrete chromatin bodies or nucleosomal units (Nagata, 2000). The short DNA fragments, regularly spaced in size give a characteristic "laddered" appearance on agar gel after electrophoresis. Above tests for DNA laddering apoptosis can differentiate between ischemic or toxic cell deaths. The cell membrane shows irregular buds called blebs. Apoptotic bodies were accumulated when the cell breaks apart into several vesicles and subsequently phagocytised.

Efferocytosis is the removal of dead cells by phagocytic cells (Vandivier et al., 2006). Dying cells at the final stages of apoptosis expose phosphatidylserine (phagocytotic molecules) on their cell surface (Li et al., 2003). Normally found on the cytosolic surface of the plasma membrane phosphatidylserine is redistributed during apoptosis to the extracellular surface (Wang et al., 2003). These molecules mark the cell for phagocytosis by macrophages (Savill et al., 2003). Phagocytes remove dying cells in an orderly manner without eliciting an inflammatory response. Marker like Annexin V allows detection of cells at these early stages of apoptosis.

1.4.3. Apoptosis and neuronal cells

Apoptosis is required for the establishment of appropriate cell numbers and for the elimination of improperly connected neurons in the developing nervous system (Pettmann and Henderson, 1998). In the adult nervous system, the inappropriate induction of apoptotic cell death contributes to neuropathology of neurodegenerative diseases. Therefore, identifying the mechanisms of neuronal apoptosis was essential for therapeutic strategies. Mitochondrial dysfunction and release of pro-apoptotic factors such as Cytocrome c or *apoptosis inducing factor* (AIF) from mitochondria are key features of neuronal cell death (Landshamer et al., 2008). AIF is a flavoprotein and normally present in the intermembrane space of mitochondria. If AIF is released from the mitochondria to the cytosol, it migrates to the cell

nucleus, binds to DNA, it signals the cell to condense its chromosomes and triggers DNA degradation and ultimately cell death (Hangen et al., 2010). Translocation of AIF to the nucleus is preceded by increasing translocation of pro-apoptotic bcl-2 family member Bid (*BH3-interacting domain death agonist*) to mitochondria, perinuclear accumulation of Bid-loaded mitochondria, and loss of mitochondrial membrane integrity (Wang et al., 1996).

After neuronal injury in response to excitotoxins, hypoxia and ischemia, death regulatory molecules like *Poly(ADP-ribose)-Polymerase* PARP, c-jun, plasma membrane death receptor ligand systems and the transcription factor p53 as key upstream initiator of cell death process have been implicated (Cregan et al., 2002). Enforced expression of p53 triggers apoptosis in post mitotic neurons (Cregan et al., 1999). Caspases as key effector molecules are involved in the execution of neuronal cell death during development and after injury. Just as well a caspase-independent mechanism of neuronal cell death exists (Rideout & Stefanis, 2001) which is mediated by AIF (Susin et al., 1999). In excitotoxic cell death, caspases are not activated and peptide-based caspase inhibitors do not invoke neuroprotection (Lankiewicz et al., 2000).

The neurogenesis is regulated by pro- and anti-apoptotic proteins. The pro-apoptotic proteins Bax and Bak (Bcl-2-antigonist) are matter for the limitation of the neural progenitor cells in the adult mouse brain, but have no influence on the differentiation of these cells (Lindsten et a., 2003). The down-regulation of Bax results in reduced apoptotic sensitivity of PC-12 cells (Vekrellis et al., 1997). Later studies showed that this occurs with a differentiation based protein expression decrease of Apaf-1 and the simultaneous increase of IAPs (Wright et al., 2004; Lindholm & Arumäe, 2004). The neurogen-active brain areas of adult rats show a 20-800 fold higher concentration of apoptotic cells based on the activation of caspase-2, -3 and –9 (Biebl et al., 2000). The anti-apoptotic protein Survivin deactivated the Caspase-3, -7 and –9 in neural mouse progenitor cells (Jiang et al., 2005). The protein Survivin is found prevalent in neurogene regions (Altura et al., 2003; Pennartz et al., 2004) and have dual functions as apoptosis inhibitor and mitosis regulator (Altieri, 2003; Jiang et al., 2005; Dohi et al., 2004; Shankar et al., 2001; Song et al., 2003; Chen et al., 2003a). Bcl-2 as anti-apoptotic protein is shown to have regulatory functions in neuronal differentiation of the human cell line Paju (Zhang et al., 1996).

2. Aim of the study

The use of biomaterials for stem cell cultivation becomes an important source for cell replacement therapies of neurodegenerative diseases. For *in vitro* studies the 3D culture is desired to better mimic 3D *in vivo* tissue growth, than standard 2D cultures. The use of an ideal material can be essential for the study. Natural derived polymers can face various challenges *in vivo* like inflammatory response, pathogen transfer and purity. This could be problematic for clinical studies. Synthetic materials instead can hold a lack of adhesion motifs. Besides the pore size of the polymers is crucial. Nanofiber structures provide a truly *in vivo* environment than micro- or macroporous polymers. The here used self-assembling hydrogel RADA-16-I functionalised with laminin seem to be ideal for the human neural progenitor cells.

In the first part the advantage of the 3D culture over the 2D culture had to analyse regarding the growth, survival and finally the neuronal differentiation of the hNPCs. Several parameters are of interest:

- the growth and distribution inside the 3D scaffold
- the contact between the cells and between cells and the scaffold
- the amount of neuronal marker during the differentiation period
- the amount of apoptotic cells (of all and only neuronal cells)
- the amount of early and late apoptotic cells
- amount of some key factors of apoptosis regulation

Either the synthetic materials possible have a lack on functional motifs, new generations of self-assembling peptide hydrogels based on RADA-16-I were designed to induce the attachment on the scaffold and the neuronal differentiation. In the second part of the study the influence of modified 3D scaffolds on neuronal differentiation of the hNPCs was of interest. Therefore scaffolds modified with bioactive peptides, called SDP and PFS (provided from BD Bioscience), were used to induce the neuronal differentiation of the hNPCs. Furthermore it was questioned if the survival of the hNPCs is influenced by the modifications of the 3D scaffolds, indicated by changing of apoptotic events. The interesting parameters are:

- the attachment or distribution of the hNPCs
- the amount of neuronal phenotypes

- the rate and the state of apoptosis for the all cells and the neuronal population

For further molecular biological studies it was of interest if the supplement of the purified functional motif PFS to monolayer cultures of hNPCs itself is able to induce the neuronal differentiation in the hNPCs.

In a third and last part of the study it was questioned if laminin has an additional effect on the hNPCs in modified 3D scaffolds. The laminin supplement to the scaffold should increase the attachment and the differentiation. Therefore the modified 3D scaffold was supplemented with laminin and these scaffolds were analysed as well regarding the neuronal differentiation and survival of the hNPCs.

3. Material and Methods

3.1. Material

3.1.1. Technical equipment

	System	Company
balance	MCBA 100	Sartorius
camera	DS2M	Nikon
cell counter	CASY	Roche
cell culture microscope	Eclipse TS100	Nikon
centrifuge	Z383K	Hermle
centrifuge	Z233MK-2	Hermle
centrifuge	3K10	Sigma
flow cytometer	FACS-Calibur	BD Bioscience
fluorescence microscope	Biozero	Keyence
heating block	Thermomixer	eppendorf
incubator	KA14060	Binder
pH-meter	Mettler	Toledo
pipettes	Reference	eppendorf
plate reader	Spectra Fluor plus	Tecan
Powerpac	PowerPac™ HC	BioRAD
scanning electron microscope	DSM 960A	ZEISS
sonicator	UR-009	ATP measurement technique
sterile working bench	Antares 48	Sterile
sterile working bench	IVF workstation L224	K Systems
transmission electron microscope	EM902A	ZEISS
vortexer	SI-0156	Scientific Industries

3.1.2. Chemicals

Routinely used chemicals were purchased with "pro analysis" grade and were supplied, if not otherwise stated, by Calbiochem, Fluka, Merck, Sigma and Roth.

3.1.3. Cell culture media, buffers and supplements

Buffer	Supplements	Company
Cell culture medium	**DMEM / F12** (Dulbecco's Modified Eagle Medium) 4.5g/l glucose FCS (fetal calf serum) Pen/Strep 100x Gentamycin B27 BFGF EGF heparin sodium salt	Invitrogen Invitrogen Invitrogen PAA Invitrogen Invitrogen Roche Roche Invitrogen
HBSS (Hank's balanced salt solution)	$CaCl_2$ $MgCl_2$	Gibco
Trypsin / Benzonase solution	25U/ml Benzonase in Trypsin-EDTA	Merck Invitrogen
Trypsin-inhibitor / Benzonase	1% HSA 25ml Benzonase 0.55mg/ml trypsin-inhibitor in DMEM/F12	Merck Sigma Invitrogen
Sucrose solution	20% (20g / 100ml aqua dest.)	Sigma
PuraMatrix	1% peptide + 99% water	BD Bioscience
Mouse Laminin I solution	1mg/ml	Trevigen
PBS	137nM NaCl 2.7nM KCl 8.1nM Na_2HPO_4 1.5nM KH_2PO_4	Biochrome AG
Immunocytochemistry fixing solution	4% PFA in PBS	Aldrich
Blocking buffer (immunocytochemistry)	5% normal goat serum 0.3% Triton-X100 in PBS	Dako Roth

Antibody incubation buffer (immunocytochemistry)	1% normal goat serum in PBS	Dako
Mowiol / Dapco (1,4-Diazabicyclo- (2,2,2) octan	6g Glycerol 2.4g Mowiol 12g of 0.2M Tris-HCL pH 8.5 25mg DABCO / ml in aqua didest.	Merck Calbiochem Roth Aldrich
FACS fixing solution	1% PFA in PBS	Aldrich
FACS saponin buffer	0.5% BSA 0.5% saponin 0.02% NaN_3 in PBS	Roth Merck Merck
FACS wash buffer	0.5% BSA 0.02% NaN_3 in PBS	Roth Merck
HBS	14mM Hepes 0.9% NaCl 1ml aqua dest., pH 7.4	Merck Roth
Wash buffer (TUNEL-Assay)	0.2% HSA in HBS	
Permeabilisation solution (TUNEL-Assay)	0.1% Triton X-100 in 0.1% sodium citrate	Roth Fluka
DNase I solution (TUNEL-Assay)	3000 IE/ml a 500µl 50µl incubation buffer (10*) 150µl DNase (10U/µl) 300µl RNase-free water	Roche
Binding buffer (Annexin staining)	0.1M Hepes/NaOH (pH 7.4) 1.4M NaCl 25mM $CaCl_2$	BD Bioscience
RIPA buffer	20mM Tris 137mM NaCl 0.1% SDS 0.5% Natriumdesoxycholic acid 1% Triton X-100 10% Glycerol 87%ig 2mM EDTA 1mM EGTA 1mM NaF 20mM sodium pyro phosphate x 10 H_2O 100ml dest. H_2O, pH 7.4 1/vol complete mini protease inhibitor cocktail 7x stock	Roth Roth Roth Roth Merck Merck Sigma-Aldrich Roche

Pierce reagent	Pierce BCA Protein Assay Kit (23225)	Thermo scientific
5x Lämmli buffer	6.25ml Tris (0.5M) 10ml Glycerol 5ml 20% SDS solution 2.5ml Mercaptoethanol 5ml 1% bromphenol blue 21.25ml aqua dest.	Roth Merck Roth Roth
Electrophoresis buffer	30.3g Tris 141g Glycine 10g SDS In 1L aqua dest	Roth Roth Roth
10% SDS solution	50g SDS 500ml aqua dest.	Roth
SDS transfer buffer (semi dry)	5.82g Tris 2.93g Glycine 3.75ml 10% SDS solution 200ml Methanol In 1L aqua dest.	Roth Roth Roth Roth
10x TBS	7.7mM Tris HCl 15mM NaCl in 1L aqua dest. working solution 1X (dilution 1:10)	Roth Roth
TTBS	100ml 10x TBS 1ml Tween 20 In 1L H_2O	Serva
WB blocking solution	3% skim milk solution	Fluka
Coomassie-Brilliant-Blue (CBB) – stock	5g Coomassie-Brillant-Blue (G-250) In 100ml aqua dest.	Serva
Colloidal Coomassie dye (CCD) - stock	50g ammonium sulphate 6ml 85% phosphoric acid 490ml H_2O dest 10ml CBB-stock	Merck Merck
Ready to use Colloidal Coomassie solution	200ml CCD-stock solution 50ml Methanol	Roth

3.1.4. Antibodies

Primary antibody	company	Catalogue number	host	Dilution for IF	Dilution for flow cytometry	Dilution for WB
Bax	BD Bioscience	610982	mouse monoclonal	-	-	1:250
Bcl-2 (100)	Santa Cruz	sc-509	mouse monoclonal	-	1:5	-
Caspase-3	Cell Signalling	#9665	rabbit polyclonal	-	-	1 :1000
GAPDH	Abcam	Ab8245	mouse monoclonal	-	-	1:10000
GFAP	Dako	Z0334	rabbit polyclonal	1:1000	1:100	-
HuC/D	Invitrogen	A21271	mouse monoclonal		1:100	-
Ki-67	Santa Cruz	Sc-15402	rabbit polyclonal	1:200	-	-
PARP-1	Cell Signalling	#9532	rabbit polyclonal	-	-	1:1000
PSA-NCAM	Millipore	MAB5324	mouse monoclonal	1:200	1:100	
PSD95	Abcam	Ab2723	mouse monoclonal	1:200	-	-
ß-Actin AC-15	Sigma	A5441	mouse monoclonal	-	-	1:10000
ßIII-tubulin	Abcam	Ab18207	rabbit polyclonal	1:2000		
Survivin	Cell Signalling	#2808	rabbit polyclonal	-	-	1:1000
Synaptophysin	Sigma	S5768-2	mouse monoclonal	1:100	-	-

TH tyrosine hydroxylase	Millipore	AB152	rabbit polyclonal	1:500	-	-
XIAP	BD Bioscience	610716	mouse monoclonal	-	-	1:200
βIII-tubulin	Santa Cruz	sc-515670	mouse monoclonal	1:500	1:100	-

Secondary antibody	**Company**	**Catalogue number**	**Host**	**Dilution for IF-IC**	**Dilution for flow cytometry**	**Dilution for WB**
Alexa Fluor 488	Molecular Probes	A11029	goat anti-mouse	1:1000	-	-
Alexa Fluor 488	Molecular Probes	A11034	goat anti-rabbit	-	1:1000	-
Alexa Fluor 568	Molecular Probes	A11036	goat anti-rabbit	1:1000	-	-
Alexa Fluor 647	Invitrogen	A21235	goat anti-mouse	-	1:1000	-
Alexa Fluor 647	Invitrogen	A21245	goat anti-rabbit	-	1:1000	-
Alexa Fluor 680	Invitrogen	A21057	goat anti-mouse	-	-	1:10000
Alexa Fluor 680	Molecular Probes	A-211098	goat anti-rabbit	-	-	1:20000
IRDye800	Rockland	610-132-121	goat anti-mouse	-	-	1:10000

3.2. Methods

3.2.1. Culture of human neural progenitor cells

The human neural progenitor cell line ReNcell VM was provided by ReNeuron (Guildford, UK). The human neural progenitor cells (hNPCs) were derived from the ventral midbrain of a 10-week-old fetus and immortalized by retroviral v-Myc transduction. The cells were cultivated in culture vessels at 37°C, 20% O_2 and 5% CO_2 in Dulbecco´s modified eagle medium (DMEM)/F12, supplemented with Glutamax, B27 media supplement, heparin sodium salt and gentamycin (all Invitrogen, Karlsruhe, Germany). For proliferation epidermal growth factor (EGF, 20ng/ml) and basic fibroblast growth factor (bFGF, 10ng/ml; both Roche, Mannheim, Germany) were added to the media. Withdrawal of the EGF and bFGF induces the differentiation of the cells (Donato et al., 2007). Different protocols of culture conditions are compared to find out the optimal growth and differentiation conditions for these cells. On one hand a monolayer culture of hNPCs on laminin coated wells (Trevigen, Gaithersburg, USA) and on the other hand 3D culture systems with the self-assembling peptide hydrogel RADA16-I (PuraMatrix^{TM}, BD Biosciences, Heidelberg, Germany).

3.2.1.1. Cultivation of the cells in a standard 2D culture system

For the 2D culture the cell culture vessels (6-well plate) were coated with laminin. Therefore the dishes were incubated with a laminin solution dissolved in (DMEM)/F12 media to a concentration of 1% for 1 to 24h at 37°C, 20% O_2 and 5% C. After washing of the well with (DMEM)/F12 media, cells were seeded with the proliferation media. When 80% confluence was reached, the hNPCs were differentiated for up to 10 days.

3.2.1.2. Cultivation of the cells in a 3D culture system

For the 3D culture the self-assembling peptide hydrogel RADA16-I (PuraMatrix^{TM}, BD Biosciences, Heidelberg, Germany) was used in a concentration of 0.25% and supplemented with laminin (8µg/100µl Matrix) further referred as PML (Ortinau et al., 2010). Furthermore modified PuraMatrix formulations PM-SDP, and PM-PFS (provided by BD Bioscience) were

tested and compared with a PuraMatrix-scaffold without laminin further referred as PM. PuraMatrix-scaffolds consisting of PM or PM-PFS and supplemented with laminin are referred as PML, and PML-PFS. For the preparation of the 3D scaffolds the cells were encapsulated in the scaffold with a concentration of 80000 cells/100µl matrix. Therefore monolayer cultured hNPCs were trypsinised with Trypsin/Benzonase. Than the hNPCs were washed and resuspended in 10% sucrose to remove salt of the solution. Two solutions were prepared 1) cell solution (hNPCs dissolved in 10% sucrose and laminin) and 2) PuraMatrix solution (PM-stock dissolved in 20% sucrose 1:1). Solution 1 was mixed with solution 2 and transferred immediately on coverslips resided in a 4-well plate. 2 x 200µl/well media was slowly added, initiating the peptide self-assembly by altering salt concentrations. After 1h incubation at 37ºC on IVF Workstation L224 with heating plate matrices were washed with 500µl media for 10min and incubated with fresh media in the incubator. In all 3D scaffolds hNPCs proliferate for 7 days after seeding inside the matrix and then were differentiated for up to 10 days with media change every 2-3 days. The growth control was done via phase contrast microscopy.

3.2.1.3. Recovering of hNPCs cultivated in a 3D scaffold

Recovering means the leaching of the cells of the scaffold to produce a single cell solution for recultivation in 2D. The 3D scaffolds with encapsulated hNPCs were washed with HBSS, mechanically disrupted by pipetting up and down and transferred to a conical tube. Next the cells were treated with Trypsin/Benzonase for 5min at 37°C, 20% O_2 and 5% CO_2. After stopping the reaction with Trypsin-inhibitor/Benzonase, the cell solution was washed two times with HBSS to remove remaining cell-cell- and cell-matrix-aggregates. Next the hNPCs were resuspended in cell culture medium and were plated on PDL and laminin coated cover slips. The next day cells were attached on the cover slips and can fixed with 4% *Paraformaldehyde* PFA (Liedmann et al., 2012a). In PBS with 0.02% NaN_3 the samples can store until staining.

3.2.2. Electron microscopy

3.2.2.1. Scanning electron microscopy

For scanning electron microscopy, hNPCs encapsulated in 3D scaffolds were fixed with glutaraldehyde (4% in PBS) for 1h or overnight, rinsed with PBS and subsequently dehydrated in acetone with increasing concentrations (30%, 50%, 75%, 90%, 100%). Specimens were dried with a critical point drier (BalTec, Germany) and sputter coated with gold. Pictures were taken with a DSM 960A scanning electron microscope (ZEISS, Germany). The preparation of the samples and imaging of the scanning electron microscope pictures were done in cooperation with the Electron Microscopic Centre of the University of Rostock (www.emz.med.uni-rostock.de).

3.2.2.1. Transmission electron microscopy

For transmission electron microscopy the 3D scaffolds containing hNPCs were fixed with glutaraldehyd (4% in PBS + Na-Cacodylat). The scaffolds were incubated 45min in osmium acid, rinsed with Na-Phosphate buffer and embedded in Agar-Agar. They were subsequently dehydrated in acetone with increasing concentrations (75%, 90%, 100%). Next the drained Agar block was embedded in Araldite and cut in ultra thin slices. The preparation of the samples and pictures were done with an EM902 transmission electron microscope (ZEISS, Germany, Oberkochen) in cooperation with the Electron Microscopic Centre of the University of Rostock (www.emz.med.uni-rostock.de).

3.2.3. Immunocytochemistry

3.2.3.1. Immunocytochemistry of 2D culture samples

The 2D culture samples were fixed with paraformaldehyde (4% in 0.1M PBS) for 15min and stored at 4°C in PBS with 0.02% NaN_3. After washing with PBS the hNPCs were incubated for 1h in blocking buffer (*Normal Goat Serum* NGS 5%, Triton X-100 0.3% in PBS). The primary antibody was incubated for 1h (ßIII-tubulin) or over night (PSD95). The cells were washed 3 times for 5min and the secondary antibody staining was performed. The secondary antibody was dissolved in PBS and 1% NGS and incubated for 1h at RT in the dark. Cell

nuclei labelling was combined with the mounting of the samples using mounting media containing DAPI (4',6-Diamidin-2'-phenylindoldihydrochlorid) (Morgan et al., 2009). The slides were fixed with nail polish. Pictures were taken with the Biozero 8000 microscope (Keyence, Germany, Karlsruhe).

3.2.3.2. Immunocytochemistry of 3D culture samples

The 3D cultures of hNPCs were fixed with paraformaldehyde (4% in 0.1M PBS) for 30min and stored at 4°C in PBS with 0.02% NaN_3. Next the matrices were incubated for 24h in blocking buffer (NGS 5%, Triton X-100 0.3% in PBS) by changing blocking buffer 4 times. Afterwards they were incubated with the primary antibody in PBS with 1% NGS over night at 4°C. After washing the cells 4 times for 2h and over night with PBS, the secondary antibody, dissolved in PBS with 1% NGS was added and matrices were incubated for 4h at RT in the dark. Before a cell nuclei labelling was performed with DAPI (100ng/ml in PBS, Sigma) the samples were washed 4-6 times for 1h and over night with PBS. After the DAPI staining three washing steps, each 30min follow, than matrices were mounted with Mowiol/Dapco. The fluorescence microscope (Biozero 8000 microscope, Keyence, Karlsruhe, Germany) was used to obtain single micrographs and z-stacks at 8 different independent areas. Each stack contains 30 single pictures with a distance of 1-2µm. Using the corresponding analyser software the blur inherent to fluorescence was removed before full projections of the z-stacks were produced (Liedmann et al., 2012b).

3.2.4. Flow cytometry

For flow cytometry, 3D scaffolds were mechanical disrupted by pipetting up and down and cells were released with a mixture of Trypsin/Benzonase from the matrices. Cells cultured in the standard 2D system were detached with Trypsin/Benzonase solution and the reaction was stopped with Trypsin-inhibitor/Benzonase solution. In the following the procedure was the same for 2D and 3D cultivated cells. After centrifugation at 3000 x g at RT for 5min, all cells were washed with HBSS puffer two times to separating cells from matrix. RADA-16 peptides or nanofibres were eliminated with the supernatant. Subsequently the remaining cell/matrix aggregates were removed with a cell strainer (70µm, BD Bioscience). After fixation of the cells with 1% PFA for 15min, the cells were resuspended in washing buffer (PBS + 0.5%

BSA + 0.02% Na-azide) and stored at 4°C in the dark. For the staining cells were centrifuged at 350 x g, 10min, 4°C and resuspended in saponin buffer (PBS + 0.5% saponin + 0.5% BSA + 0.02% Na-azide) containing the first antibody. Additional a negative control without first antibody was produced for all samples and an isotype control for each experiment. Then the cells were incubated for 2h at RT. Afterwards the cells were washed two times with saponin buffer and incubated with the secondary antibody for 1h in saponin buffer. The cells were washed again twice with saponin buffer and resuspended in wash buffer for analysis (Liedmann et al., 2012a). Measurements were done using a FACS-Calibur (BectonDickinson, San Jose, USA) in combination with Cell Quest Pro software.

3.2.5. TUNEL-Assay

Terminal deoxynucleotidyl transferase dUTP nick end labelling (TUNEL) is a method for detecting DNA fragmentation by labelling the terminal end of nucleic acids (Gavrielli et al., 1992; Negoescu et al., 1996). The In Situ Cell Death Detection Kit with the fluorochrome Fluorescein from Roche was used. In the following the procedure of the sample preparation was the same for 2D and 3D cultivated cells. The cells were prepared as described above (see 3.2.4.; Liedmann et al., 2012b). After fixing the cells with 1% PFA for 15min, the cells were resuspended in HBS with 0.2% HSA. The labelling starts with the permeabilisation of the cells with 0.1% Triton X-100 and 0.1% sodium citrate dissolved in PBS. Subsequently the cells were incubated in the TUNEL reaction mix for 1h at 37ºC in a humidified atmosphere, in darkness. Samples were subsequently washed and stored in PBS until analysis. Negative controls were incubated without TUNEL reaction mix. For positive controls cells were incubate with DNase I (3000 IE/ml) to induce DNA strand breaks. Measurement was done using the FACS-Calibur (BectonDickinson, San Jose, USA) in combination with Cell Quest Pro software.

3.2.6. Annexin V Apoptosis Detection

Annexin V is a 35-36kDa calcium dependent phospholipid-binding protein which can in combination with the vital dye propidium iodide (PI) identify apoptosis at early stage (Martin et al., 1995; van Engeland et al., 1996).

The FITC Annexin V Apoptosis Detection Kit I (BD Bioscience, San Jose, USA) was used and the cells were prepared as described above (3.2.4.) for flow cytometry without fixing the cells. For 2D cultivated cells the supernatant of the cell culture dishes was collected as well. In the following the procedure was the same for 2D and 3D cultivated cells. After washing the cells with HBSS two times and elimination of cell/matrix aggregates via a cell strainer, the cells were washed with PBS (Liedmann et al., 2012b). Next the cells were resuspended in 1x binding buffer at a concentration of $2x10^6$ cells/ml and in 100µl of the cell solution 5µl of Annexin V and 5µl propidium iodide were added. After 15min incubation at RT in the dark, 400µl of 1x binding buffer were added and measurement was done using FACS-Calibur (BectonDickinson, San Jose, USA) in combination with Cell Quest Pro software. An example of a flow cytometry measurement is shown in picture 5.

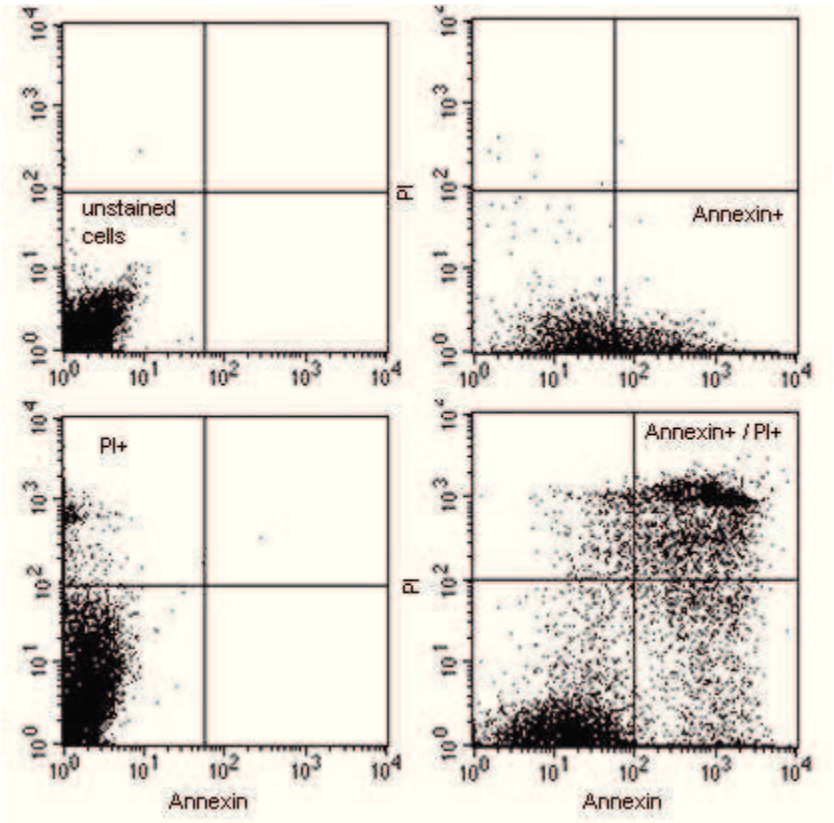

Fig. 5: The analysis of the Annexin V- PI staining is shown. The cells which were only positive for PI indicates necrotic cells, cells positive for Annexin V indicate cells in early apoptosis. Late apoptotic cells were positive for both.

The negative control was performed by blocking FITC Annexin V binding sites. Cells were incubated 15min at RT with 15µg purified recombinant Annexin V before the staining with the FITC Annexin V and PI started.

A supplement control was produced by induction of apoptosis by treatment with Camptothecin. The cells were treated with Camptothecin to get a positive control by inducing

apoptosis in the hNPCs. The 1mM stock solution of Camptothecin (in DMSO) was added to the culture medium resulting in a final concentration of 6µM. After 16h incubation of the cells at 37ºC the Annexin V assay was preceded to evaluate the amount of apoptotic cells.

3.2.7. Western blot

The sample preparation of the 3D scaffolds followed with the same procedure used for flow cytometric preparation (3.2.4.). The 2D samples and the 3D scaffolds were treated with Trypsin/Benzonase and Trypsin-inhibitor/Benzonase, washed 2 times with HBSS buffer and aggregates of matrix were separated by using a cell strainer. Next the cells were washed with PBS and lysated on ice with RIPA buffer for 20min. Then the samples were treated three times for 15s in the sonicator to enforce lysis of the cells. The samples were centrifuges afterwards for 10min at 3800 x g. 10µl of the lysate was separated for a determination of the protein amount (Pierce BCA Protein Assay Kit, Thermo scientific). Therefore the lysate solution was diluted 1:20 and 10µl of the dilution was added on well of a 96 well plate (three times). The reagent B was diluted 1:50 with Reagent A and 200µl of the resulting Pierce reagent were added to the samples in the 96 well plates. After 1h incubation the colour change was measured with a TECAN plate reader (Spectra Fluor plus). The protein content was calculated using a standard curve.

The total cell lysate for Western Blot analysing was mixed 5:1 with 5-fold Lämmli-Buffer and incubated 5min at 95°C/350rpm. The samples, with an equal amount of protein, were added to the slots of the 4-15% TRIS-HCl (Criterion) gel. The gel electrophoresis was performed in a gel chamber with electron buffer for 1h at 200V. The gel, the membrane and the filter paper were incubated for 10min on a shaker in SDS transfer buffer, subsequently. The proteins separated in the gel were blotted on a Hybond Nitrocellulose membrane (GE Healthcare) between two filter papers for 90min at 100mA. The gel was stained with Coomassie-blue to control if the blot was complete. Afterwards the membranes were blocked in 3% skim milk for 1h on a shaker. The primary antibody staining was done over night at 4°C under gentle shaking. Afterwards the membranes were washed three times for 5min with TTBS buffer. The membranes were stained for 2h at RT in the dark with the secondary antibody with gentle shaking. Before the membranes were dried they were washed two times with TTBS and ones with TBS buffer (Burnette, 1981). During the scanning of the membranes the fluorescence

was measured with the Li-COR scanner (Li-COR Inc, Lincoln, USA). For analysing the Prestained Protein Marker IV (peqlab peqGOLD) and an internal standard like GAPDH and ß-Actin AC-15 was used.

3.2.8. Statistics

All statistical analyses and graphs were performed with Prism 5 (GraphPad Prism. Inc., USA). The analysing of the ßIII-tubulin positive cells in immunocytochemistry pictures was performed by counting 8 areas of two 3D scaffolds per time point. N is given as the number of experiments and n as the number of scaffolds for each experiment. For flow cytometry analyses one 3D scaffold was used per time point, therefore N is given as the number of experiments. The values represent the mean and the aberrance was shown as *standard error of the mean* SEM. The values of the tested conditions were compared at each time point using the student's t-test. P-values ≤ 0.05 indicated by *, were considered to indicate significant statistical differences. P-values ≤ 0.01 or ≤ 0.001 are indicated by ** and *** respectively.

4. Results

Aim of the study was to elucidate the influence of a 3-dimensional environment on the proliferation and differentiation of human neural progenitor cells. Therefore cells were cultured in a standard 2D culture system and in the peptide based hydrogel PuraMatrix supplemented with laminin (PML) (4.1). Subsequently the different culture conditions were compared by several parameters like the amount of cells with a neuronal phenotype and apoptotic events. In the second part modified RADA16-I formulations (provided from BD Bioscience), namely PM-SDP and PM-PFS were tested. These formulations contained incorporated functionally modified peptide sequences to improve cell adhesion and differentiation (4.2.). Further the effect of the PFS sequence on monolayer culture was analysed (4.3.). In the last part, the effect of laminin on the hNPCs, grown in the modified matrix formulation PM-PFS, was studied to elucidate any additional effects of the combination of laminin and modified matrix (4.3.).

4.1. Cultivation of hNPCs in 3D scaffolds (PML)

In a previous study it was shown that the structure of 3D scaffolds consisting of PuraMatrix depends on the used concentration of the matrix and the functionalisation with laminin (Ortinau et al., 2010). Furthermore the formation of the matrix directly influenced the differentiation and survival of hNPCs cultured in the 3D scaffolds. As Ortinau et al. (2010) determined a PM-concentration of 0.25% as optimal for the hNPCs, I used this concentration for my studies. In the first part of the study the influence of the 3-dimensional culture system on the growth, differentiation and survival of the hNPCs was analysed.

4.1.1. Growth of hNPCs inside the 3D scaffolds (PML)

The question, how the cells grow inside the matrix was of great interest in the beginning of this work. I used a 0.25% PuraMatrix scaffold supplemented with laminin (PML) in a concentration of 8µg laminin / 100µl Matrix. The hNPCs were encapsulated in the matrix, cultured in the 3D scaffold for 7 days under proliferation conditions and subsequently differentiated for up to 10 days. Fig. 6 shows proliferated hNPCs inside the PML 3D scaffolds

(Fig. 6A, B) and cells differentiated 7 days (7dd) (Fig. 6C, D). Cells proliferated for 7 days show flat and densely packed cell aggregates with 3-dimensional loosely composed cellular structures (Fig. 6A, B). After 7 days of differentiation (Fig. 6C, D) one can see outgrowing processes and morphological changes compared to proliferating cells (Fig. 6A, B).

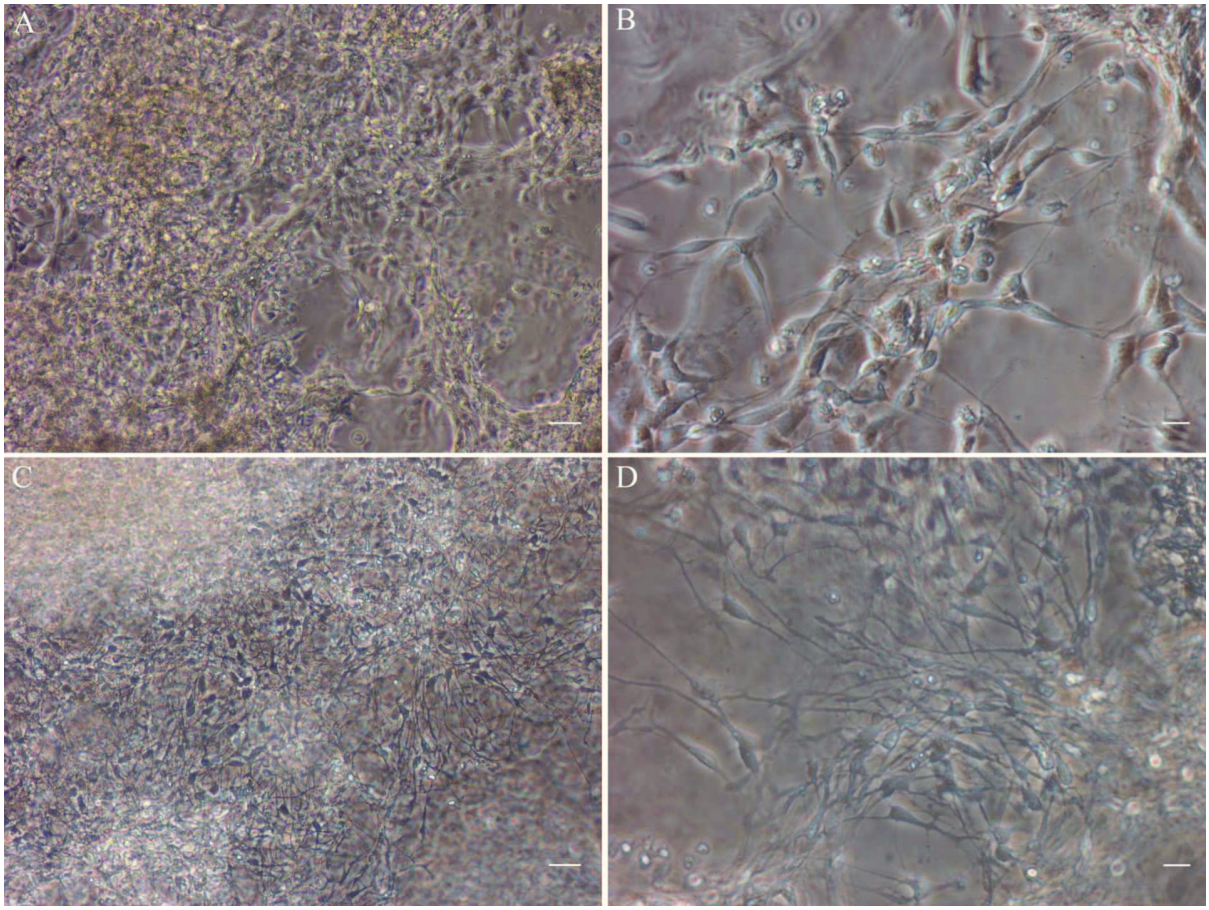

Fig. 6: Phase contrast pictures of hNPCs in 3D scaffolds (PML) 7 days under proliferation conditions (**A, B**) and 7 days differentiated (**C, D**). **A, C:** Overview, scale 20µm; **B, D:** magnification, scale 10µm.

The hNPCs grown not as neurospheres. Neurospheres are the preferred form of the hNPCs. They shown a distribution across the 3D scaffold, but the distribution is not equal in the matrix. There are parts with lower number of cells and parts with a huge number of cells and also areas without cells (Fig. 6). In a first set of experiments I analysed the structure of the scaffold by means of scanning electron microscopy to know if this may results from the structure of the matrix.

Fig. 7 shows an example of the surfaces of the PML scaffolds by using the scanning electron microscopy. The surface of the scaffold appears fissured and inhomogeneous. The PML

scaffold demonstrates cavities and lacunas (Fig. 7a, b). The dense network of regular overlapping nanofibres of the scaffold was detected with the highest magnification (right).

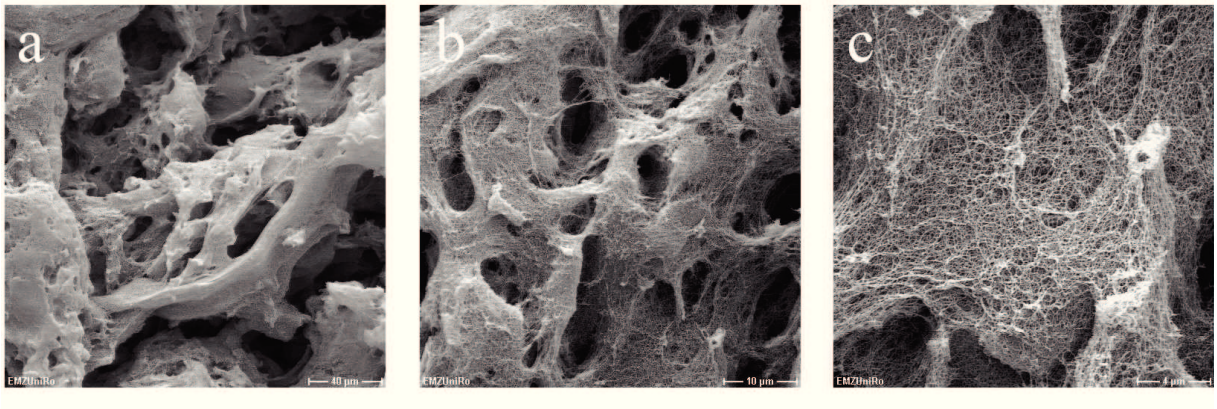

Fig. 7: Scanning electron microscopy of 3D scaffolds. The surface of the scaffold with the laminin functionalisation (PML) is shown (**a, b, c**). **a** Scale 40µm, **b** Scale 10µm, **c** Scale 4µm. The dense network of regular overlapping nanofibers was detected with the highest magnification (right, **c**).

Next, I was interested in how the hNPCs were incorporated in these structures. Therefore the cells were embedded in PML scaffolds and the growth was compared to cells cultivated in standard 2D culture system (Fig. 8). The images of the left column present an overview and the images of the right column provide a higher magnification of the samples. The pictures 8a and 8b show hNPCs grown as a monolayer in the 2D culture system. One can observe an outgrowth of processes with only few contacts between the cells.

The images 8c-h shows the network structure of the 3D scaffold and the growing of the cells within the 3D composition of the scaffold. The cells are in contact with the matrix material and avoid cavities and lacunas (8c, e). They only bridged them with processes. In higher magnification (Fig. 8d) one can see the small pore size (50-200nm) of the material in comparison to the size of the cells (5-20µm). Fig. 8e-h show hNPCs 7 days differentiated in PML scaffolds. In Fig. 8e, g a network of processes of the hNPCs is found among the scaffolds. In a higher magnification one can see a very detailed view of single cells (Fig. 8f) and a process outgrowth (Fig. 8h) of hNPCs within 3D scaffolds.

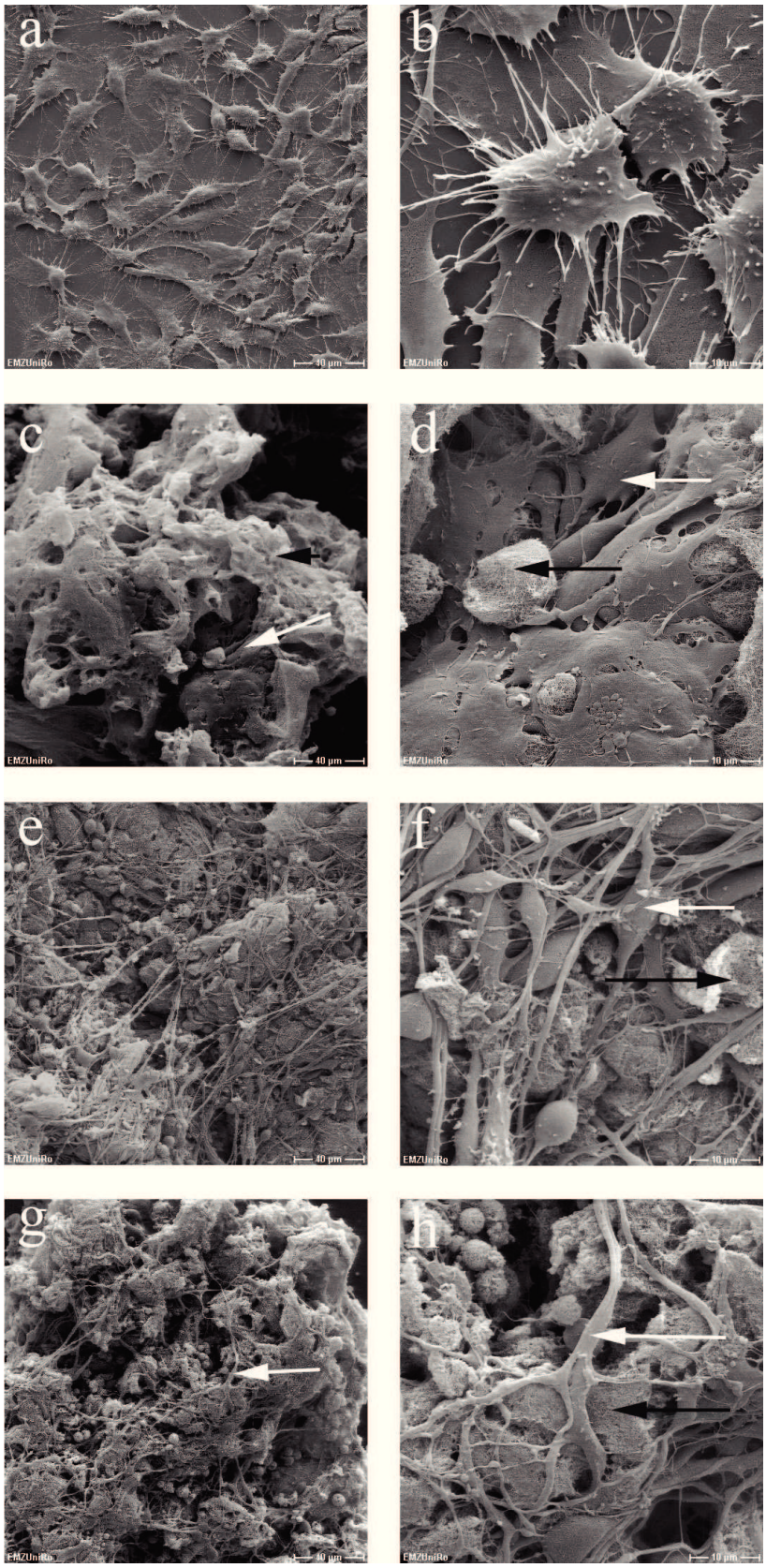

Fig. 8: Scanning electron microscopy pictures of hNPCs in 2D culture and 3D scaffolds. Left panel: scale 40 µm, right panel: scale 10 µm. **a, b** Proliferated hNPCs cultured in 2D culture, adherent on PDL and laminin coated cover slips. Proliferating cells cultured in PML 3D scaffolds for 7 days (**c:** overview, **d:** magnification) and 7 days differentiated cells in PML 3D scaffolds (**e, g:** overview; **f, h:** magnification). A very detailed view of hNPCs is shown in **d, f** and of a process in **h.** White arrows indicate hNPCs, black arrows indicate structure of the matrix.

As the scanning electron microscopy pictured only the surface of the 3D scaffolds, transmission electron microscopy was used in addition to analyse cells residing inside the matrices. Fig. 9 shows two ultra thin slices of laminin functionalised scaffolds (PML) with proliferated cells. Inside the cells one can see cell organelles like the nucleus with nucleolus, the rough endoplasmic reticulum (RER), several mitochondria, the golgi apparatus and the cell membrane (Fig. 9A). The cells are surrounded by other cells or matrix distinguishable of overlapping nanofibers. Interestingly one could observe vesicles in the cells filled with material with a structure similar to the structure of the matrix material (Fig. 9B, C), which could possible phagozytosed nanofibers from the scaffold.

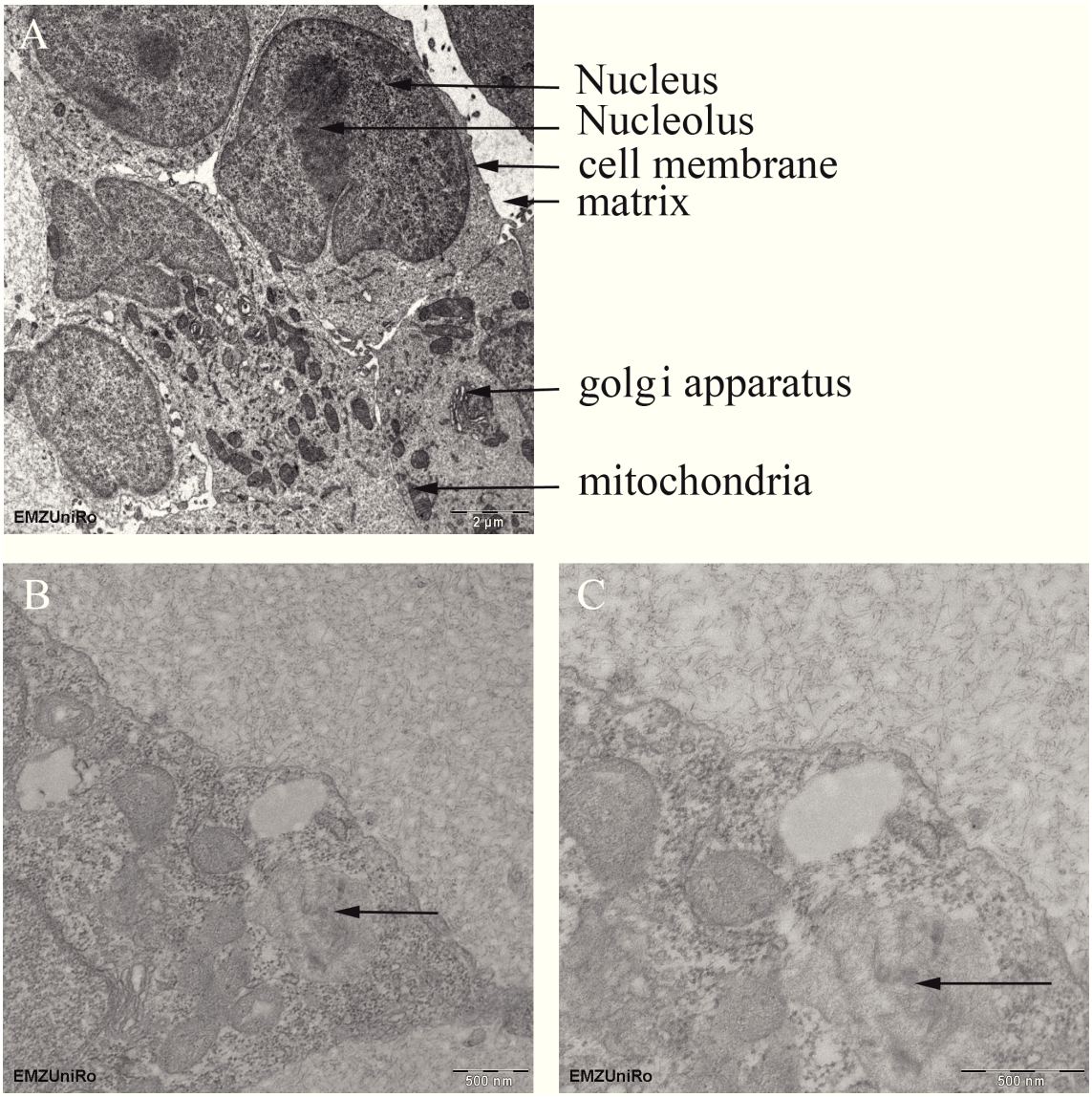

Fig. 9: Transmission electron microscopy of hNPCs cultured 4 days in 3D scaffolds supplemented with laminin (PML). **A:** Nucleus, Nucleolus, cell membrane, matrix, rough ER, mitochondrion, Golgi apparatus. Scale 2µm. **B, C:** Scale 500 nm. The structures inside the vesicle of the cells (black arrow), which looks similar to the structure of the 3D scaffold.

4.1.2. Differentiation of hNPCs in 3D scaffolds (PML)

To elucidate the influence of the 3-dimensional environment on the differentiation of the hNPCs, immunocytochemical studies were performed using neuronal marker. Further a quantification of the amount of the different phenotypes of the hNPCs was done.

The hNPCs were proliferated in PML 3D scaffolds for 7 days and subsequently differentiated for another 7 days. Different neuronal markers were used like ßIII-tubulin for mature neuronal cells, TH (tyrosine hydroxylase) for dopaminergic neurons or GFAP (Glial fibrillary acidic protein) for glial cells. Fig. 10 shows differentiated cells stained against ßIII-tubulin and GFAP (Fig. 10A), ßIII-tubulin and TH (Fig. 10B) as well as PSA-NCAM (Fig. 10C). Proliferated cells usually show GFAP, but no ßIII-tubulin or TH positive cells. The hNPCs differentiated mostly to astrocytes, shown as GFAP positive cells, only a small amount of →

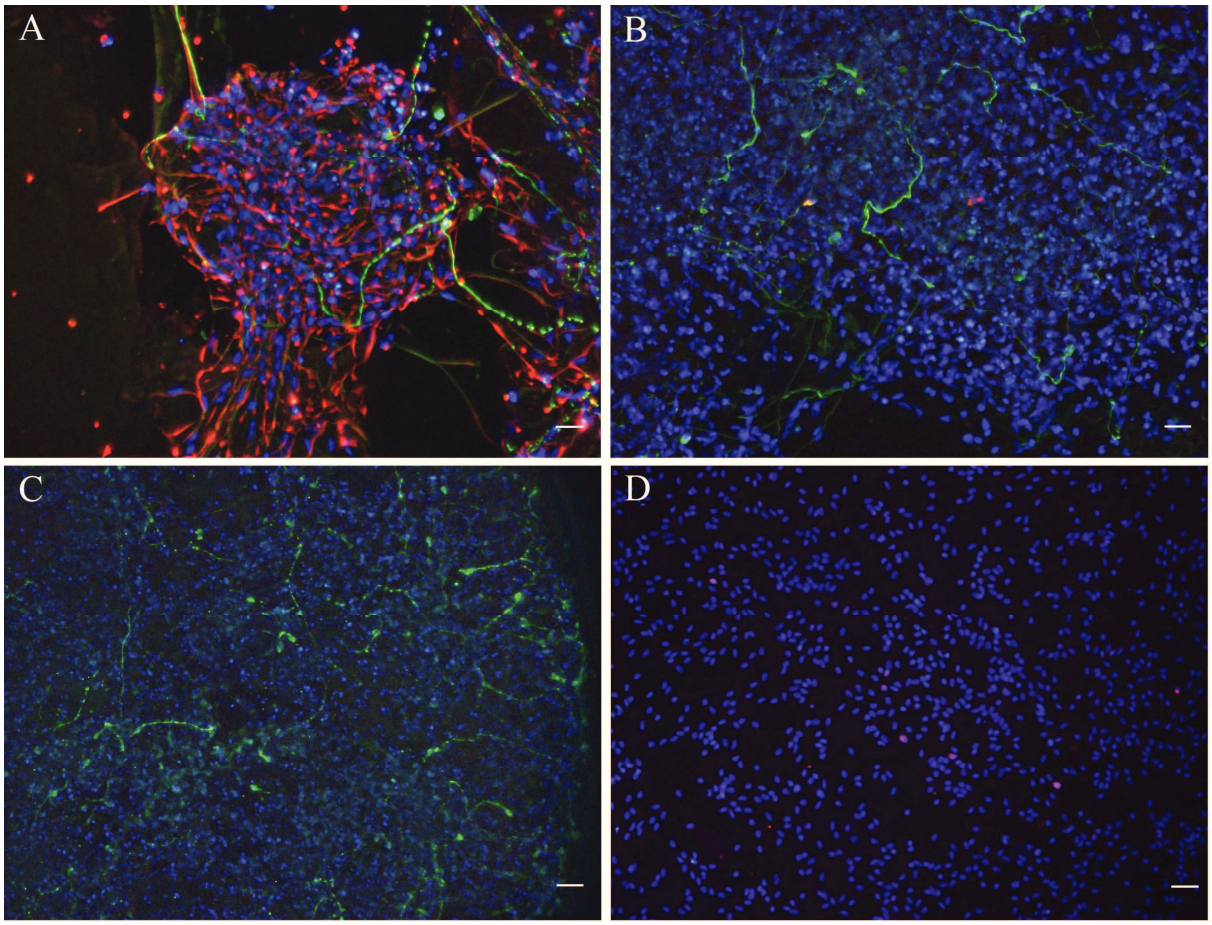

Fig. 10: Immunocytochemistry pictures of 7 days differentiated hNPCs in 3D scaffolds (PML). A: ßIII-tubulin (green) / GFAP (red), scale 20 nm. **B:** ßIII-tubulin (green) / TH (red), scale 20 nm. **C**: PSA-NCAM (green), scale 50 nm **D:** Ki-67 of released hNPCs, which were differentiated 7 days in 3D scaffolds, scale 20 nm. The distribution of cells within the matrix is shown by DAPI staining. Proliferated cells were positive for GFAP, PSA-NCAM and Ki-67. TH and ßIII-tubulin were usually only found in differentiated cells. GFAP and PSA-NCAM were found in both conditions. Also some Ki-67 positive cells were found in hNPCs when differentiated in 3D scaffolds.

ßIII-tubulin and few TH positive cells were found (Fig. 10A, B). PSA-NCAM was used as a marker for neuronal precursor cells. The hNPCs are positive for PSA-NCAM at proliferated and differentiated state in 3D scaffolds. Fig. 10C shows differentiated hNPCs positive for PSA-NCAM. If the hNPCs were differentiated in 3D scaffolds some cells were not stained for any of the described marker. Following, the in 3D scaffolds differentiated hNPCs were released of the scaffold to prove if the cells keep their proliferation potential. The differentiated cells were plated again as monolayer and stained against Ki-67. Ki-67 is a marker for dividing cells. Fig. 10D shows that some cells differentiated in 3D scaffolds were positive for Ki-67.

Fig. 11 shows the quantification of immunocytochemistry pictures with hNPCs in 3D scaffolds at different time points. The manual counting was done for cells differentiated up 20 days to define the time course for following experiments in the 3D cultures. The peak with the highest number of cells was detected at 7 days of differentiation with around 3-4% ßIII-tubulin positive cells. Then a decrease of ßIII-tubulin positive cells until 14 days was found to less than 1% positive counts.

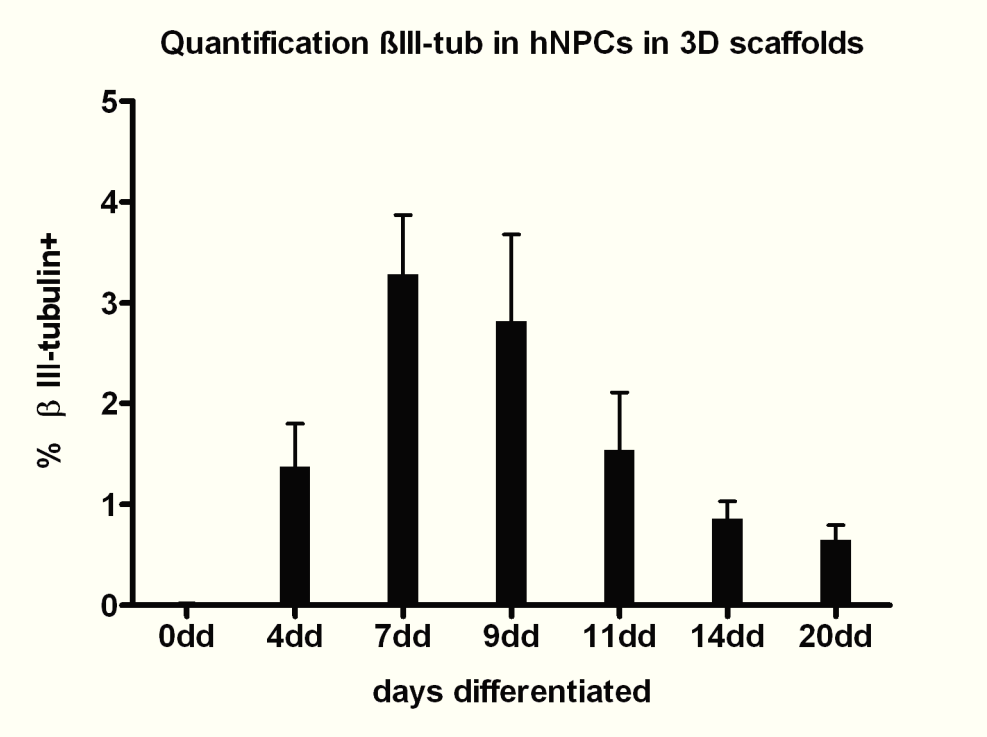

Fig. 11: Quantification of immunocytochemistry pictures of hNPCs in 3D scaffolds (PML): Number of ßIII-tubulin positive cells counted at different stages of differentiation. Total number of cells was determined by DAPI staining using GSA Image Analyser counting software. The highest number of ßIII-tubulin^{+} cells was found at 7dd. N=2-4, n=2. Mean ± SEM.

As the quantification of microphotographs is extremely time consuming and only a small subset of cells within the scaffolds can be analysed, a method to release the cells from the scaffolds was adapted. In a next approach hNPCs encapsulated in 3D scaffolds were released from the matrices and subsequently cultured in 2D culture system providing access to cells for immunocytochemical staining. Therefore the 3D scaffolds were disrupted mechanically and the cells were released and sub-cultured on PDL and laminin coated cover slips. Three conditions with PML 3D scaffolds were tested. Cells were released after 7 days of proliferation, as well as 4 and 7 days in differentiation (Fig. 12). Recovered proliferated cells adhere properly. Differentiated cells had a reduced tendency to adhere. Fig. 12 shows differentiated hNPCs recovered from PML 3D scaffold at 4dd and 7dd stained for GFAP and ßIII-tubulin (Fig. 12 A, C). The number of adhered neuronal cells was decreased from 4 to 7 days (Fig. 12 B, D). Based on these results the next experiments to detect cells positive for different marker via immunocytochemistry, were done with cells recovered from scaffolds after 4 days differentiation.

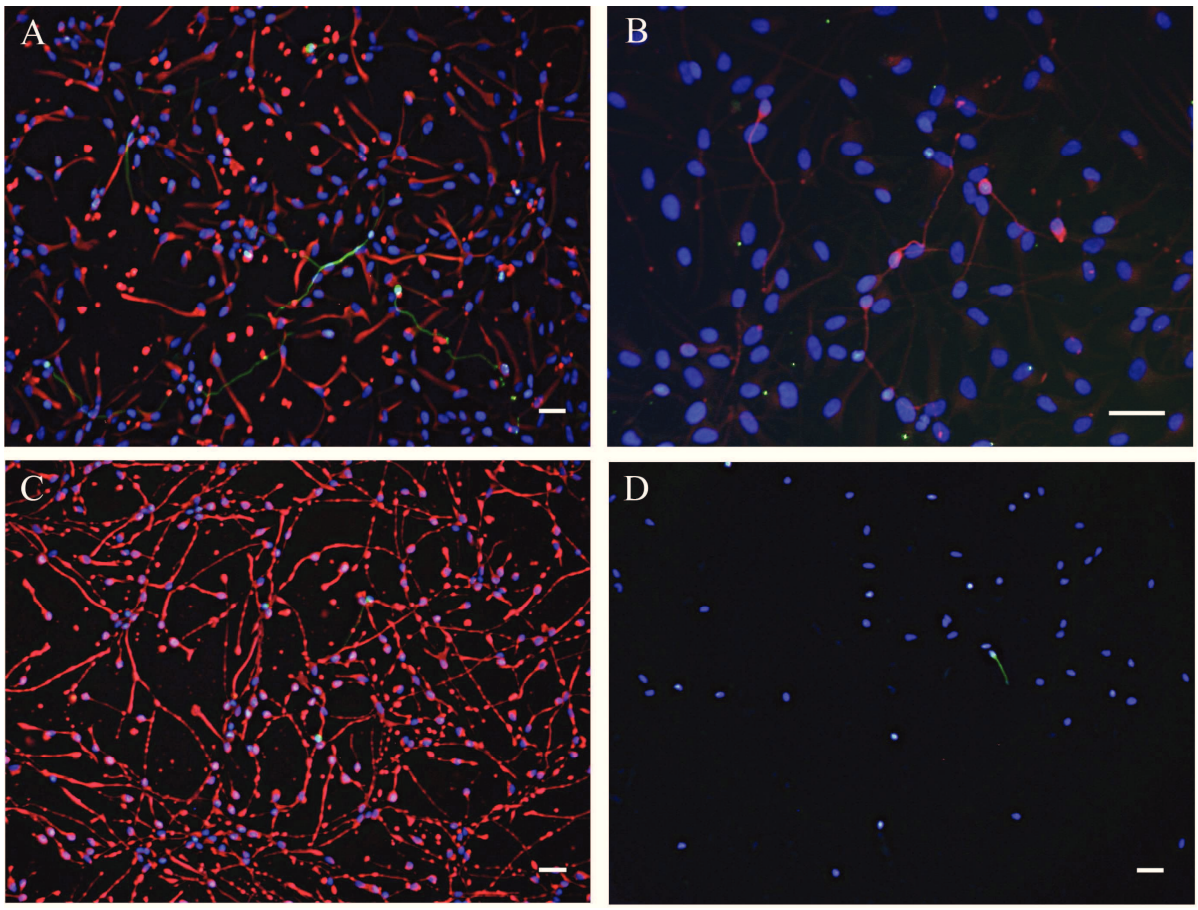

Fig. 12: Immunocytochemistry of recovered hNPCs at 4dd and 7dd stained against ßIII-tubulin and GFAP. Scale 20 nm. **A:** recovered at 4dd, ßIII-tubulin (green) / GFAP (red); **B:** recovered at 4dd, ßIII-tubulin (red); **C:** recovered at 7dd ßIII-tubulin (green) / GFAP (red); **D:** recovered at 7dd ßIII-tubulin (green). More neuronal cells adhered when recovered at 4dd.

This method provided access to an analysis of the cells by flow cytometry. Therefore the scaffolds were mechanical disrupted and cells were released by the same method to produce a single cell solution. Fig. 13A shows an example of a flow cytometry analysis to determine the amount of neuronal cells. Unstained cells were used as negative control, to set the gate (black frame, Fig. 13A) for the subsequently analysis of the amount of different marker e.g. HuC/D. To quantify the percentage of positive cells the same gate, set in the negative control, was used. Positive cells appear in the right part of the x-axis, where also intermediate population in 3D scaffolds was observed (blue frame), and most likely representing debris of cells.
The comparison of manual counted cells and cells counted by flow cytometry of ßIII-tubulin revealed a much higher proportion of positive cells, where the time dependency of the number of ßIII-tubulin^{+} was comparable, indicating the reliability of the flow cytometry protocol (Fig. 13B).

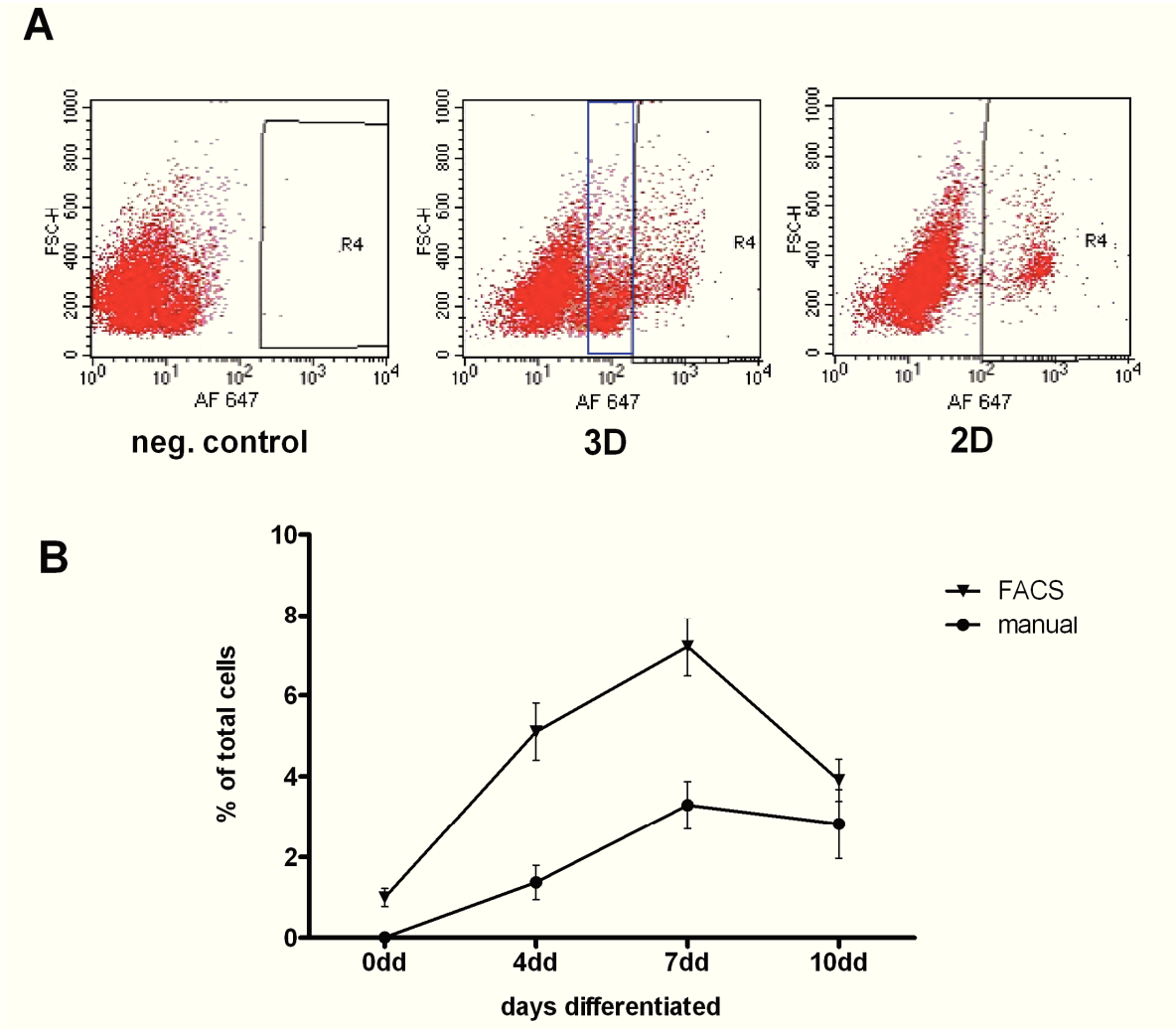

Fig. 13: Principle of flow cytometry analysis with hNPCs. A: Pictures show negative control with the secondary antibody Alexa Fluor 647 and the hNPCs, cultured in 2D and 3D scaffolds (PML), stained with HuC/D and the Alexa Fluor 647. Black gate demonstrate positive cells, blue gate intermediate population of cells. **B:** Mean ± SEM. Comparison of manual counted ßIII-tubulin+ with flow cytometry counted positive cells, time dependency was comparable.

Depending on the results of the immunocytochemistry quantification the time points 4, 7 and 10 days of differentiation were assessed for further experiments (4dd, 7dd, 10dd). The time points 1dd and 3dd were additional reviewed to compare the results with the usually used cultivation of hNPCs as adherent monolayer, where the peak of ßIII-tubulin positive cells is between 3dd and 4dd. First the amount of ßIII-tubulin$^+$ cells in the standard 2D culture system and in 3D scaffolds was compared (Fig. 14A). The expression of ßIII-tubulin was significant higher in hNPCs cultivated in 3D scaffolds at all time points especially at 7 and 10 days and with the highest amount at 7 days (7.03 ± 0.76 %). The comparison 2D vs. 3D shows that the peak of ßIII-tubulin shifts from 4dd (2D: 2.99 ± 0.45 %) to 7dd (3D: 7.03 ± 0.76 %), where a 2.4 fold higher amount was found compared to 2D cultivated cells.

As a second neuronal marker the expression of HuC/D was analysed. The expression of HuC/D was significant higher at 7 days in 3D scaffolds (2D: 2.33 ± 0.67 %; 3D: 5.55 ± 0.59 %) and lower at 1 day in 3D scaffolds (2D: 2.59 ± 0.34 %; 3D: 0.72 ± 0.38 %). The peak of HuC/D expression was after 4dd in 2D culture and 3D scaffolds (2D: 5.84 ± 0.58 %; 3D: 7.08 ± 1.07 %; Fig. 14B). Comparison with ßIII-tubulin shows that the expression of HuC/D starts earlier than ßIII-tubulin in 2D cultivation and was significant higher than ßIII-tubulin at 0dd, 1dd and 3dd (Fig. 14A, B). In 3D cultured cells the expression of HuC/D peaked earlier than ßIII-tubulin as well, but was not significant higher as ßIII-tubulin.

In addition to the neuronal markers GFAP was used to determine cells with a glial phenotype (Fig. 14C). The comparison 2D vs. 3D shows a significant lower expression of GFAP at 3dd, 7dd and 10dd in 3D scaffolds (3dd: 1.12 fold, 7dd: 1.13 folds, 10dd: 1.24 folds; Fig. 14C). The amount of GFAP positive cells in proliferated cells (0dd) was found to be comparable between the 2D and 3D culture system (2D: 91.47 ± 2.21 %; 3D: 91.35 ± 1.7 %).

Flow cytometry of PSA-NCAM, a marker for neuronal progenitor cells, was done to prove if the increase of ßIII-tubulin is based on a higher progenitor pool (Fig. 14D). The comparison between 2D cultures and 3D scaffolds showed a significant increase of PSA-NCAM in 3D scaffolds (2D: 5.17 ± 1.56 %; 3D: 41.33 ± 11.74 %). Comparing the expression of PSA-NCAM with the expression of ßIII-tubulin (Fig. 14A), it is noticed that there is a huge difference between the amounts of the markers. Nearly 40 % of the cells were positive for PSA-NCAM but only about 8 % of the hNPCs become positive for ßIII-tubulin.

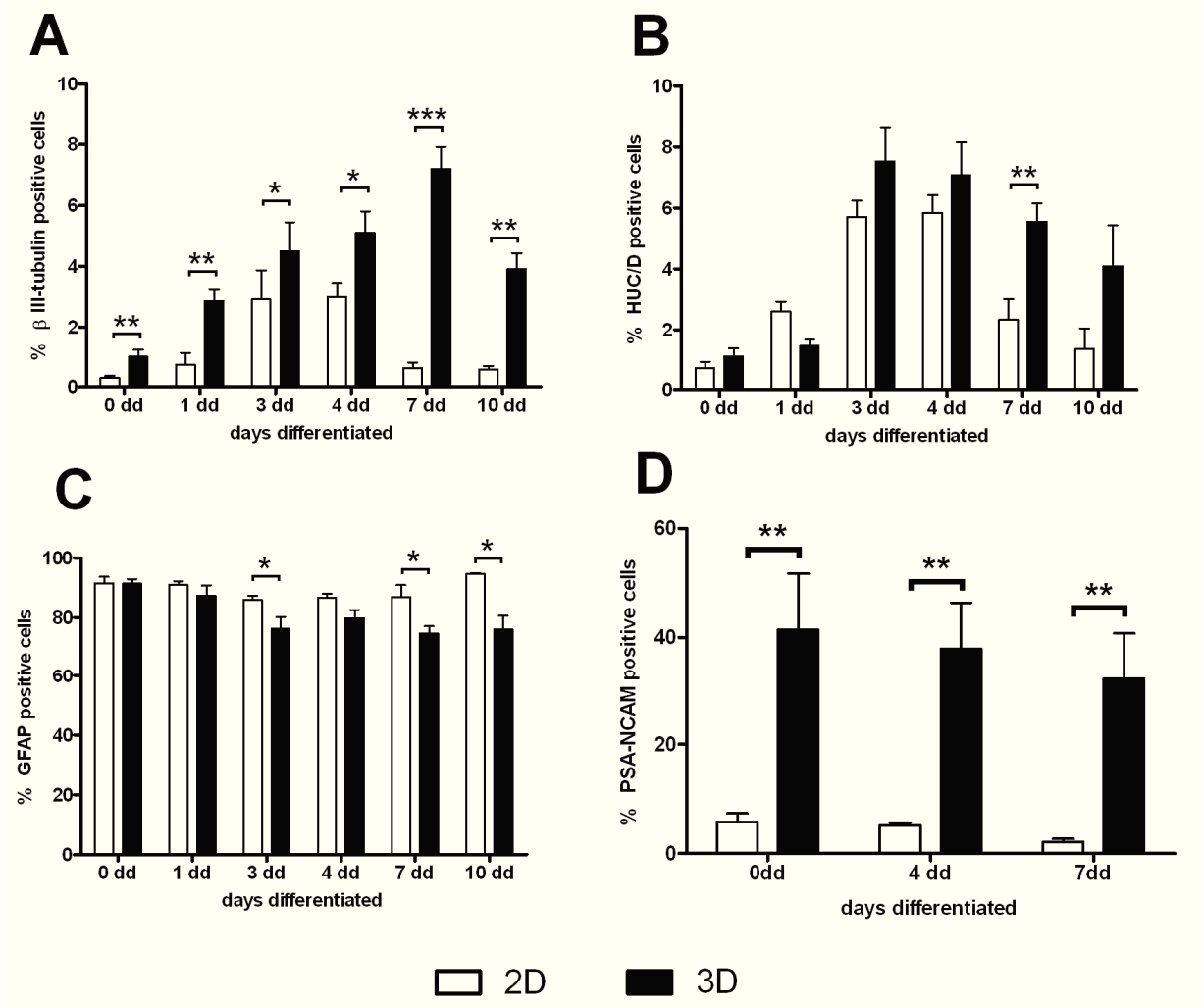

Fig. 14: Flow cytometry analysis of hNPCs cultivated in 2D and 3D scaffolds (PML). Mean ± SEM. **A:** Significant increase of ßIII-tubulin$^+$ cell in 3D scaffolds, **2D:** N = 6-13, **3D:** N = 7-12; **B:** Significant increase of HuC/D$^+$ cells in 3D scaffolds at 7dd, **2D:** N = 3-8, **3D:** N = 4-14; **C:** Significant decrease of GFAP$^+$ cells in 3D scaffolds at 3dd, 7dd, 10dd, **2D:** N = 3-7, **3D:** N = 4-9; **D:** Significant increase of PSA-NCAM$^+$ cells in 3D scaffolds, **2D:** N = 5-11, **3D:** N = 5. *, ** and *** indicates significant differences 2D to 3D.

4.1.3. Apoptosis of hNPCs in 3D scaffolds (PML)

As the neuronal population of the hNPCs seem to survive longer in the PuraMatrix-scaffolds (Fig. 14A) the rate of apoptosis was examined in the 2D culture and PML 3D scaffolds. In a first set of experiments the ratio of apoptotic events was investigated using a TUNEL-Assay (Fig. 15). The TUNEL-Assay is a common method for detecting DNA fragmentation, which is a consequence from apoptotic signalling cascades. The presence of nicks in the DNA can be identified by terminal deoxynucleotidyl transferase. This enzyme catalyzes the addition of labelled dUTPs. Also cells with severed DNA damage are labelled. For the TUNEL-Assay

the hNPCs were differentiated up to 10 days and subsequently released from the matrices as described above (3.2.5.). The amount of TUNEL-positive cells of 3D scaffolds was compared to the amount of positive cells found in the standard 2D culture.

In 2D cultivated cells a high increase of apoptotic events was detected over time, with the highest amount after 10 days (74.86 ± 9.28 %; Fig. 15). In 3D scaffolds cultivated cells the number of positive cells was always lower in comparison to 2D cultured cells and the increase of TUNEL-positive cells was less steep over time. The comparison of the number of apoptotic cells in the 2D and 3D cell culture system showed a significant lower rate of apoptosis in the 3D scaffold after 4, 7 and 10 days (Fig. 15).

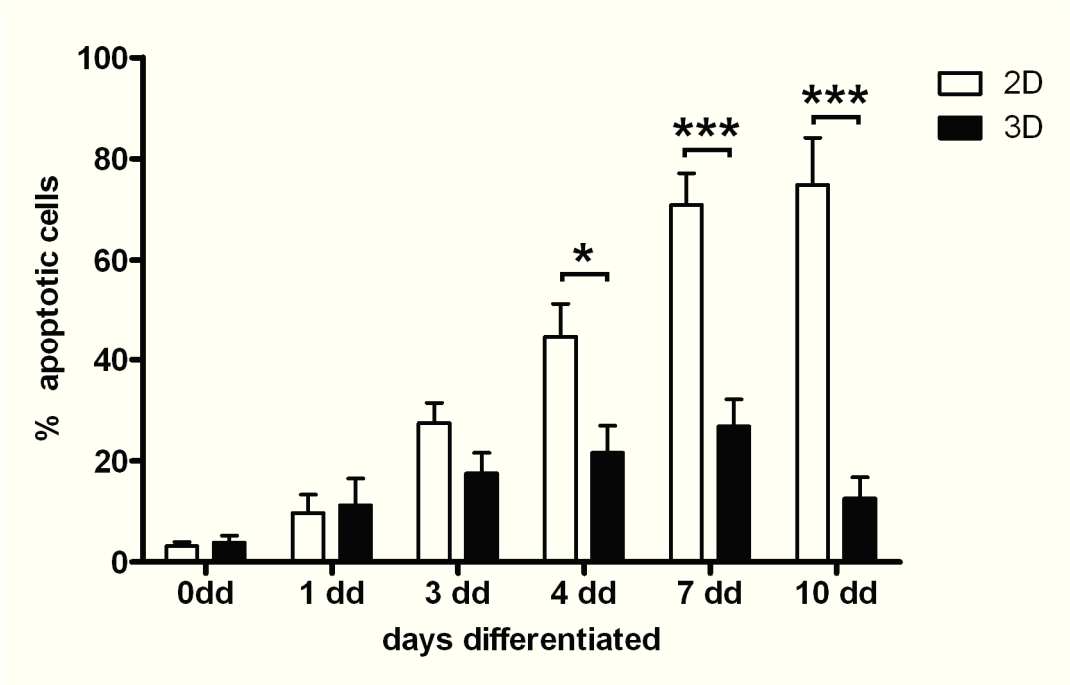

Fig. 15: TUNEL-Assay of hNPCs cultured in 2D monolayer and 3D scaffolds. Mean ± SEM. **2D:** white bars, N = 5-12, **3D:** black bars, N = 5-10. * and *** indicates significant differences 2D to 3D. Increase of apoptotic cells during differentiation up to 10 days is shown for 2D. Compared with 3D scaffolds significant differences were found.

As the TUNEL-Assay marks cells at different states of apoptosis and shows only cells within ongoing apoptosis with DNA damage but not the state of apoptosis, another assay had to be used to determine cells in the early and late state of apoptosis. The Annexin V staining can identify apoptosis at very early states of apoptosis in comparison to assays based on nuclear changes. In combination with the vital dye propidium iodide cells could discriminate between early or late apoptosis and necrotic cells. Therefore a double staining of Annexin-V and

propidium iodide was used for the next experiments. Quantification of early apoptotic cells in the hNPC population revealed an increase in both conditions during differentiation, but the amount of cells was not significantly different between cells cultured in the 2D system and 3D scaffolds (Fig. 16A).

The quantification of late apoptotic cells revealed an increase up to 7 days differentiation for 2D cultured cells (Fig. 16B). A higher proportion of cells in the late apoptosis were observed in the 2D culture compared to the 3D culture system. A significant change was found at 1dd, 4dd, 7dd and 10dd, with a fold change from 1.7 at 1dd to 2.4 at 10dd.

The population of necrotic cells was not quantified because dead cells lost the adherence to the surface in 2D culture and washed away during media change, which underestimate the real number. In 3D culture all cells dead or alive were cleaved in the scaffold. Further the necrotic cells in 3D scaffolds show no significant differences at all time points. Therefore no comparison with 2D culture of the necrotic cells was done.

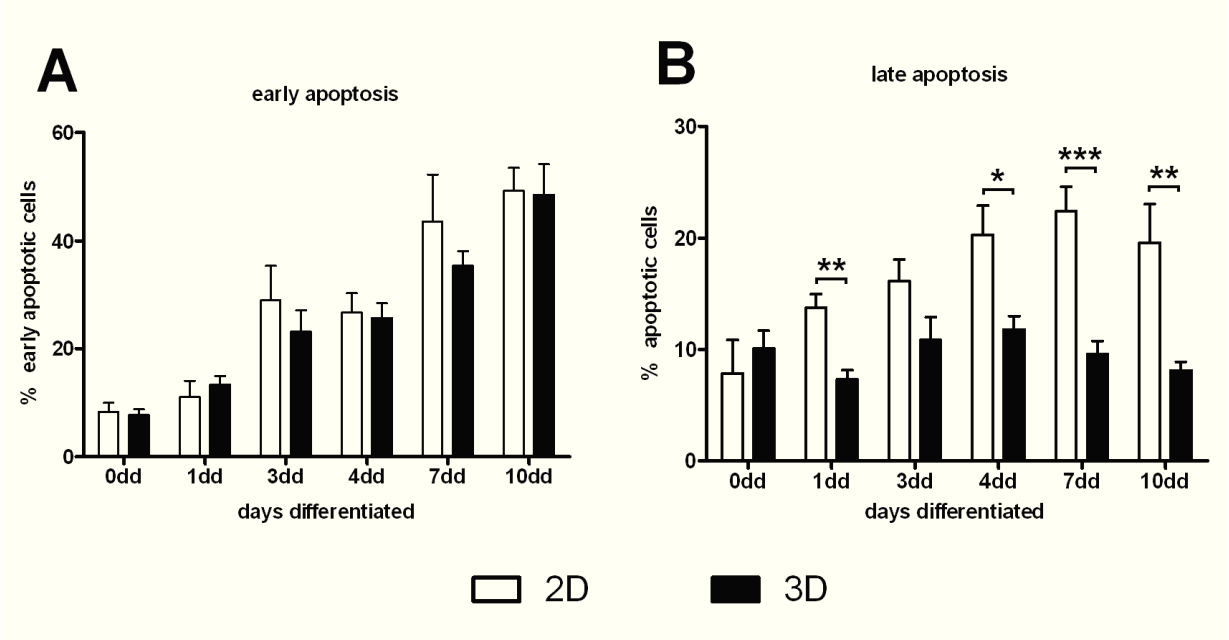

Fig. 16: Double staining of FITC coupled Annexin-V and Propidium Iodide in 2D culture and 3D scaffolds analysed via flow cytometry. Mean ± SEM. **2D:** white bars, N = 4-6, **3D:** black bars, N = 3-5. *, ** and *** indicates significant differences 2D to 3D. **A:** early apoptosis. No difference between 2D and 3D scaffolds was observed. **B:** late apoptosis. A significant lower number of apoptotic cells were determined in 3D scaffolds.

The above described experiments, of monitoring the survival and apoptotic events in 2D- and 3D cultures, contained all populations of cells, regardless of their phenotype. To study in which amount the neuronal cell population was affected by apoptosis, a TUNEL-Assay was performed in combination with ßIII-tubulin stained cells (Fig. 17). Quantification revealed

that cells cultured in monolayer showed an increase of apoptotic neurons over 7 days up to 70 % (Fig. 17). Regarding the whole population of the cells (Fig. 15) there was no difference. The apoptotic events of neuronal cells in 3D scaffolds (Fig. 17) were higher than in the whole population (Fig. 15). Compared with 2D the hNPCs in 3D scaffolds show a higher rate of apoptotic neurons up to 4 days differentiated, with a significant increase at 3dd. But they seem to survive longer, because only few ßIII-tubulin positive cells were left after 7 days of differentiation in the 2D culture, where in 3D scaffolds the highest number of neurons was found after 7 days of differentiation (Fig. 14A).

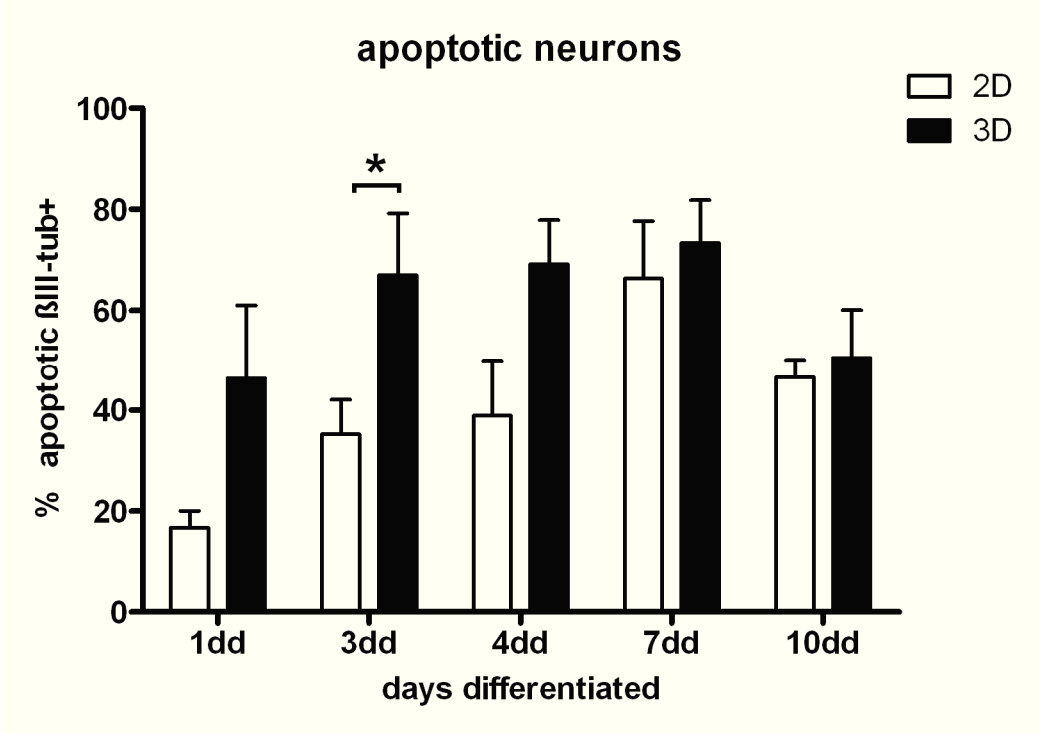

Fig. 17: Combination of TUNEL-Assay and ßIII-tubulin staining shows apoptotic neurons of hNPCs in 2D culture and 3D scaffolds. Mean ± SEM. **2D:** white bars, N = 3-6, **3D:** black bars, N = 4-7. * indicates significant differences 2D to 3D. A significant increase at 3dd in 3D scaffolds was found.

Based on the results of the TUNEL-Assay and Annexin V – PI double staining further investigation were done to study apoptotic processes. As a most likely possibility the amount of the anti-apoptotic protein Bcl-2 was analysed by means of flow cytometry. Bcl-2 plays a crucial role in the regulation of the formation of MAC, where the formation of MAC is hindered, resulting in prevention of cytochrome c release and apoptosis. Fig. 18 show the quantification of the Bcl-2 amount of the hNPCs differentiated in 2D culture and PML 3D scaffolds. The Bcl-2 expression of hNPCs in 2D culture started with a low amount and

increases during differentiation with the highest amount at 4dd (15.99 ± 2.87%). After 4 days the Bcl-2 amount decreases up to 10dd. The hNPCs in 3D scaffolds started with a high concentration of Bcl-2 at 0d (9.13 ± 3.62%). Than increases during differentiation to the highest concentration at 4dd (26.90 ± 7.50%) and was more or less stable up to 10dd. The comparison of the Bcl-2 concentration in 2D culture and 3D scaffolds showed always a higher amount in 3D scaffolds. Where a significant higher amount was found in 3D scaffolds at 0, 7 and 10 days of differentiation compared to 2D cultivated cells (Fig. 18).

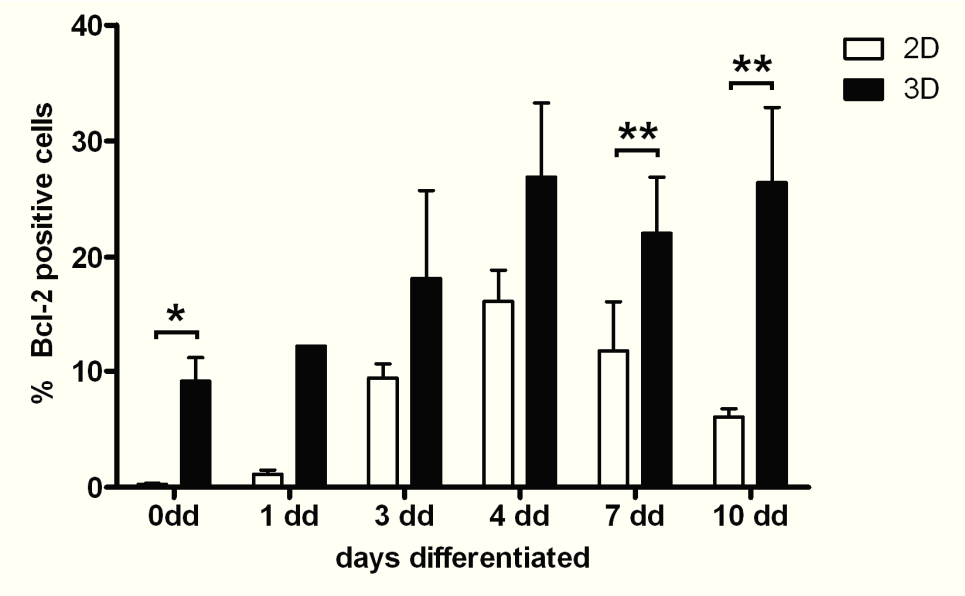

Fig. 18: Flow cytometry of Bcl-2 in hNPCs in 2D culture and 3D scaffolds. Mean ± SEM. **2D:** white bars, N = 3-6, **3D:** black bars, N = 3-6. * and ** indicates significant differences 2D to 3D. An increased Bcl-2 expression in 3D-scaffolds is shown with significant differences at 0dd, 7dd and 10dd.

Based on the finding of decreased apoptotic rate in 3D scaffolds I was next interested in the mechanism underlying this effect. The highest significant difference in apoptotic events was detected at 7dd and 10dd (Fig. 15). From previous apoptotic studies of this cell line in 2D culture is known that the expression change of apoptotic key factors started at early time points after induction of differentiation (Jaeger, 2010). Maybe 7dd are too late for 2D cultured cells. The time point 1dd could be too early for 3D cultured cells based on remaining growth factors which could not washed out before starting the differentiation. Because the highest number of ßIII-tubulin positive cells in 2D was found at 4dd and at 4dd the significant

differences of apoptotic cells between both culture conditions starts, 4dd seem to be optimal to determine the regulation of apoptosis. Several apoptotic markers were tested via Western Blot for hNPCs cultured in 3D scaffolds and 2D cultures (Fig. 19). The amount of Bax, as a pro-apoptotic marker, Caspase-3, PARP-1, the anti-apoptotic marker XIAP and Survivin were examined. Caspase-3 is an effector caspase and is activated via proteolytic cleavage. Caspase-3 (35 kDa) was detected in proliferated and differentiated hNPCs in 2D and PML 3D scaffolds. The quantification of the line intensity revealed that the expression of Caspase-3 was increased in differentiated cells. The 3D scaffolds show a lower increase, but no significant difference was detected between differentiated cells of 2D and 3D cultures.

The *Poly(ADP-ribose)-Polymerase-1* (PARP-1) was detected as a 116 kDa line in proliferated and differentiated hNPCs in 2D culture. In 3D scaffolds the expression of PARP-1 was lower and only tracks could detect in differentiated hNPCs. The quantification of line intensities shows that the expression of PARP-1 was increased in differentiated hNPCs in 2D culture. In 3D scaffolds no difference between proliferated and differentiated hNPCs was found. Comparison of 2D culture and 3D scaffolds relieved a significant decrease in 3D scaffolds during differentiation.

The expression of the *X-linked inhibitor of apoptosis protein* (XIAP), with a size of 57 kDa, was found in proliferated and differentiated hNPCs in both culture systems. The quantification of line intensities showed an increase of the XIAP expression in differentiated hNPCs. This first result indicates that XIAP is higher increased in differentiated hNPCs cultured in PML 3D scaffolds, without significant differences. The 21 kDa protein Bax could be detected in proliferated and differentiated cells. Additional a second smaller line 18 kDa known as a fragment of Bax was detected in some samples of differentiated cells in PML 3D scaffolds (Fig. 19). Quantification of the 21 kDa protein shows no difference between both cultivations (Data not shown). At last the 16 kDa protein Survivin, a member of inhibitors of apoptosis (IAP), was analysed. It was highly present in proliferated hNPCs in 2D and was decreased in differentiated hNPCs of the 2D culture. In 3D scaffolds the hNPCs expressed Survivin in lower amount, where in proliferated cells always a small line of Survivin was present, in differentiated cells only some samples showed tracks of Survivin (Fig. 19).

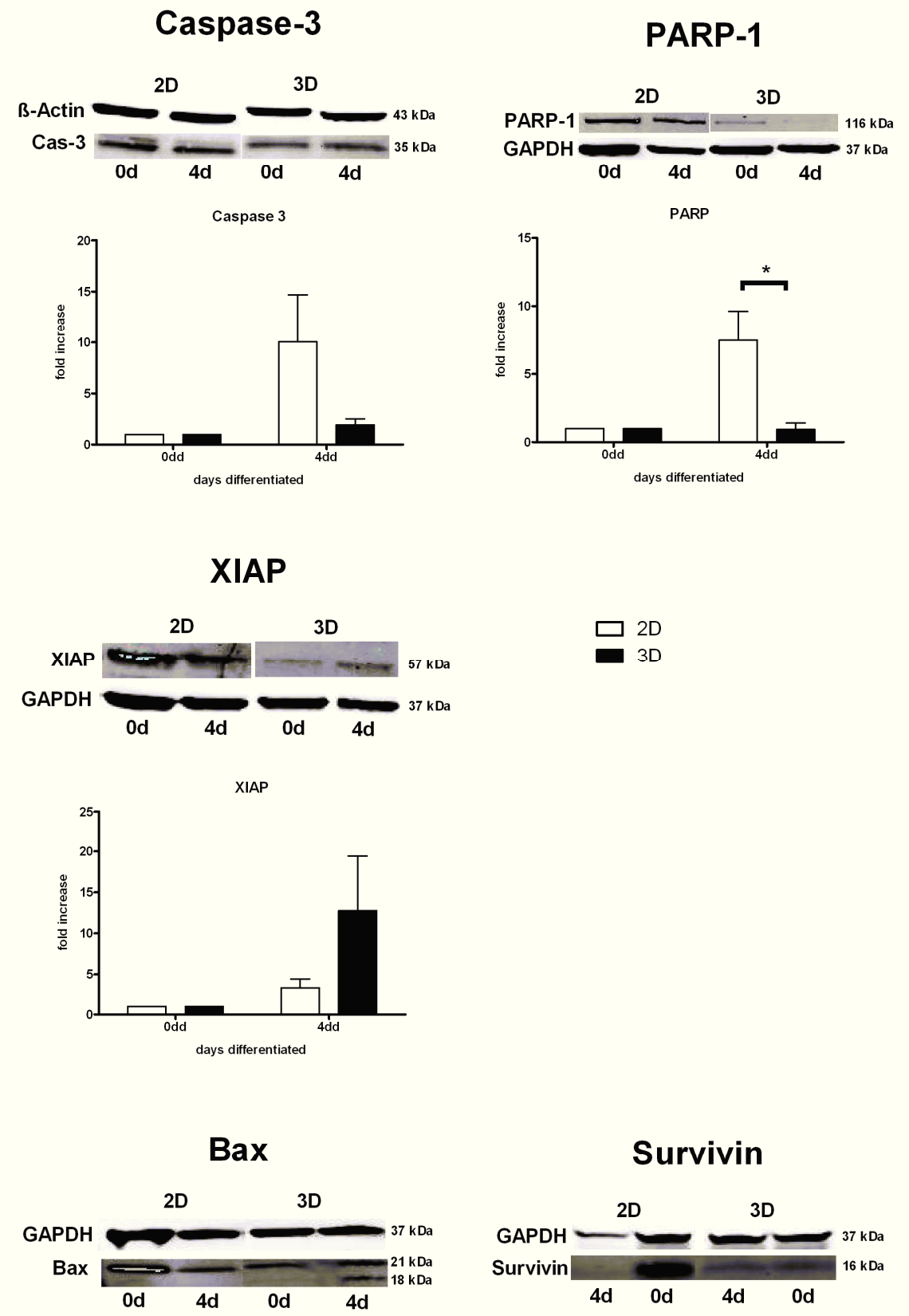

Fig. 19: Western Blot of apoptotic marker expression of two time points (0 days and 4 days differentiated) in hNPCs cultivated in 2D culture and 3D scaffolds. Lines and quantification of the line intensities related to the internal standard GAPDH or ß-Actin. Normalized to 0 days. White bars indicate 2D cultures, black bars 3D cultures. Mean ± SEM. * indicates significant differences 2D to 3D. **Caspase-3** 2D N = 4, 3D N = 3. **PARP-1** 2D N = 6, 3D N = 4. **XIAP** 2D N = 7, 3D N = 4. Compared with 2D culture a decrease of Caspase-3 and PARP and increase of XIAP is shown.

4.2. Cultivation of hNPCs in modified 3D scaffolds

4.2.1. Growth and differentiation of hNPCs in modified 3D scaffolds

In the second part of experiments modified PuraMatrix formulations, provided by BD Bioscience, were used to study the differentiation of hNPCs. The modified PuraMatrix formulations contain incorporated functionally modified peptide sequences to alter the functionalisation of the scaffolds. Two altered formulations of PuraMatrix were used.

1) **PM-SDP:** The SDP-peptide (Ac-$(RADA)_4$-GGSDPGYIGSR-NH_2) is a cell adhesion motif of laminin, promoting cell adhesion and extensibility of neural cells (Gelain et al., 2006).
2) **PM-PFS:** The PFS-peptide (Ac-$(RADA)_4$-GGPFSSTKT- NH_2) is a motif of the bone marrow homing factor shown to improve the differentiation of neural stem cells and extension of neural cells (Gelain et al., 2006).

The hNPCs were cultured in the modified matrices accordingly to the above-mentioned procedure (3.2.1.2.). The unmodified pure PuraMatrix scaffold was used as control to detect if the modifications results in increased attachment or differentiation. Fig. 20 shows hNPCs cultured in 3D scaffolds of PM, PM-SDP and PM-PFS. The cells proliferated for 7 days and were subsequently differentiated for 7 days. The hNPCs grow in PuraMatrix and modified PuraMatrix formulation in spheroid likes densely packed cell aggregates with sporadically 3-dimensional loosely composed cellular structures (Fig. 20A, C, E). The spheroids like structures are mostly less compact and smaller than typical neurospheres after 7 days of proliferation. The cells within all scaffolds mostly hold the spheroid like structure during proliferation and no visual difference could be detected between the three conditions. Upon induction of differentiation, one can see morphological changes and outgrowing processes. Differentiated cells build networks with other cells and cell aggregates (Fig. 20B, D, F).

Fig. 20B, D and F show immunocytochemistry staining against ßIII-tubulin after 4 days of differentiation. Expression of the neuronal marker ßIII-tubulin was observed in all three conditions, where an impressively higher amount of processes and cell bodies was observed in matrices consisting of PM-PFS and PM-SDP (Fig. 20D, F). The hNPCs build a dense network of outgrowths between different spheroids in the modified scaffolds PM-SDP and PM-PFS (Fig. 20D, F), but especially in scaffolds with the PFS-peptide (Fig. 20F). Further in parts with higher amounts of spheres and lower distances of the spheres the connection

between different spheres seem to be increased (Fig. 20F). The amount of ßIII-tubulin between 4dd and 7dd evidence no difference (data not shown).

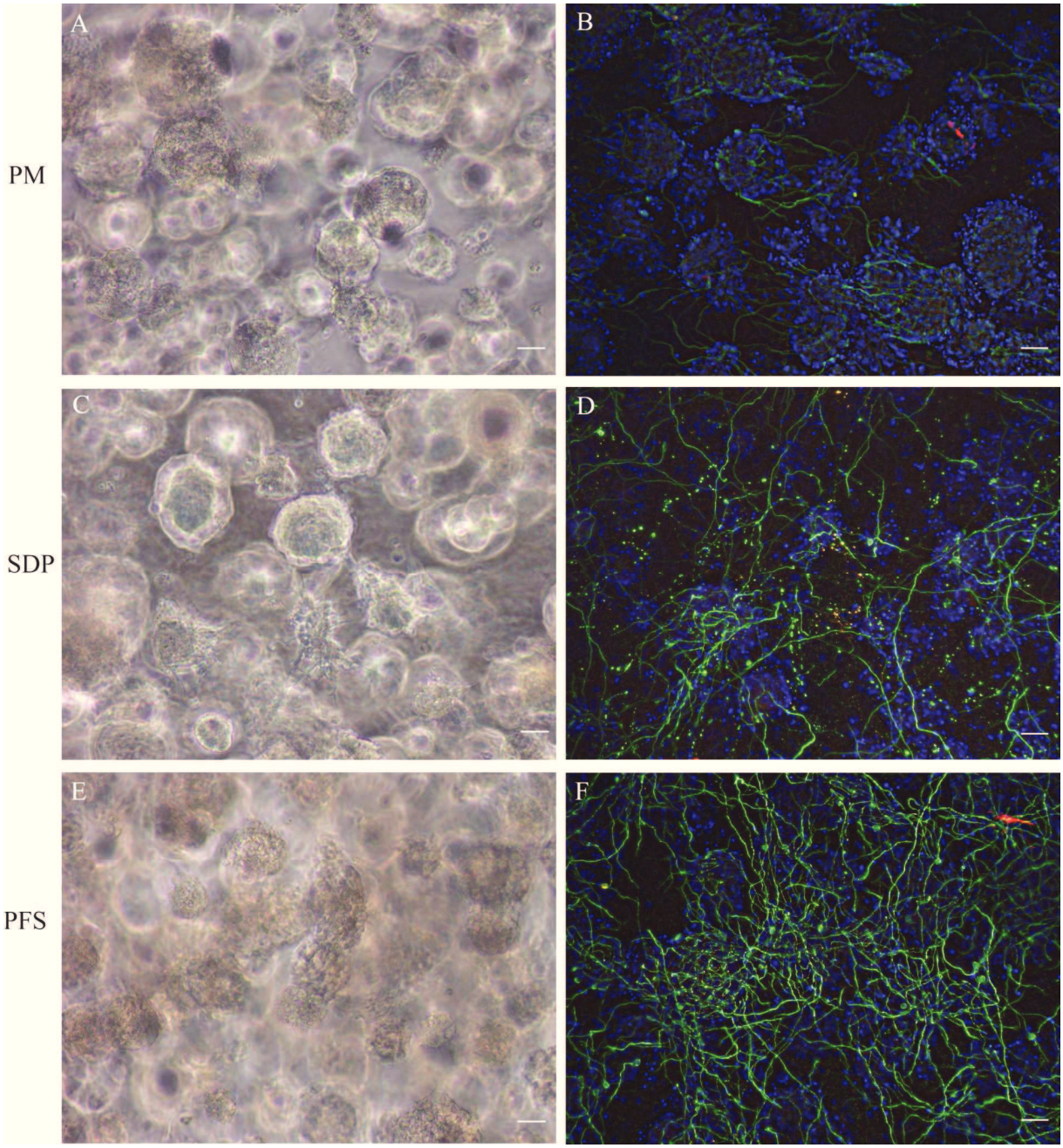

Fig. 20: The hNPCs proliferated and differentiated in 3D scaffolds of PuraMatrix and modified PuraMatrix formulations. Scale 50 nm. **PM:** PuraMatrix, **PM-SDP:** PM modified with peptide sequence of the laminin, **PM-PSF:** PM modified with peptide sequence of the bone marrow homing factor. **A, C, D:** Phase contrast pictures of proliferating cells. Spheroid like growth patterns of hNPCs were observed in all scaffolds; **B, D, F:** Immunocytochemistry pictures, 4dd, ßIII-tubulin (green) / TH (red). The distribution of cells within the matrix is shown by DAPI staining. One can observe an increased number of ßIII-tubulin^{+} cells in matrices consisting of PM-SDP and PM-PFS scaffolds.

Next the amount of the neuronal marker ßIII-tubulin, HuC/D, the glial marker GFAP and the marker for neuronal progenitor cells PSA-NCAM were quantified by means of flow cytometry. The comparison of PuraMatrix vs. the modified PuraMatrix formulations revealed significant higher numbers of ßIII-tubulin positive cells in the modified matrices at all time points (Fig. 21A). Whereas the PM-PFS scaffolds show the highest increase. All conditions show an increase with the highest amount at 10 days (PM: 8.36 ± 1.65 %, SDP: 19.01 ± 4.29 %; PFS: 25.07 ± 2.66 %). The HuC/D expression showed a little higher amount in the modified scaffolds at 4 days of differentiation, but no significant changes compared with the PM scaffold could be detected (Fig. 21B). Except in the PM-PFS scaffold a significant increase was determined at 7 days. The higher amount in PM-SDP scaffold at 10dd was not significant. →

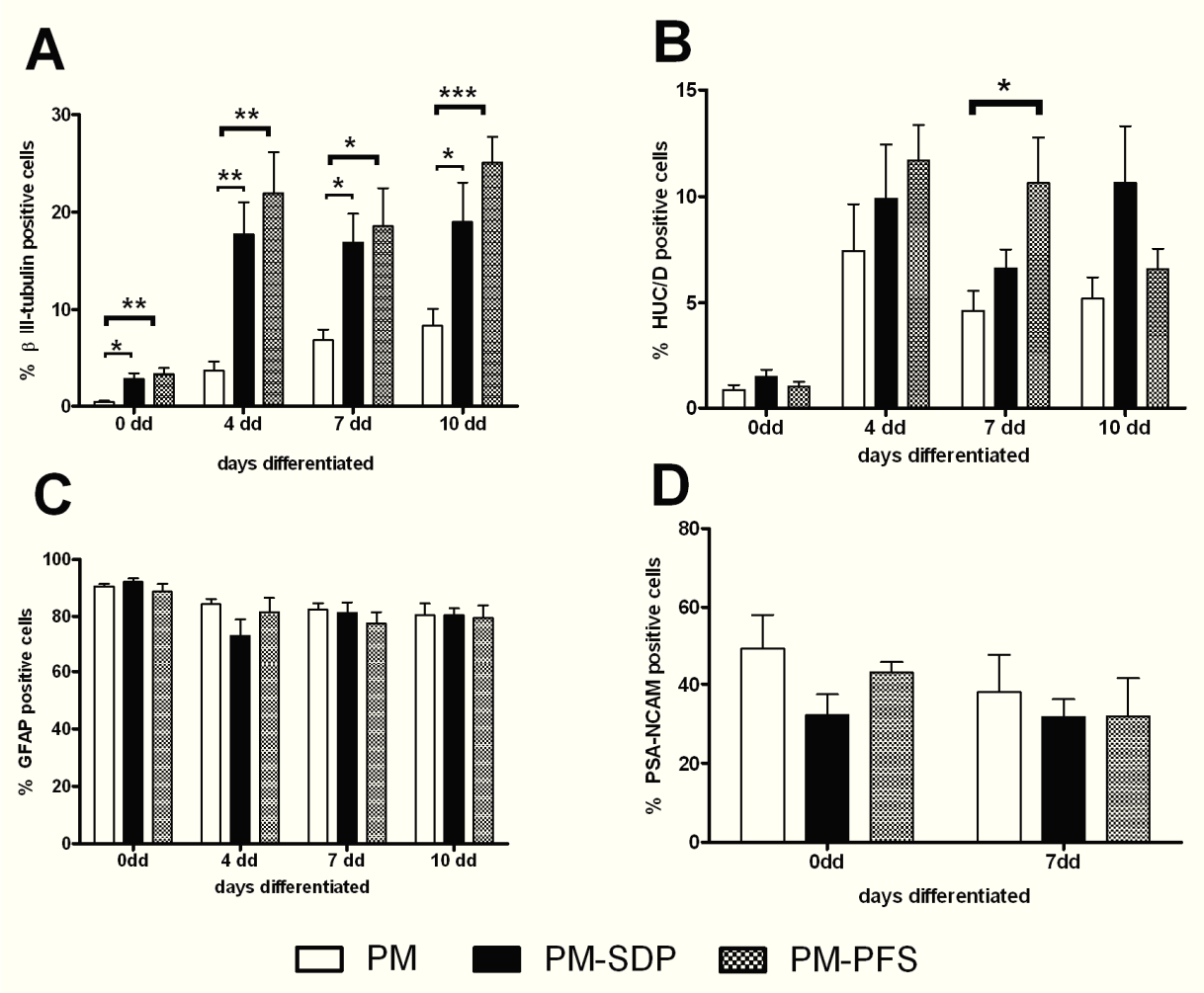

Fig. 21: Flow cytometry analysis of neuronal markers in hNPCs cultivated in PuraMatrix and modified PuraMatrix formulations. White bars indicate PM scaffolds; black bars PM-SDP scaffolds, doted bars PM-PFS scaffolds. Mean ± SEM. *, ** and *** indicates significant differences PM to mod. PM. **15A** ßIII-tubulin **PM:** N=7-8, **PM-SDP:** N = 8-10, **PM-PFS:** N = 6-9; **15B** HuC/D **PM:** N = 8-10, **PM-SDP:** N = 7-9, **PM-PFS:** N = 5-10; **15C** GFAP **PM:** N = 5, **PM-SDP:** N = 4-6, **PM-PFS**: N = 5-7; **15D** PSA-NCAM N = 4. A significant increase of ßIII-tubulin^{+} at all time points and HuC/D at 7dd. Expression of GFAP and PSA-NCAM no significant differences were found.

Surprisingly the expression of GFAP show no significant differences compared with the PM scaffold (Fig. 21C). A little decrease was found in PM-SDP scaffolds at 4 days and PM-PFS at 7 days, but no significance was observed. The amount of GFAP-positive cells was between 73 % and 81 % in the modified scaffolds.
PSA-NCAM was used to determine if the progenitor pool of the hNPCs is changed when cultured in the modified 3D scaffolds and was mostly expected in proliferated cells. Either the ßIII-tubulin expression is high increased when hNPCs cultured in modified PM formulations, I was interested if the modified scaffolds have also an effect on the expression of PSA-NCAM in the hNPCs. The quantification shows the highest amount at zero days with a decrease in differentiation (Fig. 21D). The PSA-NCAM expression of hNPCs in the modified matrices show a trend of a small decrease at both time points compared to the PM scaffold, but no significant changes were observed.

As shown in Fig. 21, culturing of hNPCs in the modified 3D scaffolds resulted in a significantly higher amount of cells with a neuronal phenotype. In a subset of experiments I examined the influence of the modified matrix on the expression of synaptic proteins, as synapses are prerequisite for synaptic transmission between neurons.
Therefore immunocytochemical staining of hNPCs, encapsulated into modified scaffolds, against synaptic marker were done, using the presynaptic marker synaptophysin and the postsynaptic marker PSD95 (data not shown). The hNPCs showed no positive staining for both markers when cultured in monolayer. Experiments with encapsulated hNPCs inside 3D scaffolds have proven disadvantageous, because the auto-fluorescence of every cell in the 3D scaffold and the high number of cells inside the scaffold resulted in a high background preventing a clear determination of positive staining.

Recovering of hNPCs cultured in modified PM formulations and staining against the synaptic marker is shown in Fig. 22. Synaptophysin could not detect in the hNPCs neither in unmodified nor in modified PM formulations. The postsynaptic marker PSD95 was usually also not found in the hNPCs in 2D culture. This was also the case for the unmodified scaffold and the scaffold modified with the SDP-peptide. Staining with the PSD95 in PM-PFS scaffolds indicates few positive cells in the PM-PFS scaffolds. Fig. 22 shows PSD95 positive cells after culturing and differentiated in PM-PFS scaffolds and subsequently released of the scaffold after 4dd.

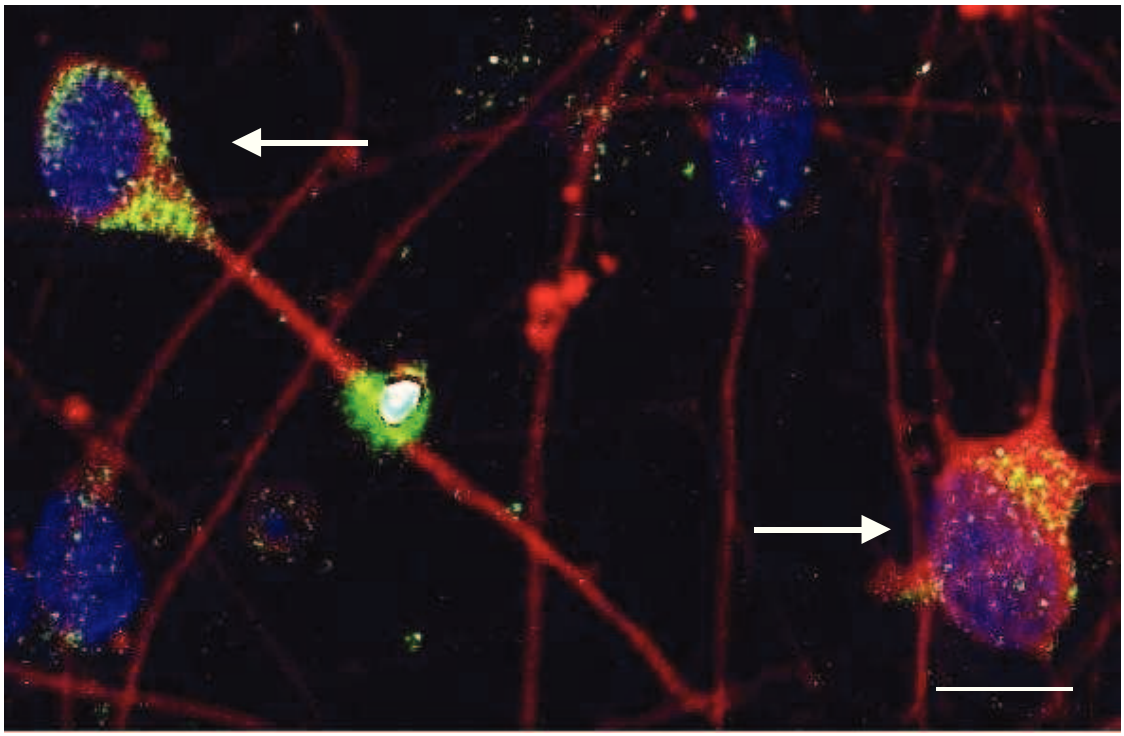

Fig. 22: Immunocytochemistry of recovered differentiate hNPCs from modified 3D scaffolds. Picture shows recovered hNPCs, which were differentiated 4 days in PM-PFS scaffolds and stained against PSD95 (green) and ßIII-tubulin (red). Scale 5 µm.

4.2.2. Survival and apoptosis of hNPCs inside modified 3D scaffolds

As demonstrated in 4.2.1. a significantly higher amount of neuronal cells was found in matrices consisting of modified PM formulations. To elucidate if these findings were based on increased differentiation or better survival of the cells, the rate of apoptosis was determined in the modified scaffolds. To evaluate the amount of apoptotic cells a TUNEL-Assay was performed with cells cultured in PM, PM-SDP and PM-PFS scaffolds. The quantification was done by flow cytometry where the whole population (Fig. 23A) as well as the neuronal population was examined (Fig. 23B). In all three types of scaffolds a bigger increase of apoptotic events was observed after 4 days of differentiation compared to 0d, followed by a small increase up to 10dd. The apoptosis of the hNPCs in both modified scaffolds was not significant different to PM scaffolds (Fig. 23A).

Fig. 23B shows the amount of apoptotic cells of the neuronal population of the hNPCs in the modified scaffolds. The apoptotic events were only in the population of neuronal cells higher than in the whole population of cells cultured in the modified scaffolds. An amount between 20 % and 30 % for all cells in the scaffolds was found, whereas between 60 % and 80 % apoptotic cells were found only for the neuronal population of hNPCs (Fig. 23A, B). The

amount of apoptotic neurons increases during differentiation in all three scaffolds. In the modified scaffolds a little lower number of apoptotic neurons were found, but based on the high variances of the experiments no significant decrease was observed (Fig. 23B).

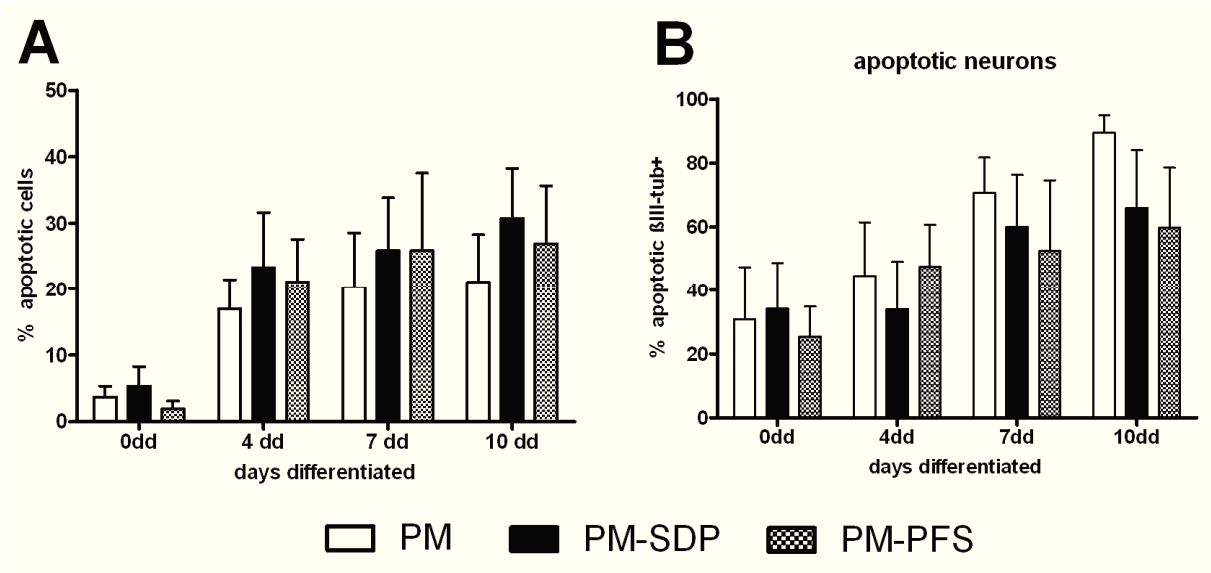

Fig. 23: Apoptosis of hNPCs in PuraMatrix and modified PuraMatrix formulations. White bars indicate PM scaffolds; black bars PM-SDP scaffolds, doted bars PM-PFS scaffolds. Mean ± SEM. **A:** TUNEL-Assay, **PM:** N = 3-5, **PM-SDP:** N = 4-5, **PM-PFS:** N = 3-5; **B:** TUNEL-Assay of ßIII-tubulin^{+} hNPCs, **PM:** N = 3-5, **PM-SDP:** N = 4-5, **PM-PFS:** N = 3-7. No significant differences were found in the modified PM scaffolds.

As the TUNEL-Assay marks cells at different state of apoptosis, a double staining of Annexin-V and propidium iodide was used to detect cells in early or late states of apoptosis. Fig. 24 shows the quantification of early and late apoptosis, as well necrotic cells of hNPCs cultured in PM, PM-SDP and PM-PFS scaffolds. The necrotic cells do not differ between the PM scaffold and the modified PM formulations. The number of cells in the early or late apoptosis was in all three conditions about 20 % after inducing differentiation (Fig. 24). Whereas the ratio of early and late apoptosis in PM scaffolds is more or less equal in PM scaffolds, in the modified PM formulations the amount of early apoptotic cells was slightly higher than the amount of late apoptotic cells. But significant differences could not be found (Fig. 24).

The apoptotic events in the modified PM formulation seem not to differ between the scaffolds compared to the PM scaffolds. The positive effect regarding the survival of the 3D scaffolds on the hNPCs, described in chapter 4.1.2. for the PML 3D scaffold, is also present in the modified PM scaffolds. An additional increased survival or a significant decreased survival was not found for the modified PM scaffolds.

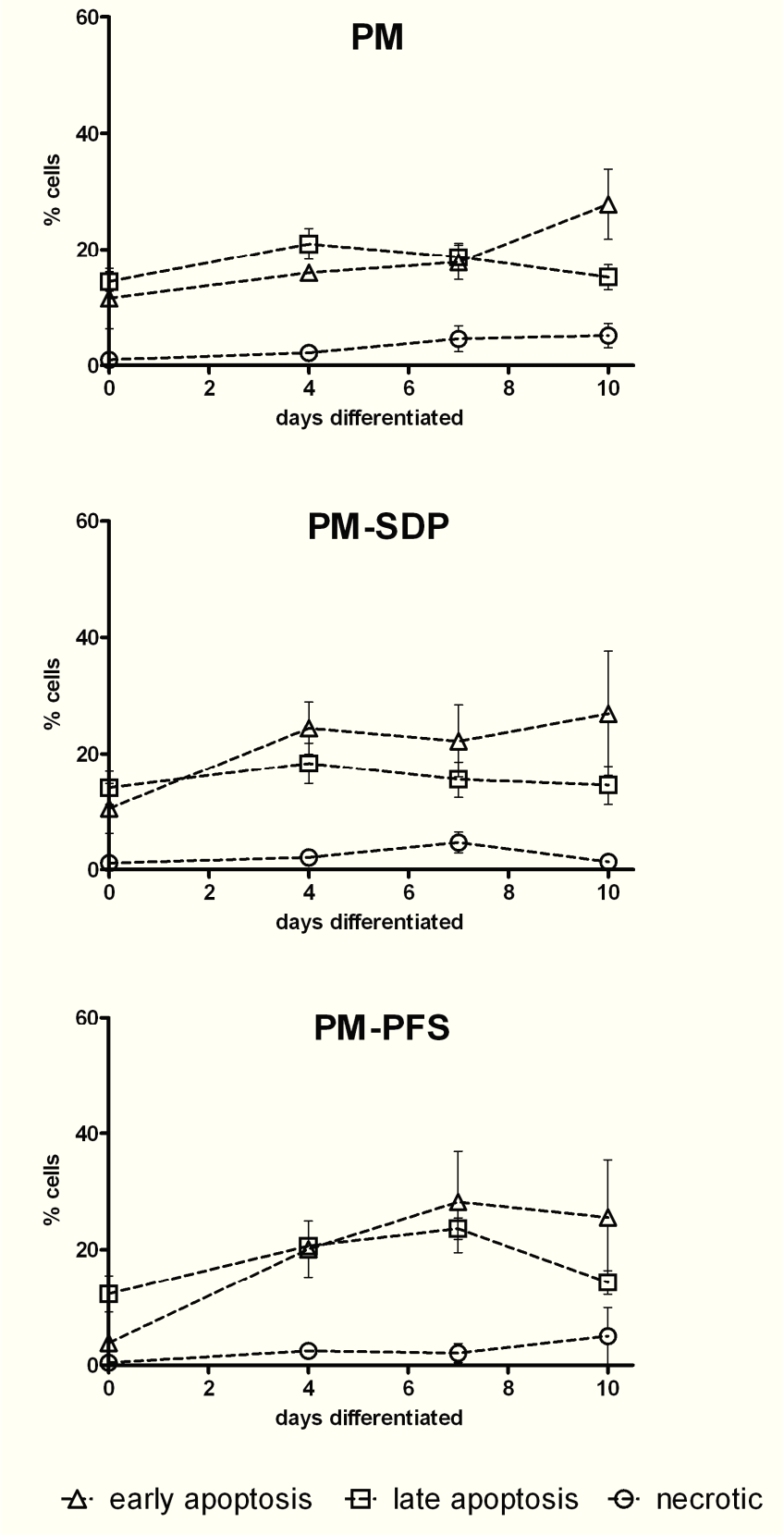

Fig. 24: Double staining of Annexin V and Propidium Iodide of hNPCs in PuraMatrix and modified PuraMatrix formulations. Triangle indicates early apoptosis, square indicates late apoptosis, and circle indicates necrosis. **PM** and **PM-SDP**: N = 4-5, **PM-PFS**: N = 3. No significant differences were found in the modified PM scaffolds.

In the last experiment, regarding apoptosis of hNPCs cultured in the modified PM scaffolds, the expression of the anti-apoptotic protein Bcl-2 was analysed. The modified PM formulation had as well a starting concentration at 0d, where the lowest concentration was found in PM-PFS scaffolds. The control and the PM-SDP scaffold showed an increase during differentiation with the highest amount at 4dd and a decrease up to 10dd. The Bcl-2 expression in PM-PFS scaffolds increases up to 7dd and at 10dd a small decrease was found. A slightly decrease of the Bcl-2 expression at 4dd was found in PM-PFS scaffolds compared to the control and the PM-SDP scaffold, but no significant differences were observed (Fig. 25).

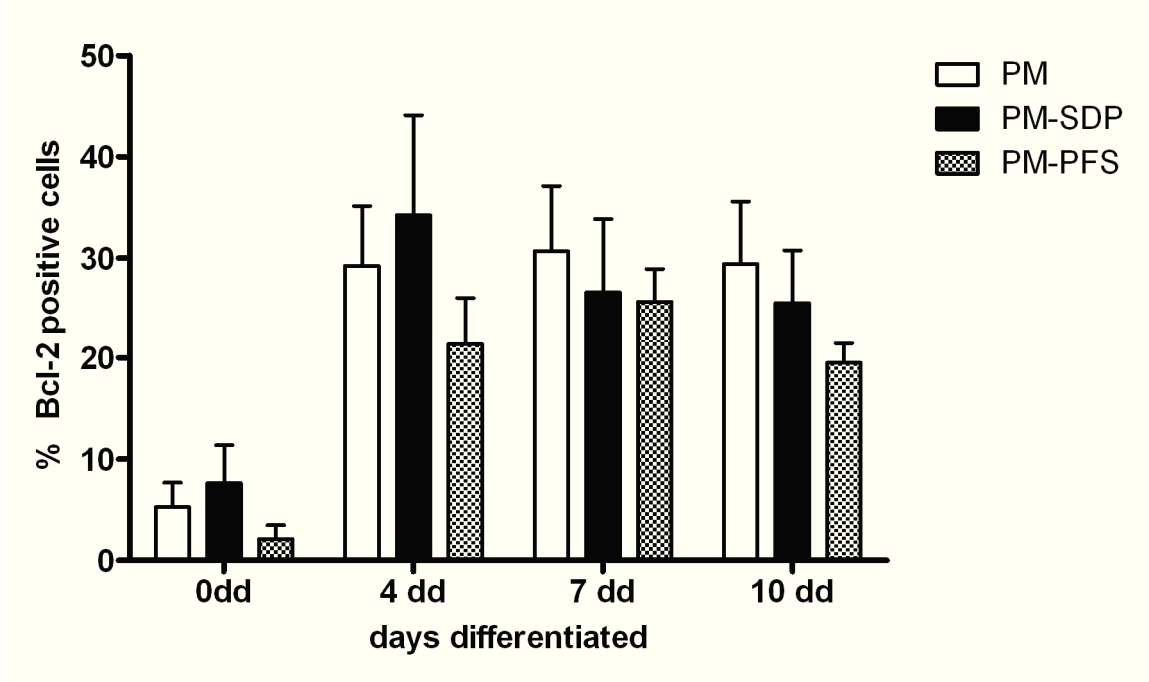

Fig. 25: Flow cytometry of Bcl-2 of hNPCs in PuraMatrix and modified PuraMatrix formulations. White bars indicate PM scaffolds; black bars PM-SDP scaffolds, doted bars PM-PFS scaffolds. Mean ± SEM. **PM:** N = 3-4, **PM-SDP:** N = 4, **PM-PFS:** N = 3-4. No significant differences were found in the modified PM scaffolds.

4.3. Effect of PFS peptide sequence on monolayer culture of hNPCs

The increased ßIII-tubulin expression of hNPCs encapsulated in the modified PM scaffold (Fig. 21) was the origin of the following set of experiments. As the highest amount of ßIII-tubulin was observed in PFS-scaffolds, experiments were done to study the effect of the PFS-peptide on hNPCs cultured as monolayer. Therefore a purified PFS peptide sequence (GGPFSSTKT) was used. This PFS-peptide sequence was added to the media of a 2D monolayer culture of hNPCs at different time points. The addition of the PFS-peptide

sequence to the sample results in a decreased attachment of the hNPCs as well proliferated and differentiated cells (Fig. 26B) compared to the control (Fig. 26A).

For the quantification of the neuronal marker ßIII-tubulin two conditions were tested. PFS-peptide supplemented during proliferation and differentiation (black bars) and only during the differentiation (doted bars). As control 2D culture of hNPCs without supplement was used (white bars). Regarding the amount of neuronal differentiated cells, a small decrease was found in both conditions compared to control, but no significant differences could observed (Fig. 26C). If the PFS-peptide was added only during differentiation no difference compared to the control was observed. A slightly higher amount of ßIII-tubulin was observed at 0 days for hNPCs proliferated with PFS-peptide, however this difference was not significant.

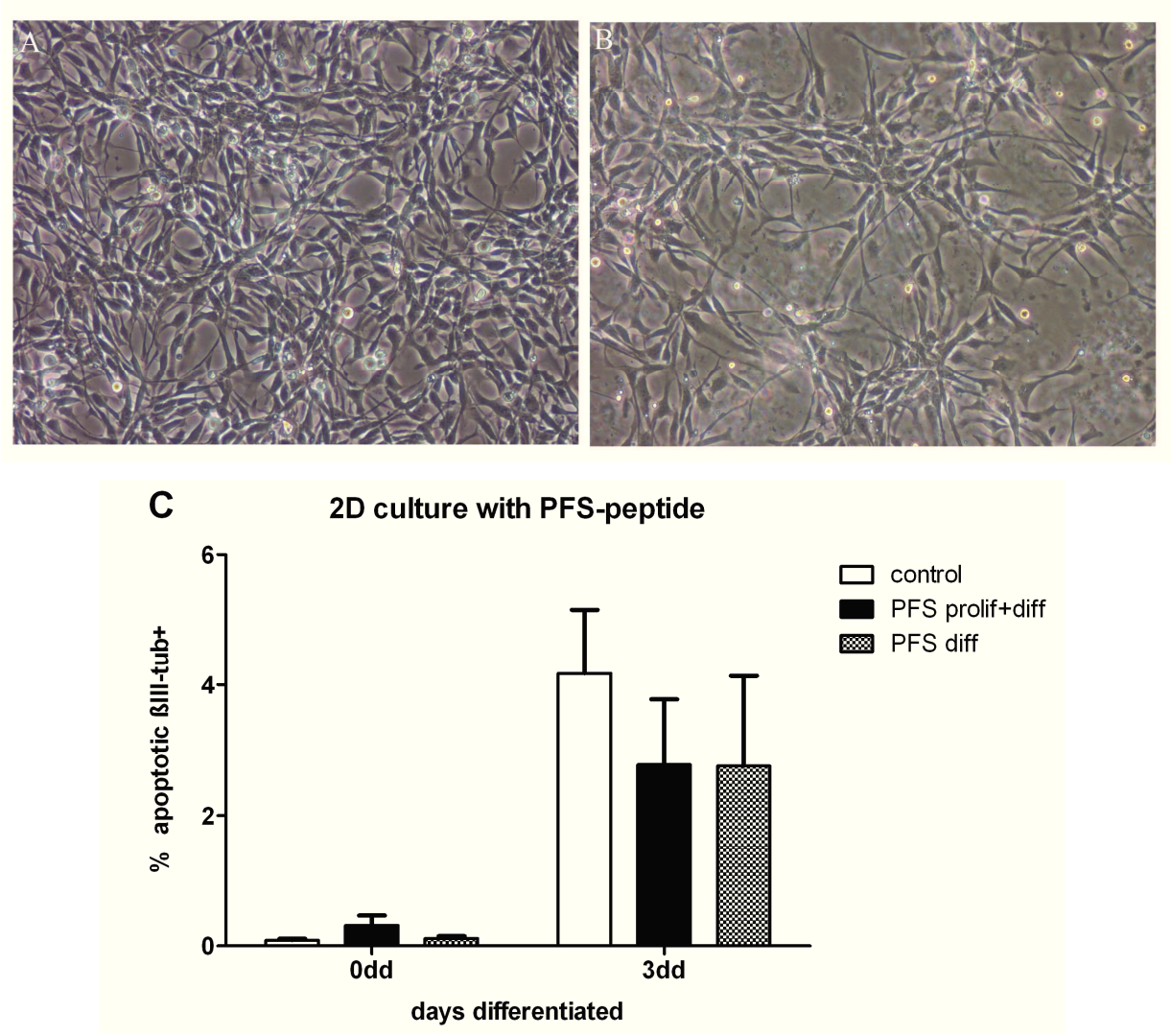

Fig. 26: hNPCs cultured in monolayer with the PFS-peptide sequence as media supplement. A, B: Phase contrast pictures of proliferated hNPCs. Scale 10µm. **A:** control. **B:** PFS-peptide as supplement. The attachment of the hNPCs is decreased under PFS-peptide treatment **C:** Flow cytometry against ßIII-tubulin**.** White bars indicate control, black bars PFS-peptide for proliferation and differentiation, doted bars PFS-peptide for differentiation. Mean ± SEM. N = 3. No effect was found under PFS-peptide treatment.

4.4. Influence of laminin on hNPCs in modified 3D scaffolds

Aim of this part of the study was to determine the influence of laminin on the hNPCs cultured in modified PM scaffolds to elucidate possible additive effects of the modified matrix and laminin. The hNPCs grew neurosphere like in the modified PM scaffolds, laminin supplement can increase the attachment of the hNPCs and prevent neurospheres shown in 4.1.1. Therefore PM-PFS scaffolds were supplemented with laminin and the growth, differentiation and survival of the hNPCs were compared to cells cultured in not modified PM scaffolds supplemented with laminin as described in 4.1. If the laminin supplement to the modified PM scaffolds had also an effect on the differentiation or the survival will be shown in this chapter.

4.4.1. Growth and differentiation of hNPCs in laminin supplemented modified 3D scaffolds

Regarding the differentiation of the hNPCs an enhancement of neuronal cells was found in PM-PFS scaffolds (Fig. 21A), where no obvious effect was observed regarding the increased adhesion of the cells (Fig. 20E). In the PML scaffold a better spreading and decreased spheroid like growing of the hNPCs were observed (Fig. 6). Hence the PM-PFS scaffold was supplemented with laminin (further referred as PML-PFS) to show if laminin can influence the adhesion and the differentiation.

The supplementation of laminin to the PFS scaffolds resulting in the same growth pattern like the PML scaffold (Fig. 6, 27). One can see flat and densely packed cell aggregates with 3-dimensional loosely composed cellular structures item (Fig. 27A).

Regarding the differentiation an increase of ßIII-tubulin positive cells after 4 days of differentiation in the PML-PFS scaffold was detected compared with the PML scaffold (Fig. 10B, 27B).

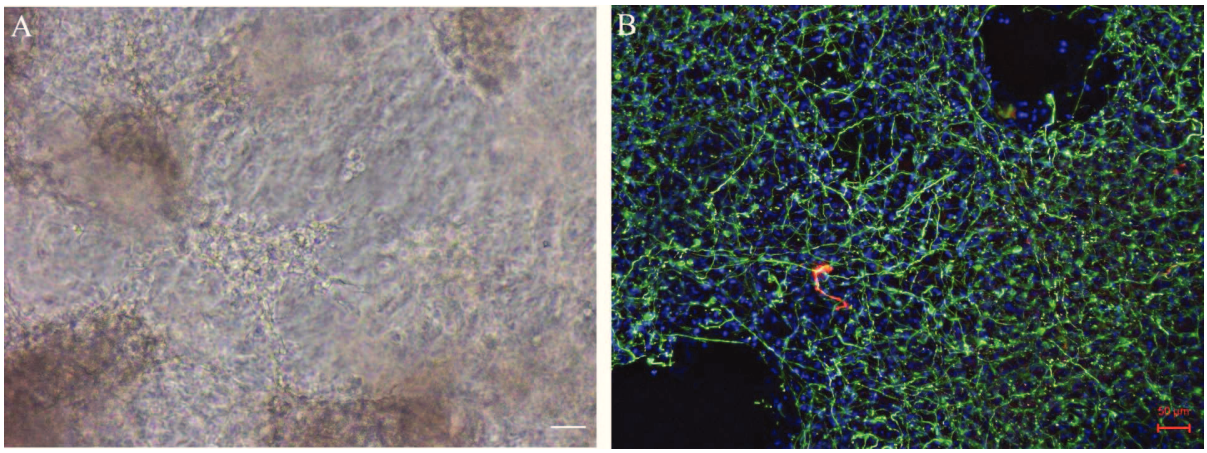

Fig. 27: The hNPCs proliferated and differentiated in PFS scaffolds supplemented with laminin (PML-PFS). Scale 50 nm. **A:** Phase contrast picture at 0dd. More distribution of the cells and less spheroid like structures of the hNPCs was found in PM-PFS scaffolds. **B:** Immunocytochemistry pictures after 4dd, ßIII-tubulin (green) / TH (red). A high amount of ßIII-tubulin and a dense network of neuronal cells were detected.

Fig. 28 shows a comparison of the tested 3D scaffolds (PM, PML, PM-PFS and PML-PFS). The addition of laminin to the PM scaffold leads to no different expression of ßIII-tubulin at 4 and 7dd. ßIII-tubulin was slightly but not significantly increased at 0dd in PML compared to PM scaffolds. At 10dd the ßIII-tubulin$^+$ cells were decreased in the scaffolds supplemented with laminin (PML). The supplementation of laminin to the modified PFS scaffold leads to an increase in ßIII-tubulin expression compared with PM and PML scaffolds. But the level of positive cells observed in the PM-PFS scaffolds was not reached in the PFS scaffolds supplemented with laminin (PML-PFS) at all time points with a significant difference at 10dd (Fig. 28A). Regarding the amount of ßIII-tubulin positive cells in proliferating cells, no significant difference was found between cells hosted in PM-PFS or PML-PFS scaffolds (Fig. 28A).

In case of the HuC/D expression there was no significant difference between PM and PML scaffolds (Fig. 28B). In PML-PFS scaffolds an increased number of HuC/D$^+$ cells were found at 0dd. After induction of the differentiation the number of HuC/D$^+$ cells was always lower in PML-PFS scaffolds compared with PM-PFS scaffolds with significant differences at 7 and 10dd. The laminin supplementation lift the positive influence of the PM-PFS scaffold for the HuC/D expression and the number of HuC/D$^+$ cells is in the range of PM and PML scaffolds (Fig 28B). Besides the neuronal marker ßIII-tubulin and HuC/D the GFAP expression was analysed. A decreased amount of GFAP positive cells was found in scaffolds supplemented with laminin (Fig. 28C). At 7dd the GFAP expression was significantly decreased in PML scaffolds compared with PM scaffolds. PML-PFS scaffolds exhibited a lower amount of

GFAP$^+$ cells than PM-PFS scaffolds at 7dd and 10dd. A significant decreased expression of GFAP was found at 7 and 10dd in PML-PFS scaffolds compared to PM scaffolds. At 10 days after differentiation the lowest amount of GFAP (64.47 ± 5.11 %) was found in PML-PFS scaffolds.

To determine the neuronal progenitor cell pool of the hNPCs the expression of PSA-NCAM was analysed (Fig. 28D). The PSA-NCAM expression of proliferated cells was slightly decreased in 3D scaffolds supplemented with laminin (PML, PML-PFS) compared with 3D-scaffolds without laminin (PM, PM-PFS), but no significant differences were found. As well no differences between the conditions were found for differentiated cells (Fig. 28D).

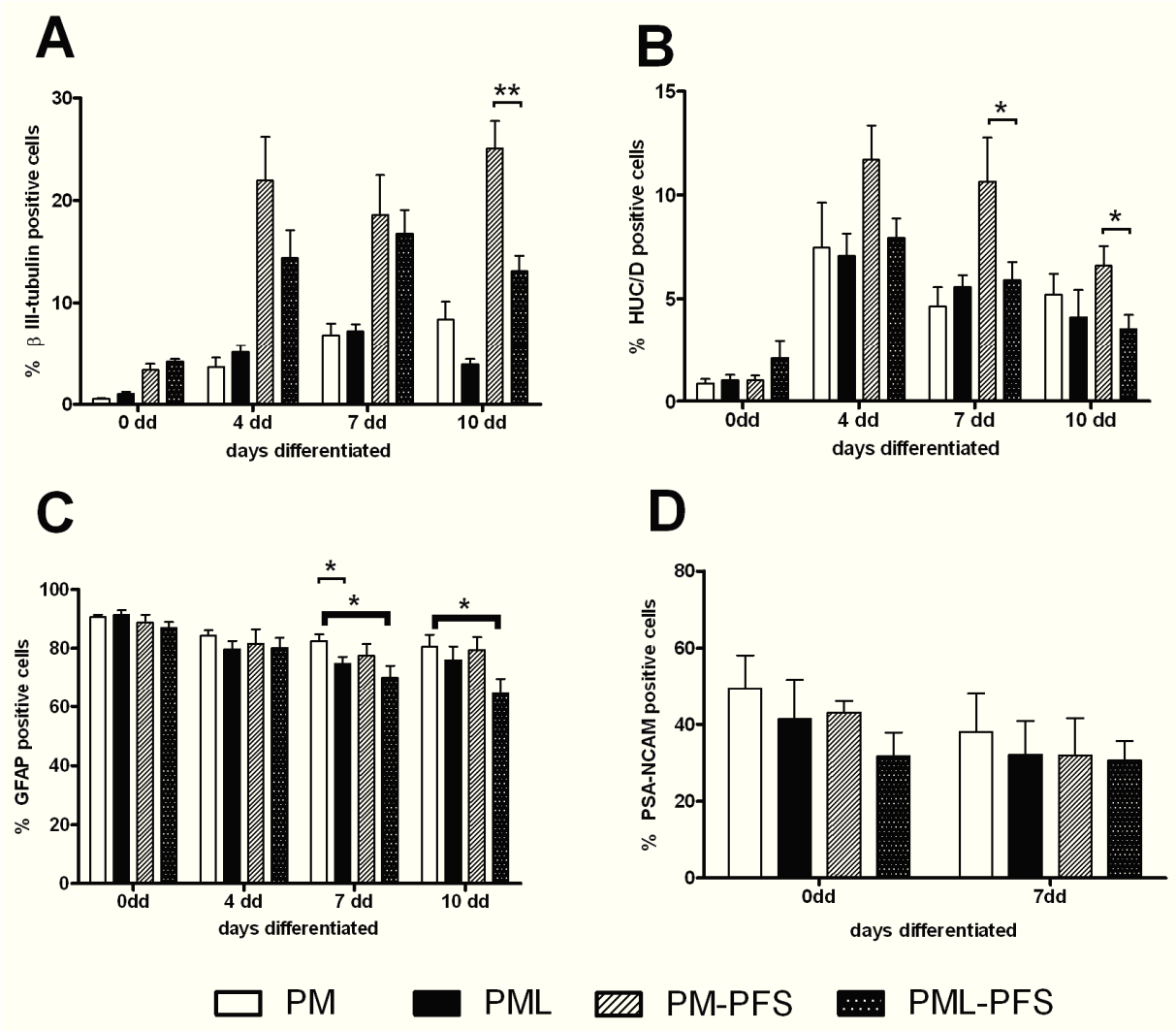

Fig. 28: Flow cytometry analysis of neuronal markers in hNPCs cultivated in PM and modified PM formulations with and without laminin. White bars indicate PM scaffolds; black bars PML scaffolds, striped bars PM-PFS scaffolds, doted bars PML-PFS scaffolds. Mean ± SEM. * and ** indicate significant differences. **A** ßIII-tubulin **PM:** N=7-9, **PML:** N = 7-10, **PM-PFS:** N = 6-9, **PML-PFS:** N = 7-9; **B** HuC/D **PM:** N = 7-10, **PML:** N = 7-12, **PM-PFS:** N = 5-10, **PML-PFS:** N = 7-8; **C** GFAP **PM:** N = 5, **PML:** N = 7-10, **PM-PFS**: N = 5-7, **PML-PFS:** N = 4-5; **D** PSA-NCAM N = 4, **PML:** N = 3-5. A significant decrease of ßIII-tubulin$^+$ at 10dd and HuC/D$^+$ at 4dd and 7dd in PML-PFS scaffolds was observed in comparison to PM-PFS. Expression of

GFAP was significant decreased at 7dd in PML and PML-PFS and at 10dd in PML-PFS scaffolds in comparison to PML scaffolds. For PSA-NCAM no significant differences were found.

4.4.2. Survival and apoptosis of hNPCs in laminin supplemented modified 3D scaffolds

In this part of the project the influence of laminin on apoptotic events in the hNPCs was of interest. Therefore laminin was supplemented to the scaffolds consisting of PM and PFS. The amount of apoptotic cells was determined at different time points of differentiation using the TUNEL-Assay and the Annexin-PI-staining.

Fig. 29 shows the results of the TUNEL-Assay of PM versus PML scaffolds (Fig. 29A) and PM-PFS versus PML-PFS scaffolds (Fig. 29B). In PM scaffolds the apoptotic cells increases up to 10dd and was slightly lower up to 7dd. The amount of apoptotic cells in PML scaffolds was increased up to 7 days of differentiation and decreased at 10 days of differentiation. A little lower amount at 10dd was found for PML scaffolds, but no significant differences could be found.

In the PFS scaffolds the amount of apoptotic cells increase over time. Where the number of apoptotic cells in PML-PFS scaffolds was slightly increased compared to PM-PFS, but no significant differences were observed.

Analysing the amount of TUNEL positive cells in the neuronal population (Fig. 29B) the PM and the PML scaffolds show an increase up to 7dd, than the apoptosis in the neurons decrease in PML scaffolds whereas apoptotic events in the PM scaffold further increases. Therefore significant differences were observed in PML scaffolds at 10dd compared to PM scaffolds.

In the PFS scaffolds namely PM-PFS and PML-PFS the apoptosis in neuronal cells increases over time in PM-PFS scaffolds. The increase of apoptotic neurons at 7dd was more or less equal between both conditions, no significant difference was observed.

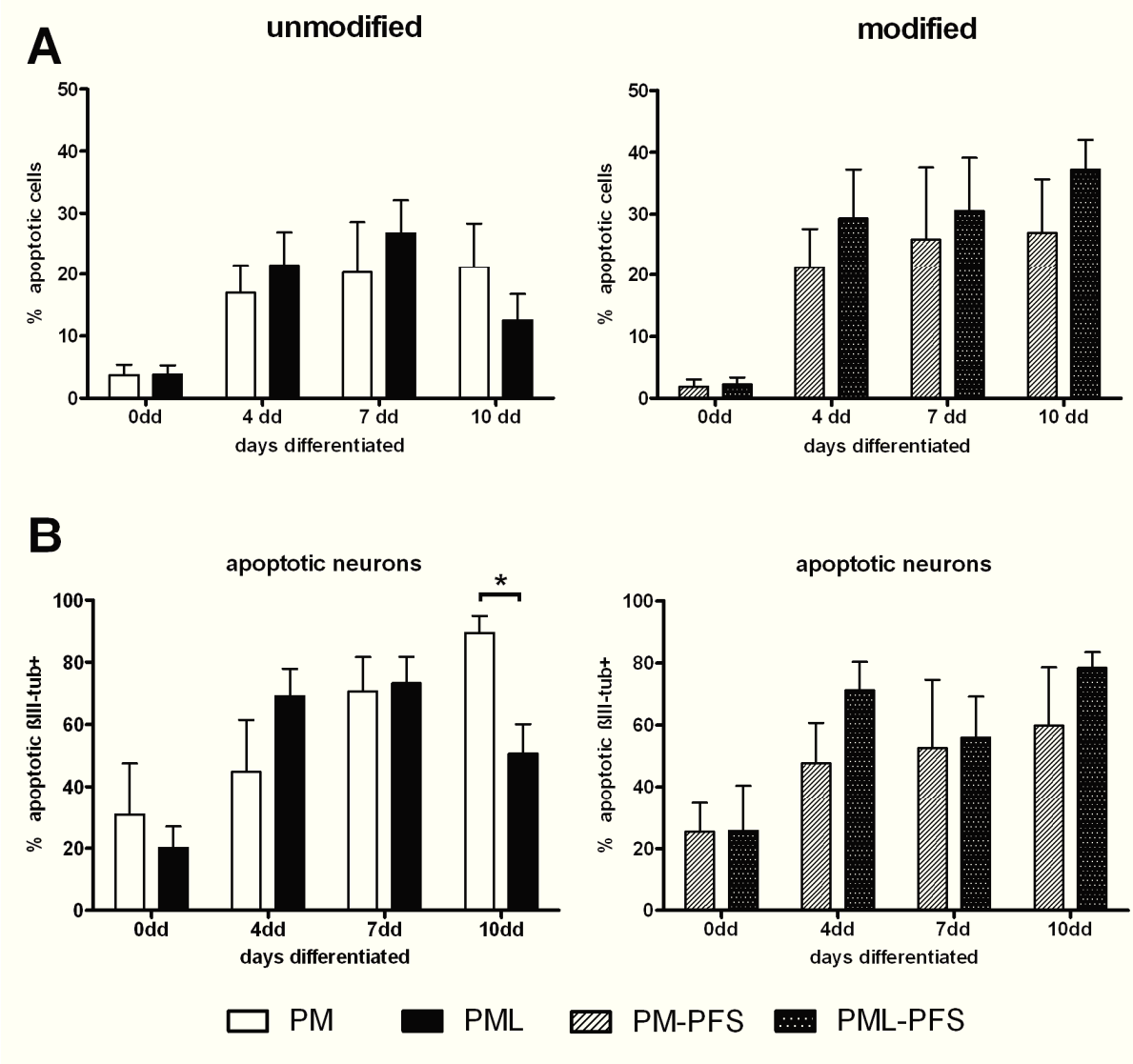

Fig. 29: Apoptotic cells of hNPCs cultivated in 3D scaffolds of PuraMatrix with and without laminin; PFS-scaffolds with and without laminin. White bars indicate PM scaffolds, black bars PML-scaffolds, striped bars PFS- and dotted bars PML-PFS-scaffolds. * indicates significant differences PFS to PML-PFS. Mean ± SEM. **A:** TUNEL-Assay, **PM**: N = 3-5, **PML**: N = 6-9, **PM-PFS** and **PML-PFS**: N = 3-6. No significant differences for the whole cell population were found. **B:** TUNEL-Assay of ßIII-tubulin positive cells, **PM**: N = 3-5; **PML**: N = 6-10, **PM-PFS**: N = 3-7**, PML-PFS**: N = 4-7. A significant decrease of apoptotic neurons was found in PML-scaffolds versus PM scaffolds at 10dd.

The next figure shows the relation between the necrotic cells, cells in early and late apoptosis (Fig. 30). To show the influence of the laminin supplement, all six tested culture conditions were compared (PM, PM-SDP, PM-PFS, PML, PML-PFS and 2D culture). One could observe differences between hNPCs cultivated in contact with laminin or without. In all three types of scaffolds cultured without laminin, namely PM and the modified scaffolds PM-SDP and PM-PFS (Fig. 30, left panel) no differences in the number of cells in the early or in the late apoptosis were observed, where the number of apoptotic cells ranged between 20 % and

→

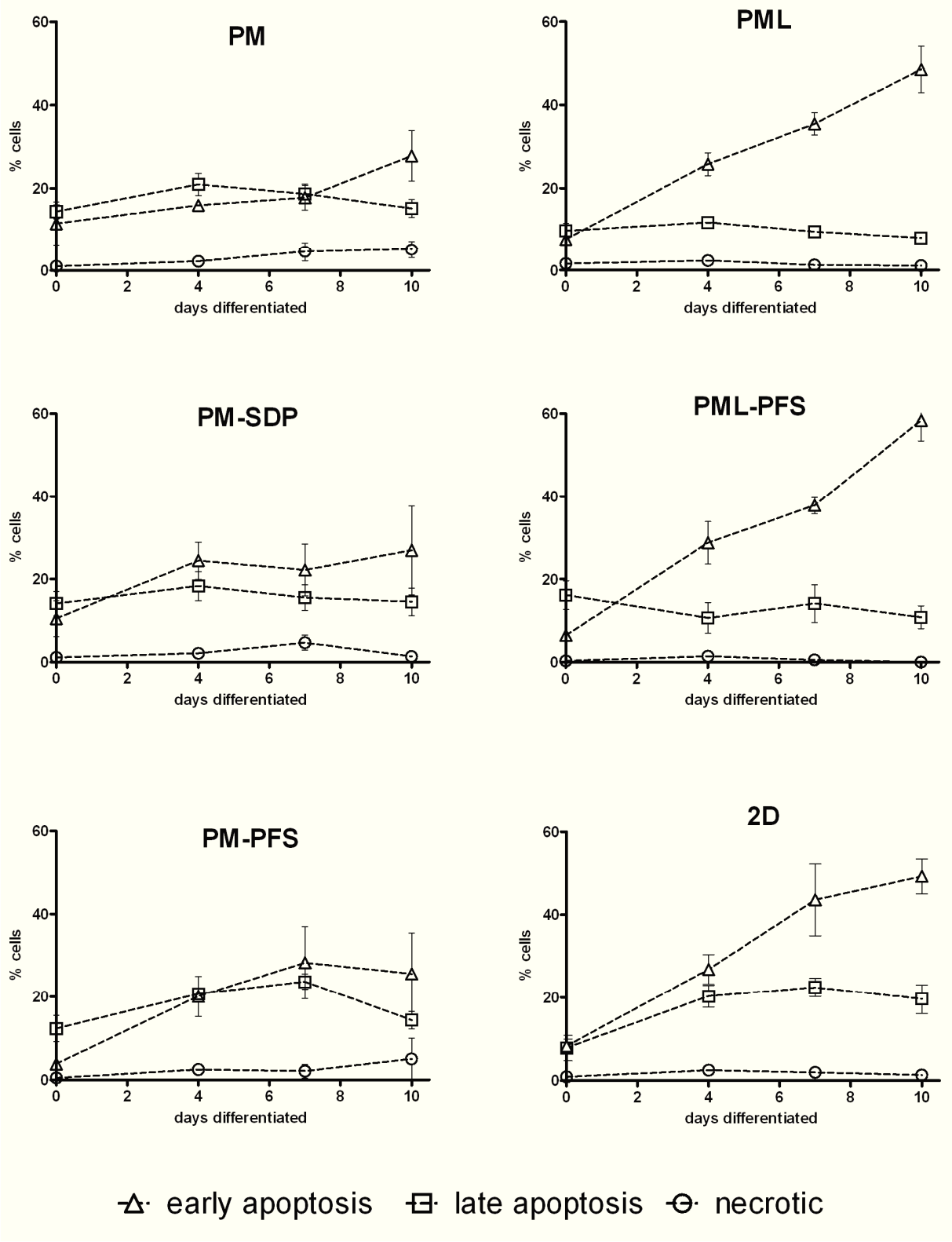

Fig. 30: Double staining Annexin V and Propidium Iodide of hNPCs cultivated in 2D, 3D scaffolds of PuraMatrix and modified PuraMatrix formulations with and without laminin. Triangles indicate early apoptosis, squares indicate late apoptosis, and circles indicate necrosis. **PM** and **PM-SDP**: N = 4-5, **PM-PFS**: N = 3, **PML**: N = 9-10, **PML-PFS**: N = 3, **2D**: N = 4-6. Left panel: No differences between early and late apoptosis in scaffolds without laminin were found. Right panel: A higher amount of early apoptotic cells was found in scaffolds supplemented with laminin and 2D cultures.

25% (Fig. 30). Cells cultivated with laminin in PML, PML-PFS scaffolds and 2D monolayer cultures (Fig. 30, right panel) reacted in difference between early and late apoptotic events.

In all three conditions more cells were found to be in the early apoptosis than in late apoptosis (Fig. 30, right panel). A high increase of cells in the late apoptosis was only found in 2D cultivated cells. The number of necrotic cells was more or less equal in cell cultures with laminin PML-PFS, PML and 2D. In scaffolds without laminin supplement PM, PM-SDP and PM-PFS the necrotic cells increases a little bit during differentiation (Fig. 30).

In a last set of experiments I analysed the effect of laminin on the expression of the anti-apoptotic protein Bcl-2 in PM and PM-PFS scaffolds (Fig. 31). The hNPCs cultured in scaffolds with laminin showed a higher expression of Bcl-2 in proliferating conditions (Fig. 31A, B). In the PML scaffolds a slightly decreased expression of Bcl-2 was observed at all time points of differentiation in comparison to the PM scaffold, but the differences were not significant (Fig. 31A). The Bcl-2 expression of hNPCs in PM-PFS scaffolds increases up to 7dd, than a decreased expression in 10dd was found (Fig. 31B). In PML-PFS scaffolds hNPCs differentiated for 7 days, showed a significant decrease of Bcl-2 in comparison to PFS-scaffolds, where as at the other time points the expression was more or less equal.

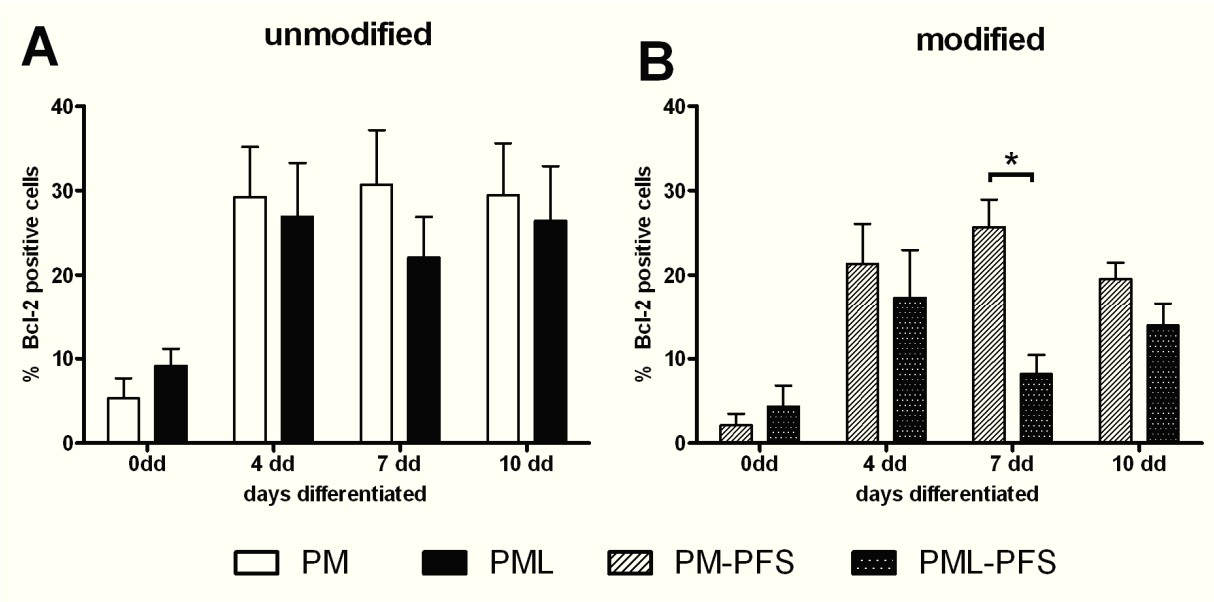

Fig. 31: Flow cytometry analysis of Bcl-2 in hNPCs cultivated in 3D scaffolds of PuraMatrix and modified PuraMatrix with and without laminin supplement. Mean ± SEM. * indicates significant differences PM-PFS to PML-PFS. **A:** White bars indicate PM scaffold, black PML scaffold. **PM**: N = 3-4, **PML**: 4-6. No significant difference in PML- compared with PM scaffolds was observed. **B:** striped bars indicate PM-PSF scaffold, dotted bars PML-PFS scaffold. N = 3-4. A significant decrease was found in PML-PFS scaffolds at 7dd.

4.5. Executive summary

As described in the first chapter (4.1.) the PML scaffold results in an increase of ßIII-tubulin positive cells and a decrease of astrocytes. Compared with the 2D culture hNPCs show 2 or 3 times more neural precursors (PSA-NCAM^{+}) when proliferated in 3D scaffolds (PML). Further the hNPCs survived longer in 3D scaffolds compared to 2D culture and a significant lower number of apoptotic cells were found in the 3D scaffolds (PML).This is combined with an increased expression of anti-apoptotic proteins (Bcl-2, XIAP) while the expression of key enzymes of apoptosis regulation was decreased in 3D scaffolds (PML).

The surprising effect in the study was the high increase of neural cells when hNPCs cultured in modified 3D scaffolds (4.2.), which resulting also in a few cells positive for the postsynaptic marker PSD95. Another important result is that all 3D scaffolds with and without modification increase the progenitor pool of hNPCs but only the cells encapsulated inside the modified matrices can use this effect to enhance the differentiation in neuronal direction. The number of apoptotic events did not differ between the 3D scaffolds modified or non-modified. Regarding the attachment, there was a different. The attachment was decreased in the modified scaffolds compared with PML scaffolds. In the modified scaffolds neurosphere like growth of the hNPCs was detected. Additional the soluble PFS-peptide itself as media supplement to hNPCs cultured in 2D does not enhance the neural differentiation.

The effect of laminin on the hNPCs cultured in 3D scaffolds is also an important finding in this work. The supplementation of laminin to the modified scaffolds results in a small decrease of neural cells and an increase in attachment of hNPCs. Furthermore laminin supplement influence apoptosis in hNPCs by increasing the amount of early apoptotic cells in laminin supplemented 3D scaffolds.

5. Discussion

The objective of this study was to examine the cultivation of human neural progenitor cells in functionalised 3D scaffolds based on the self-assembling peptide hydrogel PuraMatrix. This system was analysed regarding the growth, survival and finally the neuronal differentiation of the hNPCs. In the first part the influence of the PuraMatrix supplemented with laminin (PML) on the growth (5.1.1.) and differentiation of the hNPCs (5.1.2.) is discussed. Chapter 5.1.3. is focused on the influence of the PML scaffolds on the survival of the hNPCs. The regulation of the apoptosis in the PML 3D scaffolds by some key enzymes of the apoptotic process is the topic of chapter 5.1.4. The 3D culture could be an advantage for the stem cell research, but also provide some challenges. This will be discussed in chapter 5.1.5.
In the second part the potential of the hNPCs regarding the induction of neuronal differentiation using modified 3D scaffolds is discussed. Including the ability of the hNPCs to build functional active neuronal cells was of interest. Further the question if the survival of the hNPCs is changed, when cultivated in modified 3D scaffolds, is debated (5.2.). An additional focus in this study was the effect of the soluble PFS-peptide sequence, used as a media supplement, on the differentiation of the hNPCs (5.3.).
The last part of the discussion is focused on the influence of laminin on modified 3D scaffolds regarding the neuronal differentiation and survival of the hNPCs (5.4.).

5.1. Differentiation and survival of hNPCs inside the 3D scaffolds (PML)

5.1.1. Growth of hNPCs inside the 3D scaffolds (PML)

In the first part of the study the influence of the 3D culture on the growth and differentiation of hNPCs was analysed. In standard cultivation conditions cells mostly grow in a 2D monolayer environment on rigid flat surfaces. 3D culture systems allow defined microenvironments to better recapitulate the *in vivo* milieu. Cells forming 3D structures often resemble their *in vivo* counterparts more closely in comparison to two-dimensional systems (Falconnet et al., 2006). During early development, hESCs reside and differentiate within a

single 3D environmental milieu (Gerecht et al., 2007). The development of more realistic *in vitro* models for cell-based assays may be facilitated by applying some of the principles developed in tissue engineering in which stimulation of specific cellular responses is of great importance (Dainiak et al., 2008).

The aim of the first part of the study was to optimise the culture of hNPCs in a 3D culture system consisting of RADA-16-I (PuraMatrix) and to develop methods to quantify different parameters to be compared with 2D monolayer cultures. The hNPCs encapsulated in PuraMatrix scaffolds with laminin supplement (PML), were distributed in flat and densely packed cell aggregates with three-dimensional loosely composed cellular structures. As the functionalisation of the scaffold supports cell adhesion and prevents the formation of neurospheres (Ortinau et al., 2010), the distribution of the cells seems to be a consequence of the casual arrangement of cells during seeding, an increased attachment based on the laminin and the structure of the scaffold. The latter was concluded from the scanning electron microscopy studies (figures 7 and 8). The dense network of regular overlapping nanofibers in the 3D scaffolds is typical for the self-assembling peptide hydrogel PuraMatrix (Holmes et al., 2000). The 3D scaffolds supplemented with laminin demonstrate more cavities and lacunas as without laminin. This structural difference could be a consequence of the increase of fibres in number and length, which was shown with atomic force microscopy (Ortinau et al, 2010). These findings suggest a possible explanation for the increased instability during preparation and handling of the 3D scaffolds supplemented with laminin.

Because scanning electron microscopy pictured only the surface of the sample, transmission electron microscopy was used to show more details and to reveal structures inside the 3D scaffold. The aim was to visualize the formation of cells in the scaffolds, cell-cell or cell-matrix-contact. But neither evidence for synaptic structures nor how the cells contact the matrix compartments of the 3D scaffold could be elucidated. One possibility to analyse cells-matrix interaction are further studies on the surface of the cells and to mark the MHC-receptors or immunoglobulin with gold labelled antibodies. *In vivo* are cell-ECM interactions mediated by adhesion receptors that include integrins, dystroglycans, CD44 and thrombomodulin, and a novel subfamily of receptor tyrosine kinases called discoidin domain receptors. Integrins have emerged as the most prevalent and best-characterized ECM receptors (Zahir & Weaver, 2004). Therefore especially the integrins come in consideration for interaction with the PML scaffold, because integrins are the most important ones for laminin binding (Rodin et al., 2010). Structure differences of proliferated and differentiated cells could be analysed as well with scanning electron microscopy and transmission electron

microscopy, because integrin receptors were increased in differentiated cells (Anton et al., 1999). Furthermore synaptic contact between cells could by easier detected if they are labelled with gold-coupled antibodies.

An interesting finding was the observation of structures inside vesicles located in the cells, which looks like nanofibers from the PuraMatrix™ (Fig. 9). The mechanism by which a possible uptake might be carried out is presumably phagocytosis. The hydrogel PuraMatix consists of a repeated amino acid sequence of arginine, alanine, aspartic acid, and alanine and is described to be resorbable (Zhang et al., 2004). Zhang et al. (2004) generated a 14C, carbon radio labelled version of PuraMatrix, which was internally labelled at the third alanine site (Acetyl- (RADA)-(R- [14C(U)-Ala]-D-A)-$(RADA)_2$-$CONH_2$) as opposed to a labelled acetyl group which could be cleaved off, in order to better characterize the adsorption, degradation, metabolism and excretion of the PuraMatrix material *in vivo*. Beniash et al. (2005) showed as well that nanofibers matrices of self-assembling peptide amphiphile can be endocytosed by MC3T3-E1 cells. This indicates that nanofibers of peptide matrices can be used as a source of nutrients for the hNPCs.

5.1.2. Differentiation of hNPCs inside the 3D scaffolds (PML)

Besides the analysis how the hNPCs proliferate in the 3D scaffolds, another aspect was of special interest, namely the differentiation of the hNPCs inside the PML 3D scaffolds. The cells are known to differentiate mostly into astrocytes, some neuronal cells and only few dopaminergic neurons (Donato et al., 2007; Ortinau et al., 2010). Similar findings were obtained in hNPCs cultured in the 3D scaffolds. Proliferated and differentiated cells were positive for the *glial fibrillary acidic protein* GFAP, whereas ßIII-tubulin and *tyrosine hydroxylase* (TH) positive cells were only found after differentiation induction. Partially, spontaneous differentiation was detected in proliferating cells. Such spontaneous differentiation is also described for monolayer cultures, with a confluence of more than 80% (Donato et al., 2007). As one cannot control the distribution of cells in the 3D scaffolds as well as in a 2D culture system, the amount of cells can be higher in some part of the scaffold, leading to spontaneous differentiation. Also it can be hypothesised that the laminin functionalised PuraMatrix by itself has low capacity to induce the differentiation of the hNPCs under proliferating conditions. Ortinau et al. (2010) showed the same effect of this 3D culture system based on PuraMatrix. It is also known that scaffolds based on PuraMatrix can support neuronal cell attachment and differentiation as well extensive neurite outgrowth

(Holmes et al., 2000). Holmes and his co-workers (2000) suggested that the scaffolds are permissive substrates, because primary rat neurons form active synapses on such scaffold surfaces. The ability of PuraMatrix to support neuronal differentiation of fetal human neural stem cells (hNSCs) was also shown by Thonhoff and co-workers (2008). Self-assembling peptide scaffolds presenting laminin-derived epitopes were shown to direct neuronal differentiation of PC12 cells and significantly longer neurite outgrowth were found in matrices containing the IKVAV motive of the laminin (Li & Chau, 2010).
Additionally also cells positive for Ki-67 were detected in differentiated cells. Ki-67 is a cellular proliferation marker to determine the fraction of dividing cells (Scholzen & Gerdes, 2000, Gerdes et al., 1983). Ki-67 play an important role in the ribosomal RNA transcription and its inactivation leads to inhibition of ribosomal RNA synthesis (Bullwinkel et al., 2006; Rahmanzadeh et al., 2007). Ki-67 is present during all active phases of the cell cycle (G1, S, G2, mitosis), but absent from resting cells. Upon withdrawal of the growth factors the differentiation of the hNPCs starts and the cells stop to proliferate. The presence of dividing cells during differentiation indicates that a minor population of cells still active in proliferating in 3D scaffolds.

First the amount of ßIII-tubulin positive hNPCs was evaluated during a differentiation period of 20 days by manual counting. The peak with the highest amount was found at 7 days of differentiation (Fig. 11). This is in contrast to Ortinau et al. (2010) where the peak of ßIII-tubulin was found at 4dd with the same condition. Based on these results the time course for following experiments was set to a maximum time of 10 days differentiation. The challenge of this part was to get clear pictures to determine the number of ßIII-tubulin positive cells because of the high number of cells and the 3D structure. As the counting of cells resided in the scaffolds was extreme time consuming a new method for quantification of different parameter by changing conditions had to be found. An excellent method to count different cell types of a sample is the flow cytometry (Bader, 2010). Therefore the scaffolds had to be disrupted to get a single cell solution and cell-cell- and cell-matrix-aggregates had to be excluded. The basic preparation was given from the manufacturer (PuraMatrix user manual) and was as in a first step adapted. The protocol is comparable with protocols used to prepare e.g. tissues where a mechanical isolation of the cells is followed by a digestion of surrounding material by enzymes. A higher number of cells (flow cytometer: 50.000 per probe, manual analysis: several hundred per probe) can be analysed independent of the distribution of the cells in the 3D scaffolds, where one could found parts with many positive cells or parts with

only a few numbers of positive cells. Areas with high number of ßIII-tubulin positive cells were often thick aggregates of cells in the scaffolds, and could not be analysed with a standard fluorescence microscope. The very dense areas of matrices can hardly be analysed or high background of the matrix material resulting in an underestimation of the "real" cell number. This is not the case for flow cytometry analysis. But if flow cytometry is used for neuronal cells one topic has to be discussed. In this study neuronal cells were mainly stained with an antibody against ßIII-tubulin, resulting in staining of the complete cell, including soma and processes (Morgan et al., 2009; Ortinau et al., 2010). Based on the fact that the release of the cells from the scaffold comes along with mechanically disruption of the scaffolds, one can expect wrong positive signals through this cell debris. To overcome this challenge different experiments or controls were done. All used antibodies were tested in 2D cultured cells to assure positive staining where the samples were prepared using the same protocol to release cells from 3D scaffolds. For all samples negative controls (only secondary antibody) and isotype control were done. Beside ßIII-tubulin other marker for neuronal cells were used, namely NeuN and HuC/D. NeuN is a neuron-specific nuclear protein detected in the nucleus of neurons in a wide range of vertebrates and so it is widely used as a tool for detecting neuronal cells (Dent et al., 2010). NeuN recognizes the DNA-binding and the distributions are apparently restricted to neuronal nuclei. Dent et al. (2010) provided evidence that NeuN/Fox-3 is an intrinsic component of the neuronal nuclear matrix and a reliable marker of nuclear speckles in neurons.

The assumption that the initiation of the neuronal differentiation of the hNPCs via growth factor withdrawal results in the differentiation to NeuN positive neurons could not be verified. This result differs from the literature, where NeuN has been widely used as a reliable tool to detect most post mitotic neuronal cell types in neuroscience, developmental biology, and stem cell research fields as well as diagnostic histopathology (Kim et al., 2009). It first appears at developmental time points that correspond with the withdrawal of the neuron from the cell cycle and/or with the initiation of terminal differentiation of the neuron (Kim et al., 2009; Dent et al., 2010). We assume that the cells are still immature or arrested in an intermediate or quiescent developing state which is supported by a high number of GFAP positive cells and the high number of nestin positive cells, which were detected in our lab during differentiation (Morgan, 2011). Another possibility might be that, the NeuN protein is not expressed at the tested time points (0d, 4dd). Weyer & Schilling (2003) suggested whereas NeuN expression per se is a reliable marker of proliferative capacity, levels of NeuN expression may also be indicative of the physiological status of a post mitotic neuron.

Furthermore, neuronal marker HuC/D (human neuronal protein HuC/HuD) was tested as a neuronal RNA-binding protein and a marker for neurons in an early developmental stage (Graus et al., 1987, Graus & Ferrer, 1990). HuC/D was found in all samples of differentiated cells (Fig. 14B). This antibody showed a clear signal in flow cytometry of 2D samples as well as of 3D samples (Fig. 13). In addition in the 3D samples was an intermediate population observed (dotted frame in Fig. 13). To avoid wrong signals in the analysis, coming from debris of the cells, this population was excluded from the analysis.

Quantification of the flow cytometry measurements was shown in Fig. 14. Comparison with ßIII-tubulin shows that the expression of HuC/D starts earlier than ßIII-tubulin in 2D cultivation and was significantly higher than ßIII-tubulin at the early time points 0d to 3dd (Fig. 14A, B). This confirms the expectations, because HuC/D is a marker for early neuronal cells and Bader (2010) showed that HuC/D is expressed in neurons prior to ßIII-tubulin.

The comparison of the monolayer culture with the 3D scaffold showed an increase of ßIII-tubulin positive cells in the 3D scaffolds (Fig. 14A). Remarkable was the shift of the peak with the highest amount of ßIII-tubulin from 4dd in 2D to 7dd in 3D scaffolds. Together with the increased expression of HuC/D and the decreased GFAP expression of the hNPCs in the 3D scaffolds (Fig. 14C), the increase of ßIII-tubulin positive cells supports the importance of a 3D environment and the architecture, which resembles more the *in vivo* environment of the cells. 3D cultures contain cells with different phenotypes and the cellular heterogeneity within 3D culture models is far more realistic (Dainiak et al., 2008). The 3D culture of different cell types was shown to enhance the survival and the differentiation of these cells. 3D culture of murine embryonic stem cells and NSCs in hydrogels showed an enhanced neuronal differentiation (Brännvall et al., 2007; Willerth et al., 2006; Thonhoff et al., 2008). Several studies have explored the culture of hESCs in defined 3D settings by using a variety of natural and synthetic scaffolds for cell growth (Li et al., 2006), differentiation (Gerecht-Nir et al., 2004), or lineage guidance (Levenberg et a., 2003 & 2005; Baharvand et al., 2006; Gerami-Naini et al., 2004; Ferreira et al., 2007). Li et al. (2007) for example demonstrated that human neuroblastoma SH-SY5Y cells developed longer neurites in 3D collagen type 1 cultures than in 2D cultures. Whereas completely synthetic hyaluronic acid hydrogel matrix can support long-term self-renewal of hESCs in the presence of conditioned medium from mouse embryonic fibroblast feeder layers and direct cell differentiation (Gerecht et al., 2007). Regarding the used cells, neural progenitor cells show an induction of neuronal differentiation by using 3D culture systems (Thonhoff et al., 2008; Ortinau et al., 2010). The same might be also possible for the ReNcell VM cells in this study. Many researchers culturing NPCs in 3D

scaffolds using natural derived biomaterials. *In vitro* studies of embryonic cortical rat NSC/NPC in a 3D collagen type 1 gel revealed progenitor cell expansion, differentiation, and formation of synapses (Ma et al., 2004). Neural progenitor cells isolated from the E13.5 forebrain cortical neuroepithelium differentiated mostly into neurons and a few glial cells in hyaluronic acid hydrogel scaffolds and support the survival of NPCs, providing even phenotypic direction to become neurons (Pan et al., 2009). Different materials have different capabilities to influence the differentiation of NSCs and NPCs especially. Synthetic biomaterials like polyvinylidene fluoride (PVDF)-based material inhibit the differentiation of NSCs, whereas other materials promote their differentiation (Hung et al., 2006).

Regarding the used self-assembling peptide hydrogel RADA16-I, it tends to build soft gels and was used for *in vitro* and *in vivo* application of neural cells (Holmes et al., 2000; Ellis-Behnke et al., 2006; Thonhoff et al., 2008; Semino, 2008; Ortinau et al., 2010). Thonhoff et al. (2008) found that PuraMatrix was the most optimal hydrogel for hNPCs, when gelated in concentration of 0.25%, and it retains several crucial properties of hNPCs, including migration and neuronal differentiation. A comparable observation was shown by Ortinau et al. (2010) and as well in this study.

The observed increased neuronal differentiation in this study might be based by, apart from the 3D environment, increased attachment on the peptides of the scaffold or on the supplemented laminin. There exists an attachment of the hNPCs on the peptides of the scaffolds, shown in (Thonhoff et al., 2008) by some loosely cellular compounds of fetal hNSCs leaving neurospheres structures after 7 days. But these cells and used ReNcells forming neurosphere structures in the PuraMatrix. The supplement of laminin was used to prevent such effect, because the increased attachment of hNPCs on laminin is used for the 2D culture. Laminins are a family of heterotrimeric glycoproteins composed of α, β and γ chains, which exist as five, three and three genetically, district types forming 15 different combinations in human tissues (Aumailley et al., 2005). The different laminins show various expression patterns as well as tissue-specific localization and functions. Laminin is, together with collagen IV, entactin, and proteoglycans the main constituents of basement membranes, which provide not only mechanical support but also influences cell behaviour (Paulsson, 1992) and induce robust outgrowth of DRG neurites *in vitro* (Tonge et al., 1997). Laminin is known to be important for proper brain development (Georges-Labouesse et al., 1998; Zhang & Galileo, 1998; Anton et al., 1999).

The coating with laminin is useful to prevent neurospheres in hNPC cultures shown in Donato et al. (2007). The PM scaffolds with laminin supplement (PML) showed the same effect and a

distribution described in Ortinau et al. (2010). The addition of laminin to the hydrogel has also the ability to support the hNPCs to build neuronal cells. Yu et al. (1999) showed that laminin coupled to agarose hydrogel scaffolds enhance neurite extension from three-dimensionally cultured PC12 cells. Georges et al. (2006) found that laminin-coated soft gels encourage attachment and growth of neurons while suppressing astrocyte growth.
The mouse laminin 1, used in my study, is restricted to the early embryo and certain epithelial cells (Ekblom et al., 2003). The extracellular matrix protein laminin 1 promotes cell adhesion and was shown to stimulate neurite outgrowth in various neuronal cell types (Powell et al., 2000). Therefore I conclude that the combination of 3D environment, increased attachment on the scaffold and on laminin support the neuronal differentiation of the hNPCs in the PML 3D scaffold.

One possible mechanism underlying the increased amount of neuronal cells in the 3D scaffolds is an alteration in the pool of progenitor cells, which are determined to undergo neuronal differentiation. To test this hypothesis PSA-NCAM, a marker for neural progenitor cells was used to elucidate differences in the progenitor pool of cells cultured in 2D and 3D cultures. The significant high increase of the progenitor pool in the 3D scaffolds, observed in this study before starting the differentiation (Fig. 14D), might be a result of the proliferation period of the cells in the 3D scaffolds. Assumingly, the hNPCs change their developing state during the proliferation in the 3D scaffolds into neuronal restricted precursor cells. A neuronal restricted precursor cell can undergo self-renewal and differentiate into multiple neuronal phenotypes and is identified by its high expression of PSA-NCAM (Mayer-Proschel et al., 1997). Many neural development processes in the brain are depending on the regulated expression of *neural cell adhesion molecule* NCAM isoforms. In the developing nervous system PSA-NCAM represents the highly polysialylated form of the embryonic NCAM and it is the mainly expressed form (Kiss et al., 2001). PSA-NCAM is suggested to perform an instructive role in development by interacting with signalling molecules (Muller et al., 2000; Kiss et al., 2001). Therefore the observed high expression of PSA-NCAM in the ReNcell VM cells indicate a change in the proliferation state of the cells and the possible interacting with signalling molecules resulting in the increase of neuronal cells in the 3D scaffolds.
In my study I observed as well a small decrease of PSA-NCAM during differentiation. This depends on the fact that PSA-NCAM expression is mainly present during development (Kiss et al., 2001) and in the adult it is restricted to regions that retain plasticity (Theodosis et al., 1994). This may indicate instead, that the ReNcells starts to become mature.

Interestingly a significant difference between the amount of PSA-NCAM positive cells and ßIII-tubulin positive cells was observed in 3D scaffolds (Fig. 14A, D). About 40 % of the hNPCs in 3D scaffolds were positive for PSA-NCAM, but only about 8 % of the hNPCs were found to be positive for ßIII-tubulin. The 7 fold higher amount of PSA-NCAM positive cells enforces the hypothesis of a changed pool of progenitor cells in 3D scaffolds to neuronal restricted precursor cells. Therefore more cells are able to differentiate in neuronal like cells. This and the shift of the ßIII-tubulin expression peak from 4dd in 2D culture to 7dd in 3D culture could also indicate that an increased survival of the hNPCs in 3D scaffolds is possible. Presumptive are both mechanism possible for the positive effect of the 3D scaffolds supplemented with laminin. The PML 3D scaffold seems to prime the hNPCs effective to differentiate to neuronal phenotypes. But not all cells, which are primed to neuronal restricted precursors, become neurons (only 8%). Therefore the neuronal differentiation has to optimise. The influence of the scaffold is early, in the proliferation state, but do not really enhance the differentiation. It has to evaluate, how to utilise the increased potential of the proliferated cells. One possibility is described in the second part of the study.

For further examination of molecular changes of cells cultured in 3D scaffolds, the orientation on studies screening for high-throughput screening format for cell-based assays could be important. Dainiak and his co-workers (2008) demonstrated the possibility to combine 3D cell culture with a miniaturized screening format (96-minicolumn plate) on human colon cancer cells (HCT116), human acute myeloid leukaemia KG-1 cells, and embryonic fibroblasts.

5.1.3. Survival and apoptosis of hNPCs inside the 3D scaffolds (PML)

In the next part of the study, investigations about the survival of hNPCs in 3D scaffolds were done. It is known that the number of dead cells and apoptosis is increased in monolayer cultures of hNPCs upon induction of differentiation (Jaeger, 2010). Ortinau et al. (2010) showed that the survival of the hNPCs is increased when cultured in 3D scaffolds. They found a decreased number of dead cells compared to 2D cultures by the use of a Live/Dead-assay. Corresponding controls using this assay approved these results, where the amount of dead cells in 3D scaffolds was not changing over a period of 20 days of differentiation (data not shown). It was concluded that the apoptosis is reduced in 3D scaffolds. The results of the TUNEL-Assay affirmed this assumption. The number of apoptotic cells was 2.5 fold lower than in 2D cultures (Fig. 15). The increased survival during the differentiation fit very well to

the higher number of ßIII-tubulin neurons. An increased cell survival of neural cells in 3D scaffolds was also described by Mahoney & Anseth (2006) with poly ethylenglycol hydrogels. The use of hydrogels as scaffolds for culturing cells in a 3D environment is attractive, because hydrogels have high permeability for oxygen, nutrients and other water-soluble metabolites through their high water-content matrix, which is an excellent environment for cell growth and tissue regeneration (Alsberg et al., 2002). In contrast Silva et al. (2004) could not demonstrate significant differences in cell survival within the differentiation phase with the IKVAV hydrogel system compared to 2D composition. But they suggest that diffusion of nutrients, bioactive factors, and oxygen through these highly hydrated networks is sufficient for survival of large numbers of cells for extended periods of time. Thonhoff et al. (2008) found that PuraMatrix was the most optimal hydrogel for hNPCs, since it showed low toxicity when gelated in concentration of 0.25% and retain crucial properties of hNPCs. Orive (2009) provide that polymer encapsulation allows long-term survival of cells sourced from animals or human stem cells. Embryonic stem (ES) cells grown on polymeric scaffolds with well-defined microstructure constructed into a multilayer cell-scaffold complex using low-pressure carbon dioxide (CO_2) and nitrogen (N_2) was shown to increases the cell viability (Xie et al., 2009). Zhu et al. (2010) showed that human bone marrow stoma stem cells increased to higher levels and remained higher for longer periods with the use of the fibrin matrix.

3D cell models offer a district advantage over conventional 2D systems because they recapitulate both the architecture and the phenotypic behaviour of the differentiated tissue with reasonable fidelity (Zahir & Weaver, 2004). The cell-ECM and cell-cell interactions are necessary for maintenance of cell survival in tissues (Yu et al., 2002). Santini et al. (2000) showed that 3D spheroids undergo phenotypic switch associated with changes in tissue organisation that is linked to enhance cell-cell interactions, altered expression of integrins and increased expression of ECM proteins. Shain et al. (2002) showed that cell-ECM interactions can influence death receptor signalling by increasing the activity and expression of pro-survival genes (Sethi et al., 1999).

Further it was of interesting how much the neuronal population of the hNPCs is affected from apoptosis. The analysis of the hNPCs revealed that the largest portion was positive for the glial marker GFAP, in both examined culture systems. The number of neuronal cells was around 3 % in 2D culture and 7 % in 3D scaffolds, whereas around 90% of the analysed cells were positive for GFAP. As it is known that neurons differentiated from human neural

progenitor cells are more sensitive than astrocytes to induced cytotoxicity (Li et al., 2005), I was interested in which amount the neuronal cells were affected by apoptosis. Therefore ßIII-tubulin staining were combined with the TUNEL-Assay and analysed with flow cytometry (Fig. 17). The neuronal cells were more affected by apoptosis than the total number of cells in both conditions. Surprisingly the number of apoptotic neurons was higher in 3D scaffolds. The fact that after 7 days of differentiation in 2D cultures only few ßIII-tubulin positive cells were left, whereas the highest number of neurons was observed at 7 days in the 3D scaffolds, indicates an increased survival of the neuronal cells based on the 3D structure (Mahoney & Anseth, 2006), decreased PARP-1 activation (Midorikawa et al., 2006; Skaper, 2003), increased XIAP expression (Tamm et al., 1998) and increased Bcl-2 expression (Wang et al., 2006). But why are the neuronal cells in 3D scaffolds more affected by apoptosis? Apoptosis is required for the establishment of appropriate cell numbers and for the elimination of improperly connected neurons in the developing nervous system (Pettmann and Henderson, 1998). Either more neuronal cells could found in 3D scaffolds or no advice for active synapses, apoptosis is a consequence for improperly connected neurons during development of neuronal cells. Another possibility is the different regulation of apoptosis in 3D scaffolds. Caspases as key effector molecules are involved in the execution of neuronal cell death during development and after injury. Just as well a caspase-independent mechanism of neuronal cell death exists (Rideout & Stefanis, 2001). I concluded, because of the high mortal rate and the high number of detached dead cell in culture medium found in 2D cultured hNPCs can shift the result and that most neurons in the 2D also undergo necrosis, while in 3D scaffolds the neurons more undergo apoptosis.

The next question was which stage the apoptotic cells are. The TUNEL-Assay as a method for detecting DNA fragmentation by labelling the terminal end of nucleic acids (Negoescu et al., 1996) labelled all cells affected of apoptosis with DNA damage. A discrimination of the state of apoptosis, ranging from early effects to DNA damage and cell death cannot be resolved by this assay (Grasl-Kraupp et al., 1995). To achieve this, another assay marking cells at earlier time points during apoptosis had to be used. Therefore the Annexin – PI staining was performed to determine the different states of the apoptosis (Vermes et al., 1995). The loss of plasma membrane is one of the earliest features of the apoptotic process. In apoptotic cells, the membrane phospholipid *phosphatidylserine* PS is translocated from the inner to the outer leaflet of the plasma membrane, thereby exposing PS to the external cellular environment (Martin et al., 1995). Annexin V is a 35-36 kDa Ca2+ dependent phospholipid-binding

protein that has a high affinity for PS, and binds to cells with exposed PS (Koopman et al., 1994). Therefore Annexin V, conjugated to fluorochromes, serves as a sensitive probe for flow cytometric analysis of cells undergoing apoptosis (Vermes et al., 1995). Since externalisation of PS occurs in the earlier stages of apoptosis, FITC Annexin V staining can identify apoptosis at an earlier stage than assays based on nuclear changes such as DNA fragmentation (van Engeland et al., 1996). The loss of membrane integrity, which also accompanies the latest stages of cell death, can be a result from either apoptotic or necrotic processes. Therefore, staining with FITC Annexin V is combined with a vital dye such as *propidium iodide* PI to identify early apoptotic cells (PI negative, FITC Annexin V positive) (Lecoeur, 2002). Viable cells with intact membranes exclude PI, whereas the membranes of dead and damaged cells are permeable to PI (Moore et al., 1998).

In addition a more technical aspect had to be discussed. The hNPCs had to be detached from the surface or the scaffold and might be stressed or damaged by this protocol. As Annexin V is a very sensitive method based on binding exposed PS, cells could become positive and can influence the staining. On the other hand, for comparison of the data all samples of 2D and 3D cultures were prepared with the same protocol.

The Annexin V – PI – staining showed the same trend as the TUNEL-Assay, namely that the rate of cells in the late apoptosis is significantly lower in the 3D scaffolds in comparison to 2D culture (Fig. 16B). But an interesting new finding was the high amount of early apoptotic cells in the 3D scaffolds (Fig. 16A). Nearly the same numbers of cells in the early apoptosis were found for 2D and 3D cultured cells. The results of Annexin V – PI double staining indicate that the hNPCs in 3D scaffolds stay / rest more in the early apoptosis and no increase in late apoptotic events was detected. Cells were protected from apoptosis and accordingly survived longer when encapsulated in 3D scaffolds supplemented with laminin. I conclude that the cells are protected in an unknown way before entering later states of apoptosis. The possible mechanism of the apoptosis regulation in 3D scaffold is discussed in the next chapter.

5.1.4. Regulation of the apoptosis of hNPCs inside 3D scaffolds (PML)

Apoptosis defines a set of cascades which, when initiated, programs the cell to undergo lethal changes such as membrane blebbing, mitochondrial break down and DNA fragmentation (Elmore, 2007). After a cell received a stimulus, it undergoes organized degradation of cellular organelles by activated proteolytic caspases, like Caspase-3, 6 and 7 (Gewies, 2003).

Caspase-3 is one member of the cascade of activated proteolytic caspases. With Caspase-3 the degenerative stages of apoptosis begin (Elmore, 2007). Caspase-3 is known as an indicator for the activity of Caspase-9 (Wright et al., 2004), and Caspase-9 is included in the process of the apotosome complex (Zou et al., 1999). The increase of the apoptosis specific chromatin condensation in murine neural progenitor cells is correlated with the activation of GSK-3ß, the pro-apoptotic proteins Bax and Caspase-3 (Eom et al., 2007). A set of preliminary western blot experiments was done in this study to evaluate the underlying mechanism of the increased survival of the hNPCs in 3D scaffolds. The expression of Caspase-3 was highly increased in differentiated cells of the 2D culture, but only a small increase was found in the 3D scaffolds. That indicates that the cells might be stressed and influenced by the withdrawal of the growth factors in 2D culture and as well as in 3D scaffolds, shown in Fig. 16A by exposing phosphatidylserine. But the early degenerative stages of apoptosis did not start in 3D scaffolds (Fig. 19). The decreased Caspase-3 expression differs from recent literature. A significant increase of active Caspase-3 in ReNcell VM cells was shown during differentiation in 2D culture (Jaeger, 2010). And it is supposed that the growth factor withdrawal is correlated with the activation of Caspase-3. Miho et al. (1999) showed that the withdrawal of bFGF results in activation of Caspase-3 in murine embryonal P19-carcinoma cells during the neuronal development (Miho et al., 1999). Caspase-3 induces the genesis of neural progenitor cells in mouse by induction of protein kinase (Fernando et al., 2005) and is possible involved in the cytoskelett reorganisation during differentiation. The decreased activated Caspase-3 in the 3D scaffolds results in increased survival of the hNPCs (Fig. 15), but it is also possible to influence the differentiation of the hNPCs.

Taken together the results demonstrate that after induction of differentiation the apoptosis of the hNPCs increases in the 2D culture with high number of cells in an early and late stage of apoptosis and an increase of active Caspase-3. In contrast in 3D scaffolds a decreased expression of Caspase-3 was found and consistently a decreased number of late apoptotic cells. This indicates different ways in regulation of the apoptosis of the hNPCs cultured in 2D and 3D culture. Because from *in vivo* it is known that cells within a 3D tissue, in which multiple cell types co-exist and cell-cell and cell-ECM interactions prevail, pathways functionally linked to tissue architecture likely play a role in modulating apoptotic decisions (Zahir & Weaver, 2004). It is known for the ReNcell VM cells, that the start of the differentiation via GF withdrawal is correlated with the activation of the intrinsic apoptotic pathway (Jaeger, 2010). The intrinsic pathway is initiated by intracellular or environmental

stimuli and one of the key enzymes is the Caspase-3 (Fig. 4) (Gewies, 2003). Activated cleavage products of Caspase-3 cleave and activate Caspase-6, -7 and –9, reduce the function of the DNA-repair enzyme PARP via proteolytic cleavage and are involved in the degradation of the actin cytoskeleton (Jaeger, 2010). Therefore the decreased expression of Caspase-3 in 3D scaffolds influence another apoptotic key enzyme Poly-(ADP-ribose)-Polymerase 1 (PARP-1). PARP-1 is involved in DNA-repair (Bouchard et al., 2003). Since the proteolytic decomposition of PARP-1 is mediated by Caspase-3 during apoptosis, we used PARP-1 as a next marker to determine the regulation of apoptosis in the 3D scaffolds. As PARP-1 is involved in proliferation and differentiation, it is found in both conditions. The expression was increased in 2D culture. In 3D scaffolds the expression of PARP-1 was significantly lower in differentiated hNPCs compared to 2D culture. From the literature is known, that the survival of cells is correlated with the PARP-1 activity in different species (Midorikawa et al., 2006). In embryonal mouse neurons the amount of cleaved PARP-1 increases also under growth factor withdrawal and activation of Caspase-3 (Eom et al., 2007).

Compared with recent literature, one possible way regulating the apoptosis is PARP-1. PARP-1 has been shown to interact with p53 (Gueven et al., 2004; Malanga et al. 1998). Tumour suppressors like p53 can excite the intrinsic path by stimulating the expression of pro-apoptotic factors Bax, Bad of the Bcl-2 family resulting in the release of Cytochrome c. The hypothesis that PARPs might regulate cell fate as essential modulators of death and survival transcriptional programs is discussed with relation to nuclear factor kappaB and p53 (Skaper, 2003). After neuronal injury in response to excitotoxins, hypoxia and ischemia, death regulatory molecules like PARP, c-jun, plasma membrane death receptor ligand systems and p53 as key upstream initiator of cell death process have been implicated (Cregan et al., 2002). The excessive activation of PARP-1 can lead to significant decrements in NAD^+, ATP depletion and cell death (suicide hypothesis) (Skaper, 2003). This can play a role for 2D cultivated cells, but not for the 3D cultured hNPCs. From *in vivo* it known that tissue architecture enhances cell survival by modulating mitochondria homeostasis (Igney & Krammer, 2002; Hickman, 2002). This is achieved through activation of pathways that upregulate mitochondrial protectors (Plas & Thompson, 2002). For the 3D culture, one family of proteins called *inhibitors of apoptosis* IAPs can play a role in regulating cell death by inhibiting the process. One member of the IAP family is the human *X-linked inhibitor of apoptosis* (XIAP) an anti-apoptotic protein of the intrinsic pathway. First results show an increase of the XIAP expression of hNPCs in 3D scaffolds compared to 2D culture. The results of the 2D culture demonstrate the same result found by Jaeger (2010), where no up-

regulation of the XIAP expression coupled to the withdrawal of the growth factors was found. ReNcell VM cells show a relative constant expression in proliferation and differentiation.
XIAP binds to Caspase-3 and -7, which are known as the effector caspases in the signalling pathway of apoptosis (Tamm et al., 1998) and following inhibition of Caspase-3, -7, and –9. Therefore the XIAP seem to play an important role in the protection from apoptosis in the 3D scaffolds and the critical point is in the intrinsic pathway by suppressing the activity of caspases and arresting of the apoptotic process.

The next question was if other anti-apoptotic factors are included in the protection of the hNPCs from apoptosis in 3D scaffolds. A most likely possibility is the regulation of apoptosis by members of the Bcl-2 protein family, which control the formation of *Mitochondrial Apoptosis-Induced Channel* (MAC) (Dejean et al., 2006b). MAC is triggering the commitment step of the mitochondrial apoptotic cascade. This ion channel is an early marker of the onset of apoptosis (Guo et al., 2004). To date, the human repertoire of multidomain proteins comprises seven pro-survival members (Bcl-2, Bcl-xL, Bcl-w, Mcl-1, Bcl2l10, Bfl-1 and Bcl2l12), and up to six pro-apoptotic members (Bax, Bak, Bok, Bcl-G, Bcl-rambo and Bfk). The pro-apoptotic members Bax and/or Bak form MAC (Dejean et al., 2006a; Dejean et al., 2005) whereas the anti-apoptotic members like Bcl-2 or Bcl-xL prevent MAC formation and inhibit the release of Cytochrome c to the cytosol (Yang et al, 1997). Bax channel inhibitors (Hetz et al., 2005) and MAC inhibitors (Peixoto et al., 2009) degrade the MAC activity and results in prevention of Cytochrome c release and caspase cascade. Bcl-2 may promote cell survival by interfering with the activation of the Cytochrome c / Apaf-1 pathway through stabilization of the mitochondrial membrane (Fig. 4; Gewies, 2003). The Bcl-2 is one among many key regulators of apoptosis, which are essential for proper development, tissue homeostasis and protection against foreign pathogens (Zahir & Weaver, 2004). Human Bcl-2 is a membrane-associated and promotes cell survival through protein-protein interactions with other Bcl-2 related family members, such as the death suppressors Bcl-xl, Mcl-w and A1, or the death agonists Bax, Bak, Bik, Bad and BID (Dejean et al., 2006a). The anti-apoptotic function of Bcl-2 can also be regulated through proteolytic processing and phosphorylation.
The increased expression of Bcl-2 at 0dd, 7dd and 10dd evidenced that the protective effect of the 3D scaffold plays an important role (Fig. 18). The increase of Bcl-2 and the increase of neural cells at 7dd and 10dd in 3D scaffolds (Fig. 13) showed that Bcl-2 can act as neuron protector in the hNPCs when cultured in 3D scaffolds. Fröhlich et al. (2009) described that

the functional inhibition of Bcl-2 leading to a temporary delayed differentiation, a reduction of neurons and increased Caspase-3 activity. Many studies showed instead that over-expression of Bcl-2 in neural cells leads to increased apoptosis resistance, reduced ß-Catenin cleavage, extensive axon growth, increased expression of neuron specific enolase and decreased activity of pro-apoptotic proteins like Bax and Bak (Martinou et al., 1994; Kranenburg et al., 1996; Brancolini et al., 1997; Zhang et al., 1996; Youle, 2007; Yin et al., 1994; Wang et al., 2006). The high starting concentration of Bcl-2 on day zero in 3D scaffolds can be a reason why the apoptotic events do not increase with starting differentiation of hNPCs in 3D scaffolds. In case the hNPCs induce the Bcl-2 expression in response of stress, it can also be an advice of stress for the cells in 3D scaffolds in the beginning of the cultivation relating to the preparation of the 3D scaffolds. In the literature it is controversially discussed if the increased expression of Bcl-2 is a consequence or the reason of the differentiation. Bcl-2 as anti-apoptotic protein is shown to have regulatory functions in the forming of neuronal differentiation of the human cell line Paju (Zhang et al., 1996). Almeida et al. (2005) and Lonze & Ginty (2002) account the increase of Bcl-2 in differentiating neuronal cells with a Wnt-3a / inactive GSK-3ß induced activity of the canonic Wnt signalling pathway. Otherwise Bcl-2 could regulate the differentiation of neural cells by cell cycle regulation, instead of anti-apoptotic processes (Zinkel et al., 2006). Bcl-2 can as well force a cell cycle arrest in the G0 / G1 phase (Zinkel et al., 2006; Mazel et al., 1996; Middleton et al., 1998). This indicates that the further developing state of the hNPCs during proliferation in 3D scaffolds can also be possible for the high concentration of Bcl-2 in 3D cultures. Further the prevention of apoptosis in 3D could be regulated by cyclin-dependent kinase-5 through ERK-mediated upregulation of Bcl-2 (Wang et al., 2006)

Investigations regarding the regulation of the apoptosis in 3D scaffold could include the determination of the expression of the Bcl-2 antagonists, accordingly pro-apoptotic proteins like Bax and Bak. First results show no difference in the amount of the 21 kDa Bax protein. In 3D scaffolds in the 4 days differentiated hNPCs additional an 18 kDa Bax fragment was found. This indicates a decreased activity of pro-apoptotic proteins, correlated with the increase of Bcl-2 (Yin et al., 1994). Further experiments are necessary to approve the relationship. In case of a parallel activation of the extrinsic pathway for the regulation of apoptosis in the ReNcell VM cells, some key enzymes of this path are interesting. Darios et al. (2003) found a connection between GF withdrawal, intracellular Ceramid increase, Caspase-8 activation, subsequently Bid cleavage and increased neuronal death. Further studies prove this connection, because the phosphorylation and activation of Bak is realised

by activated GSK-3ß (Eom et al., 2007; Linseman et al., 2004; Li et al., 2000; Putcha et al., 2002; Somervaille et al., 2001). Another interesting aspect for the regulation of apoptosis in 3D cultures of hNPCs comes from Vekrellis et al. (1997). They show that the down-regulation of Bax results in reduced apoptotic sensitivity of PC-12 cells. Later studies show that this occurred with a differentiation based protein expression decrease of Apaf-1 and the simultaneous increase of IAPs (Wright et al., 2004; Lindholm & Arumäe, 2004). The high increase of IAPs like XIAP and Bcl-2 in 3D scaffolds supports this hypothesis. Interesting could be further the analysing of the Bax expression in 3D scaffolds, because Bax is downregulated during the development of the nervous system (Vekrellis et al., 1997), and is possible downregulated during differentiation of the hNPCs is 3D scaffolds.

Another *inhibitor of apoptosis* IAP tested in this study was Survivin. Survivin was discovered by its structural homology to IAP family of proteins in human B-cell lymphoma (Tamm et al., 1998). It is known that the protein Survivin is found prevalent in neurogenic regions (Altura et al., 2003; Pennartz et al., 2004) and have dual functions as apoptosis inhibitor and mitosis regulator (Altieri, 2003; Jiang et al., 2005; Dohi et al., 2004; Shankar et al., 2001; Song et al., 2003; Chen et al., 2003a). Survivin inhibiting caspase activation by physically binding to the caspase, thereby leading to negative regulation of apoptosis. As Survivin was detected in hNPCs it was of interest if Survivin is a part of the mechanism to protect the cells in 3D scaffolds from undergoing apoptosis. The results in 2D conditions show that Survivin is highly expressed in proliferated hNPCs, but a lower amount was found in differentiated hNPCs. This is consistent with Jaeger (2010), where Survivin was mainly present in proliferated ReNcell VM cells and decreased under differentiated conditions. This could be in accordance with the fact that Survivin is highly expressed in most human tumours and fetal tissue (Sah et al., 2006) and that the ReNcell VM cells are a cell line with the ability to proliferate under growth factor supplement over many passages (Donato et al., 2007). Interestingly I observed a decrease of Survivin expression in hNPCs proliferated in 3D scaffolds and the differentiated hNPCs showed an additional decreased expression. This in turn is correlated with the decrease of the proliferation activity during differentiation progress of the ReNcell VM cells. As it is known that Survivin is completely absent in terminally differentiated cells (Sah et al., 2006), the decrease was an expected result. Survivin is mostly important for the survival of proliferated cells in the central nervous system of mammals (Jiang et al., 2005). Survivin expression is highly regulated by the cell cycle and is only expressed in the G2-M phase. It controls the cytokinesis by co-localisation with centrosomes

and spindle apparatus (Altieri, 2003). This plays a role in hyperproliferated cancer cells. The decrease of Survivin in proliferated cells of 3D scaffolds indicates that something changed in hNPCs when cultured in 3D scaffolds. A disruption of Survivin induction pathways usually leads to an increase of apoptosis. Either the decreased Survivin expression in 3D scaffolds during proliferation do not leads to increased apoptosis of hNPCs, indicates that the Survivin pathway do not play a role for regulation of the apoptosis in 3D scaffolds for proliferating cells.

The decrease of Survivin in hNPCs proliferated in 3D scaffolds seems to be compensated by the anti-apoptotic protein Bcl-2, as the Bcl-2 expression of proliferated cells in 3D scaffolds was up to 8 folds higher than in 2D cultured hNPCs (Fig. 18). It seems that the protection against apoptosis of the hNPCs in 3D scaffolds starts during the proliferation in the 3D scaffolds and results in a lower increase of apoptosis during differentiation. Further studies may also include the changes during the proliferation period in the 3D scaffolds.

Another question to be asked is, if the decreased expression of Survivin is due to altered with a change in the differentiation state of the hNPCs during proliferation. The hNPCs proliferate 7 days in the 3D scaffold and only a low rate of spontaneous differentiation was observed, terminal differentiation does not really starts. Based on the fact that Survivin is highly expressed in fetal tissue and completely absent in terminally differentiated cells (Sah et al. 2006), Survivin could possibly decrease in neuronal-restricted precursors and further differentiated cells. Therefore, the high amount of PSA-NCAM positive cells in 3D scaffolds can be correlated with the decrease of Survivin. Nearly 40 % of the proliferated cells were positive for PSA-NCAM and consequently more directed to neuronal lineage. This is an additional hint that the developmental state of the hNPCs changed during the culturing in 3D scaffolds. The molecular mechanism of Survivin regulation is not well understood. But Survivin is upregulated by beta-catenin and a direct target gene of the Wnt pathway (Olie et al., 2000). Therefore may be correlated with the differentiation.

Taken together growth in 3D per se appears to induce fundamental change in cell physiology and to regulate cell responsiveness to apoptotic stimuli, and appears to be linked to cell adhesion (Zahir & Weaver, 2004). The mechanisms whereby adhesive interactions regulate the spatio-temporal viability of cells in tissues are poorly understood. During tissue development ECM-dependent activation of integrins has been implicated in cell survival (Zahir & Weaver, 2004). The enhanced survival of the hNPCs in 3D scaffolds can be triggered by synergistic interactions between activated integrins and growth factor receptors,

because the supplemented laminin, as a member of the ECM, could mimic ECM-cell interaction. Such crosstalk facilitates stimulation of associated signalling molecules such as focal adhesion kinase, *tyrosinkinase* src, integrin-linked kinase, *mitogen-activated protein kinase* (ERK) and *phosphinositide 3-kinase* (PI3-K). These signalling cascades then actively repress cell death by increasing the expression and / or activity of anti-apoptotic molecules including bcl-2 family dimers, and *kappa-light-chain-enhancer* NFkB and *protein kinase B* (AKT) which in turn regulate expression of molecules such as folkhead and IAP proteins (Zahir & Weaver, 2004).

Also the polarity of the peptide scaffold can play a role in apoptosis resistance of the hNPCs in 3D scaffolds. Boudreau et al. (1996) found that polarized mammary structures are able to sustain long term viability in culture and are able to resist multiple extrinsic and intrinsic apoptotic stimuli (Weaver et al., 2002). This depends upon laminin induced ligation of α6ß4 integrin which activate NFkB and induce tissue polarity and apoptosis in 3D structures through PI3-K and ERK-independent activation of RAC (GTPase) (Zahir et al., 2003). Further studies are necessary to achieve this.

5.1.5. Challenges using 3D culture systems

The 3D culture based on self-assembling peptide hydrogels provides a lot of advantages regarding differentiation and survival of the cells discussed above. However, some more technical aspects appeared to limit the use of the 3D scaffolds. The huge number of cells inside the scaffolds was shown to provide problems during microscopy, high background and auto-fluorescence of the samples makes it difficult to test some new antibodies. In addition cells cultured inside 3D scaffolds cannot be used directly for functional assays like electrophysiological recordings.

The mechanical treatment used to release the cells from the 3D scaffolds could provide breaks of outgrowth, which influence the measurement via flow cytometry. And do not forget the high variance between experiments and the resulting additional work and expense for truly statistical analysing. The variance of the experiments may result of normal behaviour of the cells, little changes in treatment, little temperature and pH changes. This can influence the cells, but also the self-assembling of the scaffolds. All handling of the 3D scaffolds had been standardised and were done as best as possible. The used cell line is known to consist of NSC and NPC (Donato et al., 2007) and varied from batch to batch. Also the scaffold plays a role

in the variance, the third dimension enforce this additional. The self-assembling of the peptide sequences can be influenced on differ temperature, pH and percussion. Some studies focus on more controlled self-assembling of scaffolds not based on peptides (Perale et al., 2011) But the peptides, described above, especially the functional peptides were effective for the cells. The use of a template molecule to control the length of a self-assembling nanofibre of peptide amphiphiles is more interesting (Moxham, 2008). Further studies show that the creation of functional scaffolds changes the self-assembling and stiffness, that the scaffolds were able to recover from breakdowns of the scaffolds (Gelain et al., 2011). These possibilities provide more controllable conditions in 3D scaffolds for future approaches.

5.2. Differentiation and apoptosis of hNPCs inside modified 3D scaffolds

Along with biochemical modifications, surface characteristics of the underlying material such as hydrophobicity, charge, and mechanical compliance are also important surface cues, which substantially affect cellular responses (Brodbeck et al., 2001; Allen et al., 2003; Pelham & Wang, 1997).

The aim of the second part of my study was to examine the influence of modified PuraMatrix formulations. In this modified matrices short functionally amino acid sequences were incorporated to the RADA-16 backbone of the hydrogel matrices to improve cell adhesion and differentiation (Fig. 3). The both modified RADA16-I formulations used for this study were provided from BD Bioscience. The SDP-peptide, a cell adhesion motif in laminin (Ac-$(RADA)_4$-GGSDPGYIGSR-NH_2), is described to promote cell adhesion and extensibility of neural cells (Gelain et al., 2006). The PFS-peptide is a motif of the bone marrow homing factor (Ac-$(RADA)_4$-GGPFSSTKT- NH_2) and is thought to improve the differentiation of neural stem cells to neural cell and extension of neural cells (Gelain et al., 2006; Taraballi et al., 2010).

In the modified 3D scaffolds also the growth pattern was analysed. The observed neurosphere like growth of hNPCs (Fig. 20A, C, E) is known from Thonhoff et al. (2008) and Ortinau et al. (2010). The expectation that the modified matrix with the SDP-peptide also increase the attachment of hNPCs on the scaffold, which is known from 3D scaffolds supplemented with laminin (Fig. 6A, C), was not observed. The same spheroids like growing, as described for the

PM and the PM-PFS scaffold, was found (Fig. 20A, C, E). The spheroid like growing of the cells inside the modified matrices can direct to problems in visualisation under the microscope, preparation and separation for flow cytometric analysis. I suggested that the SDP peptide was not ideal for the attachment of the hNPCs, because there was no difference to the control. The SDP peptide could influence the hNPCs in a different way. From literature is known that the interactions between cells and hydrogel depend on the chemical properties of the polymers and on the presence of biologically active molecules exposed at the surfaces (Woerly et al., 2008). Cell adhesion and neurite outgrowth-promoting sites have been identified in the C-terminal site of α1 and α2 chain of laminin (Tashiro et al., 1989; Skubitz et al., 1991; Calof et al., 1994; Richard et al., 1996; Nomizu et al., 1995) in the cross-region of the molecule (Edgar et al., 1984, Tashiro et al., 1994), in the γ1 chain (Liesi et al., 1989 & 1992; Nomizu et al., 1997) and in the N-terminal region of the α2 chain (Nomizu et al., 1996). May be sequences of other regions in the laminin provide the possibility to enhance the attachment of the hNPC.

Besides the growth, the modified 3D scaffolds PM-SDP and PM-PFS were analysed regarding the neuronal differentiation. The results demonstrated an increased expression of ßIII-tubulin of cells differentiated in the modified 3D scaffolds (Fig. 21A). The enhancement of ßIII-tubulin up to 4.2 fold for PM-SDP scaffolds and 5.3 fold for PM-PFS scaffold exceed the expectations for this cell line. In Gelain et al. (2006) it was showed that the PuraMatrix hydrogel with such modified peptide sequences induced the neuronal differentiation of murine neural stem cells. Especially for the BMHP from the bone marrow homing factor, this is similar to the PFS-peptide.

Regarding the used cell line such high number of ßIII-tubulin positive cells is described for the first time. Usually 95 % of the ReNcell VM cells differentiate to GFAP positive cells and only 3% to the neuronal linage. A lot of applications of small molecules (Schmöle et al., 2010) as well as the activation of the Wnt pathway (Hübner et al., 2010) were shown to improve the differentiation of the ReNcell VM cells into neuronal direction. Although the observed changes in the number of neuronal phenotypes were small. This could be based of the unknown composition of neural stem and neural progenitor cells (Donato et al., 2007). The shift from two dimensional monolayer to 3-dimensional environment to create more physiological conditions leads to a significant increase of neuronal phenotypes as described above (Fig. 14) and in Ortinau et al. (2010). But this cell line needs more direction to induce the differentiation potential. This was shown in Morgan et al. (2011) by co-cultivation of

hNPCs with brain slice culture. The direct contact of these cells with primary rat NPCs or brain slice culture results in functional active neuronal cells.

Coming back to the modified 3D scaffolds it is known that, modified self-assembling 3D scaffolds with functional motifs promote neuronal differentiation of adult mouse neural stem cells (Gelain et al., 2006; Taraballi et al., 2010). Taraballi et al. (2010) also showed that the addition of glycine linker between the backbone of the PuraMatrix peptide and the functional motive increases the effect additionally. The possibility to induce the potential of the ReNcell VM cells via modified 3D scaffolds is a big step in controlling the neuronal differentiation and to push NPCs in the neuronal direction. The observed decreased expression of astrocytes enforces this hypothesis (Fig. 21C).

But why does the scaffold modified with the functional peptide sequence have such effect on the hNPCs? The SDP-peptide a cell adhesion motif in laminin (Ac-$(RADA)_4$-GGSDPGYIGSR-NH_2) is due to promote cell adhesion and extensibility of neural cells (Gelain et al., 2006). Laminin is usually used in our lab as functionalisation of surfaces of culture dishes for attachment of hNPCs on surfaces. As some studies show that the use of mouse laminin for human stem cells can be disadvantageous for the differentiation (Rodin et al., 2010), it is important to use only the functional sequences (Silva et al., 2004) or domains (Nomizu et al., 1995; Tashiro et al., 1994; Nomizu et al., 1997) of laminin not the whole protein. A wide variety of signalling peptides derived from laminin were described, which have the potency to interact with neurite outgrowth and differentiation (Powel et al., 2000). The well described laminin epitope IKVAV was used to functionalise surfaces (Kam et al., 2002; Tong & Shoichet, 2001; Li & Chau, 2010) and 3D scaffolds (Silva et al., 2004). Silva et al. (2004) were able to demonstrate that the IKVAV, integrated into a 3D matrix, was able to initiate neuronal differentiation of murine NPCs. Wei et al. (2007) showed that hyaluronic acid hydrogels with IKVAV peptides has the potential for tissue repair and axonal regeneration in an injured rat brain. These signalling peptides might act different depending on various cell types; therefore pre-test of the signalling peptides for their effect on the desired cell line could necessary before using them in a 3D approach. The SDP-peptide acts similar to these sequences regarding the potential to initiate neuronal differentiation and can used as a source to induce neuronal differentiation of hNPCs, especially for human cell lines like the ReNcell VM cells.

The PFS-peptide (Ac-$(RADA)_4$-GGPFSSTKT- NH_2) based on the Bone marrow homing peptide (BMHP) which functional motif (PFSSTKT) was demonstrated to stimulate neural

stem cell (NSC) viability and differentiation when linked to self-assembling peptide hydrogel (Gelain et al., 2006). Gelain and his co-workers also tested another motif, BMHP1 (SKPPGTSS). Both belong to a family of peptides (bone marrow homing peptides) rich in K, P, F, S, and T. They have been shown to home into bone marrow *in vivo* (Nowakowski et al., 2004). Bone marrow is one source of adult stem cells, which have the ability to differentiate into endothelial, muscle and connective tissue and neuronal cells. It is likely that bone marrow cells have some of the same differentiating pathways and adhesion receptors as NSCs (Gelain et al., 2006). Bjornson et al. (1999) for example demonstrated the possibility to turning brain into blood, in which a haematopoietic fate adopted by adult neural stem cells *in vivo*. Whereas bone marrow stromal cells extensively proliferate, migrate into the lesion, and express the neural cell markers and improving neurological function, when transplanted into animal models of cerebral infarct (Chen et al., 2001, 2003b; Shichinohe et al., 2004; Yano et al., 2005b), traumatic brain injury (Mahmood et al., 2003 & 2006), and spinal cord injury (Chopp et al., 2000; Lee et al., 2003; Yano et al., 2005a). That means transplantation of hSC / PC from bone marrow into the hippocampus of mice is able to promote neurogenesis of endogenous NSCs (Munoz et al., 2005). Also the survival of neuronal cells could be increased. The stromal cell-derived factor-1α, involved in the trafficking of haematopoietic stem cells from bone marrow to peripheral blood, was found to extent neuroprotectic effects that rescued primary cortical cultures from H_2O_2 neurotoxicity, and to modulate neurotrophic factor expression (Shyu et al., 2008). Kabos et al. (2002) described the *in vitro* generation of NPC from whole adult bone marrow. As well encapsulation in 3D scaffolds provides the possibility for differentiation of human bone marrow mesenchymal SC into nerve cells (Wang et al., 2010). Multiple mechanisms are possible for this phenomenon. Jori et al. (2005) emphasized the importance of cAMP and MEK-ERK MAP kinase in neural differentiation of bone marrow SC. The used PFS-peptide could increase the neuronal differentiation of hNPCs by the activation of the MEK-ERK MAP-kinase.

Further investigation of the modified scaffolds by Gelain et al. (2011) described a novel ensemble of self-assembling peptides developed from bone marrow homing factor with additional motives. Thirty-two sequences, including biotinylated and unbiotinylated sequences, as well a hybrid peptide-peptoid sequence were designed. Most show self-healing properties mean they recover their stiffness after rupture of the assembled gels. This enlarges the set of potential applications of these novel self-assembling peptides. The RGD-functionalisation (adhesion peptide, Arg-Gly-Asp) and the hybrid peptide-peptoid self-assembling sequences opened the door for additional functionalisation with further bioactive

motifs like IKVAV or the *neural adhesion molecule* L1 (Gelain et al., 2011; Azemi et al., 2008). L1 is expressed in developing and differentiated neurons of the central nervous system and Schwann cells of the peripheral nervous system, and can specifically promote neuronal attachment, neurite outgrowth and neuronal survival *in vitro* (Lagenaur & Lemmon, 1987; Lemmon et al., 1992; Dihné et al., 2003). Coating of the L1 bio-molecule on a silicon surface or polystyrene substrates show higher levels of neuron attachment and neurite outgrowth, while inhibiting the attachment of astrocytes (Azemi et al., 2008) as well as the astrocytic differentiation of NPCs (Lagenaur & Lemmon, 1987; Lemmon et al., 1992; Dihné et al., 2003). Interesting for further studies is the question, if PM-PSF scaffolds, additionally modified with L1, can induce the attachment of the hNPCs while inducing neural differentiation and suppressing differentiation of astrocytes.

In consideration of the PSA-NCAM expression the expectations were not delivered in modified 3D matrices. 2D culture compared with 3D scaffolds show a high increase of PSA-NCAM in 3D scaffolds that leads to the conclusion that 3D culture results in an increase of the progenitor pool. The PSA-NCAM expression of hNPCs in the modified matrices is equal to the expression in pure PuraMatrix, this indicates that the modified scaffolds increase the ßIII-tubulin expression but do not enhance the progenitor pool in additive manner in hNPCs like known from PuraMatrix without modifications.

Based on the induced neuronal differentiation of the modified 3D scaffolds and on increased PSA-NCAM and increased ßIII-tubulin expression, it was of great interest if the modified scaffolds are able to produce functional active neural cells. In a first step immunocytochemical staining against synaptic marker were done. Synaptophysin as a presynaptic marker and PSD95 as postsynaptic marker were chosen for the staining. Synaptophysin is a synaptic vesicle glycoprotein. It is present in neuroendocrine cells and in virtually all neurons in the brain and spinal cord that participate in synaptic transmission. Thus it is used for immunostainings and for quantification of synapses (Calhoun et al., 1996). It interacts with the essential synaptic vesicle protein synaptobrevin (McMahon et al., 1996). PSD95 (postsynaptic density protein 95) also known as *synapse-associated protein 90* SAP-90 and is a member of the *membrane-associated guanylate kinase* MAGUK family. It is almost exclusively located in the postsynaptic density of neurons and is involved in anchoring synaptic proteins (Hunt et al., 1996). In 2D culture no positive staining of both antibodies was found. Either the immunocytochemistry staining in 3D scaffolds were problematical because of background and auto-fluorescence of the huge number of cells. After reculturing of the hNPCs, which differentiated before in PM-PFS scaffolds, on coated cover slips were only few

PSD95 positive cells monitored. This indicates that the hNPCs cultured in PM-PFS scaffolds were able to build functional active neuronal cells. The increased expression of the PSA-NCAM of hNPCs in 3D scaffolds opens the door for further changes in the cell line, as PSA-NCAM may be related to synaptic rearrangement and plasticity (Muller et al., 1996).
The measure of functional activity of hNPCs differentiated in modified 3D scaffolds is inside the scaffold not possible. The differentiated cells had to be recultured on cover slips. First results of patch clamp studies, done in cooperation, indicated an evaluated number of cells expressing functional Na+ channels. Here 7 % of cells differentiated in PM expressed functional Na+ channels, in comparison to 12 % and 20 % of cells hosted in PM-SDP and PM-PFS (Liedmann et al., 2012b). That leads to the importance of using directed functionalised 3D scaffolds or modified surfaces to induce neuronal differentiation and to produce functional active neuronal cells *in vitro*.

If enhanced survival plays a role for the induced neuronal differentiation in the modified 3D scaffolds, the modified scaffolds were tested for apoptotic events. The apoptosis of the hNPCs in both modified scaffolds was not significant different to the control considering all cells of the scaffold (Fig. 23A) or only the neuronal cells (Fig. 23B). Also the amount of early and late apoptotic cells did not differ significant from the control. Nearly the same number of early and late apoptotic cells was found in PM-SDP, PM-PFS scaffold and in the control. That leads to the conclusion that the modified 3D scaffolds protect the encapsulated cells in the same manner like the 3D scaffolds described in chapter 5.1.3., that and the increased survival was not only the reason for the increased ßIII-tubulin expression of hNPCs in modified 3D scaffolds. Possible for the induced differentiation is the combination of inhibited apoptosis of the 3D environment (chapter 5.1.4.) and activation of the MAPK/ERK pathway by the peptide sequences.

5.2.1. Outlook for modified 3D scaffolds

Further development of functionalised scaffolds for co-cultivation of multiple cell types like primary neuronal or bone marrow cells can induce differentiation and further to functional active networks of neuronal cells types *in vitro*. Morgan et al. (2011) showed that the cultivation of hNPCs on hippocampal slice cultures results in neuronal cells positive for synaptic marker. The functional network integration of embryonic stem cells-derived astrocytes in hippocampal slice cultures by gap junction-mediated coupling between donor

and host cells permits widespread delivery of dye from single donor cells (Scheffler et al., 2003). Also Namba et al. (2007) showed that the co-culture of neural precursor cells with hippocampal slice cultures efficient neuronal production. The transplantation of hSC/PC from bone marrow into the hippocampus of mice promotes neurogenesis of endogenous NSCs (Munoz et al., 2005).

The additional modification of the PM-PFS scaffold with the cell adhesive peptide RGD or L1 (Lagenaur & Lemmon, 1987; Lemmon et al., 1992; Dihné et al., 2003) may improve the adhesion of the hNPCs on the scaffold and to reach more spreading of the cells and prevent neurospheres like growing in the PM-PFS scaffold. To simplify the culture conditions for further molecular assays, go away from encapsulation, cell seeding on surface of the scaffold (Holmes et al., 2000) or coating of a monolayer culture with the scaffold (Semino et al., 2004) could be an alternative.

As 3D culture enhances the PSA-NCAM expression, it opens the door for further experiments. The hNPCs could proliferate in 3D scaffolds for 7 days and recovered, marked alive against PSA-NCAM and subsequently sorted with a FACS sorter. The PSA-NCAM positive cells could be recultured to increase the neuronal phenotypes. Ekici et al. (2008) for example discriminate neuronal progenitors of a ReNcell VM culture and produce an adapted cell line. For additional improving of the neuronal differentiation of the separated cells, they could be encapsulates again by using the PM-PFS scaffold.

5.3. Could the use of the soluble PFS peptide sequence as supplement for monolayer culture of hNPCs imitate the effect of the PFS scaffold?

To overcome some technical drawbacks of the 3D culture, some experiments with the soluble PFS-peptide were done in the 2D culture system. This part is focused on first experiments with the soluble peptide sequence PFS to show if the peptide it self is able to enhance the neuronal differentiation. The question if the PFS-peptide alone induces the differentiation of the hNPCs by simply supplement of the peptide could be answered easily. No effect was found. Induction of neuronal differentiation by supplement of substances is described in many studies. Schmöle et al. (2010) showed that the addition of small molecules to monolayer cultures of hNPCs is able to influence or in best case increase the differentiation towards neuronal phenotypes. Synthetically produced *tyrosine-rich amelogenin peptide* TRAP and its unique C-terminal 12 amino acid sequence (TCT) is shown to suppressed bone-forming cells,

whereas *leucine-rich amelogenin peptide* LRAP and its unique C-terminal 23 amino acid sequence (LCT) markedly enhanced terminal differentiation of bone-forming cells (Amin et al., 2012). The supplementation of soluble inhibitory peptide sequences instead was shown to decrease neurite extension on 2D collagen substrates and within 3D collagen gels (Blewitt & Willits, 2007). Some examples using soluble peptide sequences could found, but most studies focus about coupled peptide sequences on surfaces or scaffolds. This could be the reason for the result. The hNPCs seem to need another presentation of the peptide sequence. The presentation of the peptide can be important for the cell reaction, therefore no higher amount of ßIII-tubulin in hNPCs could be detected in monolayer culture with PFS-peptide supplement. Surface modulation or coating with the peptide, which is described in many studies (Tashiro et al., 1989; Kam et al., 2002; Nomizu et al., 1995; Tong & Soichet, 2001), is more usefully. One possibility is electrospinning. This method is used to create thin films of different coating designs (Buchko et al., 1999). The peptide coating of cover slips via glycinee spacer could be another possibility. It is shown that glycinee as linkers between the self-assembling peptides and the motifs can increase the differentiation of neural cells (Taraballi et al., 2010). The use of functional sequences is well described in the literature. One example is the pentapeptide epitope *isolucine-lysine-valine-alanine-valine* IKVAV-peptide, this improve the neuronal differentiation in surface modulation (Tashiro et al., 1989; Kam et al., 2002; Nomizu et al., 1995; Tong & Soichet, 2001) and in 3D scaffolds (Gunn et al., 2005; Silva et al., 2004; Wei et al., 2007; Sreejalekshmi & Nair, 2011). Silva et al. (2004) describe the incorporation of the epitope IKVAV into a peptide amphiphile nanofiber scaffold, which results in selective differentiation of NPCs. Interestingly, not all cells do act in a similar way to those peptides; the neurite outgrowth activity of some sites is cell type specific (Richard et al., 1996; Malinda et al., 1999; Ponce et al., 1999). More over the orientation or the presentation of the peptide to the cells is important. If the IKVAV-peptide is linked not on the terminal site but between two self-assembling RADA-16 peptides, which change the presentation of the peptide to the cells, no neurite outgrowth of PC12 cells encapsulated in 3D scaffolds could be detected (Li & Chau, 2010). Additional glycinee spacer between the self-assembling RADA-16 peptide and the functional motif sequence change the differentiation potential (Taraballi et al., 2010). Longer spacer of glycinees, the more effective is the functional motif in eliciting NSCs adhesion, improving their viability and increasing their differentiation, because bioactive motifs are more exposed to the solvent. They concluded that the presentation of the functional peptide plays an important role in the 3D culture. Gelain et al. (2011) showed that the modification of the peptide, the biotinlylation and the RGD

functionalisation shift the properties of the scaffolds and the differentiation properties of the cells. RGD unit enhance the adhesion of cell to the surface of the hydrogels.

Thus the stiffness of the surrounding matrix is important and has implications on development, differentiation, disease, and regeneration (Discher et al., 2005). Plating cells on hydrogels with controllable stiffness has identified how mechanical parameters affect cell behaviour (Pelham & Wang, 1997). For instance, substrate stiffness modulates cell motility and spreading (Pelham & Wang, 1997), and through alterations in the cell shape it is able to modulate gene expression (Maniotis et al., 1997). Mechanical and biochemical properties of an aNSC microenvironment can turn to regulate the self-renewal and differentiation of aNSCs. (Saha et al., 2008). Synthetic, interfacial hydrogel culture systems, termed *variable moduli interpenetrating polymer networks* vmIPNs, are used to assess the effects of soluble signals, adhesion ligand presentation, and material moduli on adult neural stem-cell behaviour. The proportion of neurons versus glia is a strong function of elastic modulus, softer gels favoured neurons, and harder gels promoted glial cultures. The stiffness of materials required for optimal neuronal growth, characterized by an elastic modulus of several hundred Pa, is in the range measured for intact rat brain (Georges et al., 2006). Brain is a soft tissue and has an elastic modulus ~10 times softer than liver and nearly 50 times softer than muscle (Discher et al., 2005). The rate of human mesenchymal SC proliferation increased with the decrease in stiffness of the hydrogel (Wang et al., 2010). Also the neurogenesis of human mesenchymal SC was controlled by the hydrogel stiffness in a 3D context, they expressed more neuronal protein markers in hydrogels with lower stiffness (Wang et al., 2010). Turning the mechanical properties of a synthetic culture substrate offers a means to modulate or control neural stem-cell behaviour (Saha et al., 2008). The effect of gel stiffness on neurite extension is described in many studies for different hydrogels synthetic as well as natural hydrogels (Willits & Skornia, 2004; Gunn et al., 2005). That indicates that not only the 3D culture also the mechanically properties of hydrogels have a strong influence on the differentiation of neural stem cells which are sensitive to the mechanical properties of surrounding or underlying environment.

Apart from the mechanical stiffness and the presentation of the functional motif the modified 3D scaffold with the PFS-peptide seem to be ideal for the differentiation of the hNPCs. The elasticity of the PuraMatrix is attributed to a network nanostructure consisting of fibrous self-assemblies. The stiffness of this scaffold is in the same range of the native brain tissue and the presentation of the functional motif is good as well (Taraballi et al., 2010). All these facts and the advantages of the 3D environment together, like the architecture and the overall contact

between the cells and the scaffold, play a big role in the high increase of neuronal cells. This could never be mimicked by 2D culture systems. The coating with the peptide could support the differentiation, but not in the same range of the PM-PFS scaffold.

5.4. Effect of laminin supplement on differentiation and survival of hNPCs in modified 3D scaffolds

Different laminins show various expression patterns as well as tissue-specific locations and functions. LN-211 and LN-221 are primarily present in basement membranes of muscle cells and motor neuron synapses (Miner & Yurchenco, 2004). LN-332 is specific for subepithelial basement membranes (Kallunki et al., 1992), LN-411 is located in subendothelial basement membranes (Iivanainen et al., 1997), LN-511 is expressed ubiquitously (Miner et al., 1995), and LN-111 is restricted to the early embryo and certain epithelial cells (Ekblom et al., 2003). The influence of laminin 1 on growth, differentiation and survival of hNPCs encapsulated in modified PM-PFS scaffolds was analysed in this part to compare the results with the PML scaffold (5.1.). The functionalisation of the scaffolds with laminin supports cell adhesion and prevents the formation of neurospheres (Fig. 6A, C). Ortinau et al. (2010) showed that the growth pattern of the hNPCs can influence the differentiation. The supplementation of laminin and the following changing of the spreading of the cells in the 3D scaffolds can also influence the neuronal differentiation of the hNPCs in the PFS-scaffolds. Therefore four different conditions were compared, PM, PML, PM-PFS and PML-PFS scaffolds. The better spreading and decreased spheroid like growing of the hNPCs in the PML scaffold was already show from PML-PFS scaffolds (Fig. 27). The main result of the quantification of neuronal marker was that the positive effect of the PM-PFS scaffold is decreased when the PM-PFS scaffold was supplemented with laminin (PML-PFS) (Fig. 28). The decrease of ßIII-tubulin at 10dd in PML and PML-PFS scaffolds may results on the kind of growth inside the matrix, whether the cells are distributed or growth in spheroid like manner. The HuC/D expression was significant decreased in PML-PFS scaffold compared with the PM-PFS scaffold. The laminin in 3D scaffolds was usually shown to induce the enhancement of neurite outgrowth of neural cells (Labrador et al., 1998; Yu et al., 1999; Rangappa et al., 2000; Koh et al., 2008; Ortinau et al., 2010). As it was shown in literature that the use of laminin for 3D scaffolds induces the neuronal differentiation, I conclude that the changed distribution of the cells is the underlying effect for the decrease. The cell line is well described and it is known that the differentiation is induced if the distance between the cells is smaller and reduced if the

distance between the cells is higher (Donato et al., 2007). They suggested that this might be based on the fact that the isolation protocol of the ReNcell VM cells resulted in a bulk-like and not clonal cell isolate. The addition of laminin can also change the self-assembling of the scaffold peptides as described from Ortinau et al. (2010). The length and the fibre diameter of the nanofibers in the PM-PFS scaffold could be changed, resulting in little changed environment for the hNPCs.

If the supplement of laminin can influence the differentiation, the survival of the cells could also be effected. Considering the survival of the hNPCs (Fig. 30) a prominent difference was found between the culture conditions with and without laminin. Regarding the number of cells in an early state of apoptosis, in culture conditions with laminin, namely 2D cultures, PML and PML-PFS scaffolds, the amount was higher in comparison to 3D scaffolds without laminin (Fig. 30). In 3D scaffolds without laminin, namely PM, PM-PFS and PM-SDP scaffolds, the ratio of early and late apoptosis was equal (Fig. 30, left panel). Laminin can have an impact on the cells in three ways. At first the addition of laminin to a 3D scaffold or the coating of a surface for 2D cultures, will change the attachment, distribution and finally the growth of the hNPCs. The used cell line is growing in neurospheres in absence of laminin coating (Donato et al., 2007). The contact of cells inside the neurospheres is very close. The neuronal differentiation and the survival of the hNPCs are known to be increased in neurospheres (Donato et al., 2007). The integrin expression observed in spheroids resembles quite closely the expression pattern found in *in vivo* and the amount of cell–cell contacts and the spheroid microenvironment can modulate the integrin expression (Waleh et al., 1994). The spheroid like growing of the hNPCs in 3D scaffolds without laminin provides more direct contact of cells among each other, than in 3D scaffolds with laminin. Using laminin modified scaffolds can support the attachment and viability of PC12 cells (Koh et al., 2008). But laminin has a higher tendency to promote neurit outgrowth than to enhance viability of nerve cells (Luckenbill-Edds, 1997).

A second aspect is the used laminin. In this study laminin 1 obtained from mice was employed to supplement the matrices or to coat 2D culture dishes. The combination of human cells with mouse laminin might be not optimal. Rodin et al. (2010) described that the use of human recombinant laminin-511 for culturing hES and iPS cells supports the adhesion, the survival and the self-renewal. The laminin is shown to interact with surface receptors, such as integrin receptors $\alpha1\beta1$, $\alpha6\beta1$ and $\alpha6\beta4$, to activate signalling pathways that influence cell

viability and functions (Chen & Strickland, 2003). This may result in different mechanisms to enhance neurit outgrowth and neuronal differentiation.

Third, atomic force microscopy studies in Ortinau et al. (2010) show that the different growth patterns are linked to the assembly of the 3D scaffolds. The matrix structure is build from beta-sheets and aggregates or bundles of those. The supplement of laminin to the scaffold directly influences the formation of the PuraMatrix scaffold by increasing the number of aggregates and increases the distance between fibres by shifting the composition of beta-sheets and bundles more towards the bundles. This changes the stiffness and the stability of the scaffold, which can also influence the cells inside the scaffolds regarding survival and differentiation. This fact enforces the trend to use only the functional sequences and not the whole protein. Surface modulation adjusted for the cells and the application were possible also for 2D culture conditions. As described above (5.1.4.) that the high number of early apoptotic cells is not correlated with the onset of the caspases during apoptosis, indicates that the distribution of the hNPCs inside the scaffolds makes the cells be more vulnerable to changes during cultivation and the shift from proliferation media to differentiation media. The survival signals, which come from cell surface adhesion, must be substituted by those arising from cell–cell contact (Dainiak et al., 2008). Dainiak et al., 2008 demonstrate that formation of aggregates enhanced resistance of the cells grown on these matrices to the drug treatment.

Regarding the neuronal cells, they were influenced by laminin. The increase of apoptotic events in neuronal cells at 4dd and the following decrease at 7dd in the PML-PFS scaffold indicated that the apoptosis is mainly completed and the Surviving neurons were hardened. It also may compensate of new generated neurons.

Li et al. (2007) suggest complex cell-material interactions, in which the dimension of the culture material influences gene expression and cell spreading and the structural and mechanical properties of the culture material influence gene expression and neurite outgrowth. The cells exhibited differential expression of genes in collagen I, including those relevant to cytoskeleton, extracellular matrix, and neurite outgrowth via microarray analysis. *Real-time reverse transcriptase polymerase chain reaction* experiments (RT-PCR) compared collagen I and matrigel show differentially regulating genes associated with actin in similar patterns and the expression of the gene encoding for neurofilament varied with the type of material. RT-PCR and microarray analysis comparing 2D culture and the 3D scaffolds formulations could test whether the differential growth and gene expression reflected influences of culture dimension or culture material.

6. Conclusion

Conventional cell culture studies have been performed on 2D surfaces, resulting in flat, extended cell growth. More relevant studies are desired to better mimic 3D *in vivo* tissue growth. Effective generation of patterned 3D cultures will lead to improved cell study results by better modelling *in vivo* growth environments and increasing efficiency and specificity of cell studies. The self-assembling peptide hydrogel provide a good *in vitro* environment for hNPCs, because neuronal differentiation of the hNPCs was increased in all tested 3D culture conditions compared to 2D culture. This study demonstrates that the 3D culture increase the survival of the hNPCs compared to standard monolayer culture, providing a good architecture to mimic natural environment of these cells. The apoptosis is regulated in a different way like known from 2D culture, where the intrinsic pathway is the critical point, indicated by the decrease of Caspase-3 and PARP-1 expression in the 3D scaffolds. The hNPCs seems to be protected from apoptosis by increased expression of inhibitor of apoptosis like Bcl-2, by preventing the formation of *Mitochondrial Apoptosis-Induced Channel* and inhibiting the release of Cytochrome c to the cytosol, and XIAP, by suppressing the activity of caspases and arresting of the apoptotic process. I conclude that the hNPCs especially the neuronal cells survive longer in 3D scaffolds, indicated by the shift of the ßIII-tubulin positive cells from 4dd to 7dd in 3D scaffolds. Another possibility for the significant increase of ßIII-tubulin positive cells is a change of the developing state of the hNPCs during the proliferation in the 3D scaffolds into neuronal restricted precursor cells, indicated by the significant high increase of PSA-NCAM and the decrease of Survivin.

The modified PuraMatrix formulation enhance the neuronal differentiation of the hNPCs resulted in a 2 –3 times significant higher amount of ßIII-tubulin positive cells. The modified scaffolds seem to protect the differentiating hNPCs in the same manner like the PML scaffold. The hNPCs in modified scaffolds use the induced progenitor pool to differentiate into neuronal phenotype. That leads to the conclusion that the incorporated peptides of the modified 3D scaffolds were really able to enhance the differentiation of the hNPCs and that most likely not a single mechanism underlies the increased proportion of neuronal cells but a combination of an elevated neuronal differentiation and a protective effect of the modified matrices on the neuronal cells.

The addition of laminin to the PFS scaffold increases the attachment, but influences the cells regarding the apoptosis. The spheroid like structure seems to be protecting the hNPCs from outer factors like growth factor withdrawal resulting in less number of cells affected from early apoptotic events. The limitation of nutrients and oxygen, which occur sometimes in the middle of neurospheres, can also limiting the positive effect, shown by the little increase of cells in the late apoptosis in scaffolds without laminin.

The study shows that not only the 3D microenvironment is of importance. More directed functional biomaterials are needed for different cell types or different usage to induce neuronal differentiation and produce a functional neuronal networks for neural regenerative medicine applications. The simply functionalisation with biologic active peptides of theses scaffolds suited for the user needs, make it attractive as well. The tested modified scaffolds with incorporated peptide sequences increase the differentiation additional toward neuronal phenotypes. The potential of the resulting cells to communicate by building active synapses open the door for clinical applications. The next generation of biomaterials for neuroscience research does not only act as architecture for seeding and natural environment, they are functionalised with biological signals to control the differentiation of stem cells or progenitor cells transplanted or of endogenous sources. This controlled neural differentiation of hNPCs might become an important source for cell replacement therapies in the field of neurodegenerative diseases like Alzheimer's disease, Parkinson and Huntington's disease.. The field of tissue engineered scaffolds play an increasing role in methods for the treatment of neurological disorders like traumatic brain injury and stroke. Scaffolds with nanoscale features like the PuraMatrix have the potential to improve the specificity and accuracy of materials for a number of neural-engineering applications, ranging from neural probes for Parkinson's patients to guidance scaffolds for axonal regeneration in patients with traumatic nerve injuries.

7. References

Ahmed Z, Underwood S, Brown RA. Nerve guide material made from fibronectin: assessment of in vitro properties. Tissue Eng. 2003 Apr;9(2):219

Akdemir ZS, Akçakaya H, Kahraman MV, Ceyhan T, Kayaman-Apohan N, Güngör A. Photopolymerized injectable RGD-modified fumarated poly(ethylene glycol) diglycidyl ether hydrogels for cell growth. Macromol Biosci. 2008 Sep 9;8(9):852-62.

Allen LT, Fox EJ, Blute I, Kelly ZD, Rochev Y, Keenan AK, Dawson KA, Gallagher WM. Interaction of soft condensed materials with living cells: phenotype/transcriptome correlations for the hydrophobic effect. Proc Natl Acad Sci U S A. 2003 May 27;100(11):6331-6.

Almeida M, Han L, Bellido T, Manolagas SC, Kousteni S. Wnt proteins prevent apoptosis of both uncommitted osteoblast progenitors and differentiated osteoblasts by beta-catenin-dependent and -independent signaling cascades involving Src/ERK and phosphatidylinositol 3-kinase/AKT. J Biol Chem. 2005 Dec 16;280(50):41342-51.

Alsberg E, Anderson KW, Albeiruti A, Rowley JA, Mooney DJ. Engineering growing tissues. Proc Natl Acad Sci U S A. 2002 Sep 17;99(19):12025-30.

Altieri DC. Survivin, versatile modulation of cell division and apoptosis in cancer. Oncogene. 2003 Nov 24;22(53):8581-9.

Altura RA, Olshefski RS, Jiang Y, Boué DR. Nuclear expression of Survivin in paediatric ependymomas and choroid plexus tumours correlates with morphologic tumour grade. Br J Cancer. 2003 Nov 3;89(9):1743-9.

Amin HD, Olsen I, Knowles JC, Donos N. Differential effect of amelogenin peptides on osteogenic differentiation *in vitro*: identification of possible new drugs for bone repair and regeneration. Tissue Eng Part A. 2012 Jun;18(11-12):1193-202.

Anton ES, Kreidberg JA, Rakic P. Distinct functions of alpha3 and alpha(v) integrin receptors in neuronal migration and laminar organization of the cerebral cortex. Neuron. 1999 Feb;22(2):277-89.

Arsenijevic Y, Villemure JG, Brunet JF, Bloch JJ, Déglon N, Kostic C, Zurn A, Aebischer P. Isolation of multipotent neural precursors residing in the cortex of the adult human brain. Exp Neurol. 2001 Jul;170(1):48-62.

Aumailley M, Bruckner-Tuderman L, Carter WG, Deutzmann R, Edgar D, Ekblom P, Engel J, Engvall E, Hohenester E, Jones JC, Kleinman HK, Marinkovich MP, Martin GR, Mayer U, Meneguzzi G, Miner JH, Miyazaki K, Patarroyo M, Paulsson M, Quaranta V, Sanes JR, Sasaki T, Sekiguchi K, Sorokin LM, Talts JF, Tryggvason K, Uitto J, Virtanen I, von der Mark K, Wewer UM, Yamada Y, Yurchenco PD. A simplified laminin nomenclature. Matrix Biol. 2005 Aug;24(5):326-32.

Azemi E, Stauffer WR, Gostock MS, Lagenaur CF, Cui XT. Surface immobilization of neural adhesion molecule L1 for improving the biocompatibility of chronic neural probes: *In vitro* characterization. Acta Biomater. 2008 Sep;4(5):1208-17.

Bader B, Spatio-temporal control of Wnt/_-catenin signaling during fate commitment of human neural progenitor cells. April 2010. Dissertation. University of Rostock.

Baharvand H, Hashemi SM, Kazemi Ashtiani S, Farrokhi A. Differentiation of human embryonic stem cells into hepatocytes in 2D and 3D culture systems *in vitro*. Int J Dev Biol. 2006;50(7):645-52.

Beniash E, Hartgerink JD, Storrie H, Stendahl JC, Stupp SI. Self-assembling peptide amphiphile nanofiber matrices for cell entrapment. Acta Biomater. 2005 Jul;1(4):387-97.

Biebl M, Cooper CM, Winkler J, Kuhn HG. Analysis of neurogenesis and programmed cell death reveals a self-renewing capacity in the adult rat brain. Neurosci Lett. 2000 Sep 8;291(1):17-20.

Bjornson CR, Rietze RL, Reynolds BA, Magli MC, Vescovi AL. Turning brain into blood: a hematopoietic fate adopted by adult neural stem cells *in vivo*. Science. 1999 Jan 22;283(5401):534-7.

Blewitt MJ, Willits RK. The effect of soluble peptide sequences on neurite extension on 2D collagen substrates and within 3D collagen gels. Ann Biomed Eng. 2007 Dec;35(12):2159-67.

Blow N. Stem cells: in search of common ground. Nature. 2008 Feb 14;451(7180):855-8.

Bosch M, Pineda JR, Suñol C, Petriz J, Cattaneo E, Alberch J, Canals JM. Induction of GABAergic phenotype in a neural stem cell line for transplantation in an excitotoxic model of Huntington's disease. Exp Neurol. 2004 Nov;190(1):42-58.

Bouchard VJ, Rouleau M, Poirier GG. PARP-1, a determinant of cell survival in response to DNA damage. Exp Hematol. 2003 Jun;31(6):446-54.

Brancolini C, Lazarevic D, Rodriguez J, Schneider C. Dismantling cell-cell contacts during apoptosis is coupled to a caspase-dependent proteolytic cleavage of beta-catenin. J Cell Biol. 1997 Nov 3;139(3):759-71.

Brännvall K, Bergman K, Wallenquist U, Svahn S, Bowden T, Hilborn J, Forsberg-Nilsson K. Enhanced neuronal differentiation in a three-dimensional collagen-hyaluronan matrix. J Neurosci Res. 2007 Aug 1;85(10):2138-46.

Brodbeck WG, Shive MS, Colton E, Nakayama Y, Matsuda T, Anderson JM. Influence of biomaterial surface chemistry on the apoptosis of adherent cells. J Biomed Mater Res. 2001 Jun 15;55(4):661-8.

Brüne B. Nitric oxide: NO apoptosis or turning it ON? Cell Death Differ. 2003 Aug;10(8):864-9.

Buchko GW, Iakoucheva LM, Kennedy MA, Ackerman EJ, Hess NJ. Extended X-ray absorption fine structure evidence for a single metal binding domain in Xenopus laevis nucleotide excision repair protein XPA. Biochem Biophys Res Commun. 1999 Jan 8;254(1):109-13.

Bullwinkel J, Baron-Lühr B, Lüdemann A, Wohlenberg C, Gerdes J, Scholzen T. Ki-67 protein is associated with ribosomal RNA transcription in quiescent and proliferating cells. J Cell Physiol. 2006 Mar;206(3):624-35.

Bunge MB. Bridging the transected or contused adult rat spinal cord with Schwann cell and olfactory ensheathing glia transplants. Prog Brain Res. 2002;137:275-82.

Calhoun ME, Jucker M, Martin LJ, Thinakaran G, Price DL, Mouton PR. Comparative evaluation of synaptophysin-based methods for quantification of synapses. J Neurocytol. 1996 Dec;25(12):821-8.

Calof AL, Campanero MR, O'Rear JJ, Yurchenco PD, Lander AD. Domain-specific activation of neuronal migration and neurite outgrowth-promoting activities of laminin. Neuron. 1994 Jul;13(1):117-30.

Cao H, Liu T, Chew SY. The application of nanofibrous scaffolds in neural tissue engineering. Adv Drug Deliv Rev. 2009 Oct 5;61(12):1055-64.

Cencetti C, Bellini D, Longinotti C, Martinelli A, Matricardi P. Preparation and characterization of a new gellan gum and sulphated hyaluronic acid hydrogel designed for epidural scar prevention. J Mater Sci Mater Med. 2011 Feb;22(2):263-71.

Cha C, Kim ES, Kim IW, Kong H. Integrative design of a poly(ethylene glycol)-poly(propylene glycol)-alginate hydrogel to control three dimensional biomineralization. Biomaterials. 2011 Apr;32(11):2695-703.

Chau Y, Luo Y, Cheung AC, Nagai Y, Zhang S, Kobler JB, Zeitels SM, Langer R. Incorporation of a matrix metalloproteinase-sensitive substrate into self-assembling peptides - a model for biofunctional scaffolds. Biomaterials. 2008 Apr;29(11):1713-9.

Chen J, Li Y, Wang L, Lu M, Zhang X, Chopp M. Therapeutic benefit of intracerebral transplantation of bone marrow stromal cells after cerebral ischemia in rats. J Neurol Sci. 2001 Aug 15;189(1-2):49-57.

Chen G, Goeddel DV. TNF-R1 signaling: a beautiful pathway. Science. 2002 May 31;296(5573):1634-5.

Chen J, Jin S, Tahir SK, Zhang H, Liu X, Sarthy AV, McGonigal TP, Liu Z, Rosenberg SH, Ng SC. Survivin enhances Aurora-B kinase activity and localizes Aurora-B in human cells. J Biol Chem. 2003 Jan 3;278(1):486-90.

Chen J, Li Y, Katakowski M, Chen X, Wang L, Lu D, Lu M, Gautam SC, Chopp M. Intravenous bone marrow stromal cell therapy reduces apoptosis and promotes endogenous cell proliferation after stroke in female rat. J Neurosci Res. 2003 Sep 15;73(6):778-86.

Chen ZL, Strickland S. Laminin gamma1 is critical for Schwann cell differentiation, axon myelination, and regeneration in the peripheral nerve. J Cell Biol. 2003 Nov 24;163(4):889-99.

Cheung KC, Renaud P, Tanila H, Djupsund K. Flexible polyimide microelectrode array for *in vivo* recordings and current source density analysis. Biosens Bioelectron. 2007 Mar 15;22(8):1783-90.

Chopp M, Zhang XH, Li Y, Wang L, Chen J, Lu D, Lu M, Rosenblum M. Spinal cord injury in rat: treatment with bone marrow stromal cell transplantation. Neuroreport. 2000 Sep 11;11(13):3001-5.

Cregan SP, Fortin A, MacLaurin JG, Callaghan SM, Cecconi F, Yu SW, Dawson TM, Dawson VL, Park DS, Kroemer G, Slack RS. Apoptosis-inducing factor is involved in the regulation of caspase-independent neuronal cell death. J Cell Biol. 2002 Aug 5;158(3):507-17.

Cregan SP, MacLaurin JG, Craig CG, Robertson GS, Nicholson DW, Park DS, Slack RS. Bax-dependent caspase-3 activation is a key determinant in p53-induced apoptosis in neurons. J Neurosci. 1999 Sep 15;19(18):7860-9.

Dainiak MB, Savina IN, Musolino I, Kumar A, Mattiasson B, Galaev IY. Biomimetic macroporous hydrogel scaffolds in a high-throughput screening format for cell-based assays. Biotechnol Prog. 2008 Nov-Dec;24(6):1373-83.

Darios F, Lambeng N, Troadec JD, Michel PP, Ruberg M. Ceramide increases mitochondrial free calcium levels via caspase 8 and Bid: role in initiation of cell death. J Neurochem. 2003 Feb;84(4):643-54.

Dejean LM, Martinez-Caballero S, Guo L, Hughes C, Teijido O, Ducret T, Ichas F, Korsmeyer SJ, Antonsson B, Jonas EA, Kinnally KW. Oligomeric Bax is a component of the putative cytochrome c release channel MAC, mitochondrial apoptosis-induced channel. Mol Biol Cell. 2005 May;16(5):2424-32.

Dejean LM, Martinez-Caballero S, Manon S, Kinnally KW. Regulation of the mitochondrial apoptosis-induced channel, MAC, by BCL-2 family proteins. Biochim Biophys Acta. 2006 Feb;1762(2):191-201.

Dejean LM, Martinez-Caballero S, Kinnally KW. Is MAC the knife that cuts cytochrome c from mitochondria during apoptosis? Cell Death Differ. 2006 Aug;13(8):1387-95.

Dent MA, Segura-Anaya E, Alva-Medina J, Aranda-Anzaldo A. NeuN/Fox-3 is an intrinsic component of the neuronal nuclear matrix. FEBS Lett. 2010 Jul 2;584(13):2767-71.

Dihné M, Bernreuther C, Sibbe M, Paulus W, Schachner M. A new role for the cell adhesion molecule L1 in neural precursor cell proliferation, differentiation, and transmitter-specific subtype generation. J Neurosci. 2003 Jul 23;23(16):6638-50.

Discher DE, Janmey P, Wang YL. Tissue cells feel and respond to the stiffness of their substrate. Science. 2005 Nov 18;310(5751):1139-43.

Dohi T, Beltrami E, Wall NR, Plescia J, Altieri DC. Mitochondrial Survivin inhibits apoptosis and promotes tumorigenesis. J Clin Invest. 2004 Oct;114(8):1117-27.

Donato R, Miljan EA, Hines SJ, Aouabdi S, Pollock K, Patel S, Edwards FA, Sinden JD. Differential development of neuronal physiological responsiveness in two human neural stem cell lines. BMC Neurosci. 2007 May 25;8:36.

Edgar D, Timpl R, Thoenen H. The heparin-binding domain of laminin is responsible for its effects on neurite outgrowth and neuronal survival. EMBO J. 1984 Jul;3(7):1463-8.

Ekblom P, Lonai P, Talts JF. Expression and biological role of laminin-1. Matrix Biol. 2003 Mar;22(1):35-47.

Ekici M, Hohl M, Schuit F, Martínez-Serrano A, Thiel G. Transcription of genes encoding synaptic vesicle proteins in human neural stem cells: chromatin accessibility, histone methylation pattern, and the essential role of rest. J Biol Chem. 2008 Apr 4;283(14):9257-68.

Ellis-Behnke RG, Liang YX, You SW, Tay DK, Zhang S, So KF, Schneider GE. Nano neuro knitting: peptide nanofiber scaffold for brain repair and axon regeneration with functional return of vision. Proc Natl Acad Sci U S A. 2006 Mar 28; 103(13):5054-9.

Eom TY, Roth KA, Jope RS. Neural precursor cells are protected from apoptosis induced by trophic factor withdrawal or genotoxic stress by inhibitors of glycogen synthase kinase 3. J Biol Chem. 2007 Aug 3;282(31):22856-64.

Falconnet D, Csucs G, Grandin HM, Textor M. Surface engineering approaches to micropattern surfaces for cell-based assays. Biomaterials. 2006 Jun;27(16):3044-63.

Fernando P, Brunette S, Megeney LA. Neural stem cell differentiation is dependent upon endogenous caspase 3 activity. FASEB J. 2005 Oct;19(12):1671-3.

Ferreira LS, Gerecht S, Fuller J, Shieh HF, Vunjak-Novakovic G, Langer R. Bioactive hydrogel scaffolds for controllable vascular differentiation of human embryonic stem cells. Biomaterials. 2007 Jun;28(17):2706-17. Epub 2007 Jan 16.

Fesik SW, Shi Y. Structural biology. Controlling the caspases. Science. 2001 Nov 16;294(5546):1477-8.

Fields GB, Lauer JL, Dori Y, Forns P, Yu YC, Tirrell M. Protein-like molecular architecture: biomaterial applications for inducing cellular receptor binding and signal transduction. Biopolymers. 1998;47(2):143-51.

Flynn L, Dalton PD, Shoichet MS. Fiber templating of poly(2-hydroxyethyl methacrylate) for neural tissue engineering. Biomaterials. 2003 Oct;24(23):4265-72.

Friedl P, Zänker KS, Bröcker EB. Cell migration strategies in 3-D extracellular matrix: differences in morphology, cell matrix interactions, and integrin function. Microsc Res Tech. 1998 Dec 1;43(5):369-78.

Fröhlich M, Jaeger A, Weiss DG, Kriehuber R. Specific inhibition of Bcl-2 leads to diminished neuronal differentiation in VM197 cells. 19th Annual Conference of the German Society for Cytometry (DGFZ), Leipzig, Germany, 2009, Oct 14-16, Abstract Book, p.63.

Gavrieli Y, Sherman Y, Ben-Sasson SA. Identification of programmed cell death in situ via specific labeling of nuclear DNA fragmentation. J Cell Biol. 1992 Nov;119(3):493-501.

Geever LM, Cooney CC, Lyons JG, Kennedy JE, Nugent MJ, Devery S, Higginbotham CL. Characterisation and controlled drug release from novel drug-loaded hydrogels. Eur J Pharm Biopharm. 2008 Aug;69(3):1147-59.

Gelain F, Bottai D, Vescovi A, Zhang S. Designer self-assembling peptide nanofiber scaffolds for adult mouse neural stem cell 3-dimensional cultures. PLoS One. 2006 Dec 27; 1:e119.

Gelain F, Unsworth LD, Zhang S. Slow and sustained release of active cytokines from self-assembling peptide scaffolds. J Control Release. 2010 Aug 3;145(3):231-9.

Gelain F, Silva D, Caprini A, Taraballi F, Natalello A, Villa O, Nam KT, Zuckermann RN, Doglia SM, Vescovi A. BMHP1-derived self-assembling peptides: hierarchically assembled structures with self-healing propensity and potential for tissue engineering applications. ACS Nano. 2011 Mar 22;5(3):1845-59.

Georges PC, Miller WJ, Meaney DF, Sawyer ES, Janmey PA. Matrices with compliance comparable to that of brain tissue select neuronal over glial growth in mixed cortical cultures. Biophys J. 2006 Apr 15;90(8):3012-8.

Georges-Labouesse E, Mark M, Messaddeq N, Gansmüller A. Essential role of alpha 6 integrins in cortical and retinal lamination. Curr Biol. 1998 Aug 27;8(17):983-6.

Gerami-Naini B, Dovzhenko OV, Durning M, Wegner FH, Thomson JA, Golos TG. Trophoblast differentiation in embryoid bodies derived from human embryonic stem cells. Endocrinology. 2004 Apr;145(4):1517-24.

Gerdes J, Schwab U, Lemke H, Stein H. Production of a mouse monoclonal antibody reactive with a human nuclear antigen associated with cell proliferation. Int J Cancer. 1983 Jan 15;31(1):13-20.

Gerecht S, Burdick JA, Ferreira LS, Townsend SA, Langer R, Vunjak-Novakovic G. Hyaluronic acid hydrogel for controlled self-renewal and differentiation of human embryonic stem cells. Proc Natl Acad Sci U S A. 2007 Jul 3; 104(27):11298-303.

Gerecht-Nir S, Cohen S, Ziskind A, Itskovitz-Eldor J. Three-dimensional porous alginate scaffolds provide a conducive environment for generation of well-vascularized embryoid bodies from human embryonic stem cells. Biotechnol Bioeng. 2004 Nov 5;88(3):313-20.

Gewies A. ApoReview - Introduction to Apoptosis. 2003.
http://www.celldeath.de/encyclo/aporev/aporev.htm

Giese AK, Frahm J, Hübner R, Luo J, Wree A, Frech MJ, Rolfs A, Ortinau S. Erythropoietin and the effect of oxygen during proliferation and differentiation of human neural progenitor cells. BMC Cell Biol. 2010 Dec 2;11:94.

Gould E, Reeves AJ, Graziano MS, Gross CG. Neurogenesis in the neocortex of adult primates. Science. 1999 Oct 15;286(5439):548-52.

Grasl-Kraupp B, Ruttkay-Nedecky B, Koudelka H, Bukowska K, Bursch W, Schulte-Hermann R. In situ detection of fragmented DNA (TUNEL assay) fails to discriminate among apoptosis, necrosis, and autolytic cell death: a cautionary note. Hepatology. 1995 May;21(5):1465-8.

Graus F, Elkon KB, Lloberes P, Ribalta T, Torres A, Ussetti P, Valls J, Obach J, Agusti-Vidal A. Neuronal antinuclear antibody (anti-Hu) in paraneoplastic encephalomyelitis simulating acute polyneuritis. Acta Neurol Scand. 1987 Apr;75(4):249-52.

Graus F, Ferrer I. Analysis of a neuronal antigen (Hu) expression in the developing rat brain detected by autoantibodies from patients with paraneoplastic encephalomyelitis. Neurosci Lett. 1990 Apr 20;112(1):14-8.

Green D, Walsh D, Mann S, Oreffo RO. The potential of biomimesis in bone tissue engineering: lessons from the design and synthesis of invertebrate skeletons. Bone. 2002 Jun;30(6):810-5.

Greene LA, Tischler AS. Establishment of a noradrenergic clonal line of rat adrenal pheochromocytoma cells which respond to nerve growth factor. Proc Natl Acad Sci U S A. 1976 Jul;73(7):2424-8.

Gueven N, Becherel OJ, Kijas AW, Chen P, Howe O, Rudolph JH, Gatti R, Date H, Onodera O, Taucher-Scholz G, Lavin MF. Aprataxin, a novel protein that protects against genotoxic stress. Hum Mol Genet. 2004 May 15;13(10):1081-93.

Gunn JW, Turner SD, Mann BK. Adhesive and mechanical properties of hydrogels influence

neurite extension. J Biomed Mater Res A. 2005 Jan 1;72(1):91-7.
Guo L, Pietkiewicz D, Pavlov EV, Grigoriev SM, Kasianowicz JJ, Dejean LM, Korsmeyer SJ, Antonsson B, Kinnally KW. Effects of cytochrome c on the mitochondrial apoptosis-induced channel MAC. Am J Physiol Cell Physiol. 2004 May;286(5):C1109-17.

Hangen E, Blomgren K, Bénit P, Kroemer G, Modjtahedi N. Life with or without AIF. Trends Biochem Sci. 2010 May;35(5):278-87. Epub 2010 Feb 6.

Hartgerink JD, Beniash E, Stupp SI. Self-assembly and mineralization of peptide-amphiphile nanofibers. Science. 2001 Nov 23;294(5547):1684-8.

Hartgerink JD, Beniash E, Stupp SI. Peptide-amphiphile nanofibers: a versatile scaffold for the preparation of self-assembling materials. Proc Natl Acad Sci U S A. 2002 Apr 16;99(8):5133-8.

Harting MT, Baumgartner JE, Worth LL, Ewing-Cobbs L, Gee AP, Day MC, Cox CS Jr. Cell therapies for traumatic brain injury. Neurosurg Focus. 2008;24(3-4):E18.

Hayman MW, Smith KH, Cameron NR, Przyborski SA. Enhanced neurite outgrowth by human neurons grown on solid three-dimensional scaffolds. Biochem Biophys Res Commun. 2004 Feb 6;314(2):483-8.

Hetz C, Vitte PA, Bombrun A, Rostovtseva TK, Montessuit S, Hiver A, Schwarz MK, Church DJ, Korsmeyer SJ, Martinou JC, Antonsson B. Bax channel inhibitors prevent mitochondrion-mediated apoptosis and protect neurons in a model of global brain ischemia. J Biol Chem. 2005 Dec 30;280(52):42960-70.

Hickman JA. Apoptosis and tumourigenesis. Curr Opin Genet Dev. 2002 Feb;12(1):67-72.

Hirabayashi Y, Gotoh Y. Stage-dependent fate determination of neural precursor cells in mouse forebrain. Neurosci Res. 2005 Apr;51(4):331-6.

Hnasko R, Bruederle CE. Inoculation of scrapie with the self-assembling RADA-peptide disrupts prion accumulation and extends hamster survival. PLoS One. 2009;4(2):e4440.

Hoffrogge R, Mikkat S, Scharf C, Beyer S, Christoph H, Pahnke J, Mix E, Berth M, Uhrmacher A, Zubrzycki IZ, Miljan E, Völker U, Rolfs A. 2-DE proteome analysis of a proliferating and differentiating human neuronal stem cell line (ReNcell VM). Proteomics. 2006 Mar;6(6):1833-47.

Holmes TC, de Lacalle S, Su X, Liu G, Rich A, Zhang S. Extensive neurite outgrowth and active synapse formation on self-assembling peptide scaffolds. Proc Natl Acad Sci U S A. 2000 Jun 6;97(12):6728-33.

Hou S, Xu Q, Tian W, Cui F, Cai Q, Ma J, Lee IS. The repair of brain lesion by implantation of hyaluronic acid hydrogels modified with laminin. J Neurosci Methods. 2005 Oct 15;148(1):60-70.

Hou S, Tian W, Xu Q, Cui F, Zhang J, Lu Q, Zhao C. The enhancement of cell adherence and inducement of neurite outgrowth of dorsal root ganglia co-cultured with hyaluronic acid hydrogels modified with Nogo-66 receptor antagonist *in vitro*. Neuroscience. 2006;137(2):519-29.

Hrynyk M, Martins-Green M, Barron AE, Neufeld RJ. Alginate-PEG Sponge Architecture and Role in the Design of Insulin Release Dressings. Biomacromolecules. 2012 May

14;13(5):1478-85.

Hübner R, Schmöle AC, Liedmann A, Frech MJ, Rolfs A, Luo J. Differentiation of human neural progenitor cells regulated by Wnt-3a. Biochem Biophys Res Commun. 2010 Sep 24;400(3):358-62.

Hung CH, Lin YL, Young TH. The effect of chitosan and PVDF substrates on the behavior of embryonic rat cerebral cortical stem cells. Biomaterials. 2006 Sep;27(25):4461-9.

Hunt CA, Schenker LJ, Kennedy MB. PSD-95 is associated with the postsynaptic density and not with the presynaptic membrane at forebrain synapses. J Neurosci. 1996 Feb 15;16(4):1380-8.

Igney FH, Krammer PH. Death and anti-death: tumour resistance to apoptosis. Nat Rev Cancer. 2002 Apr;2(4):277-88.

Iivanainen A, Kortesmaa J, Sahlberg C, Morita T, Bergmann U, Thesleff I, Tryggvason K. Primary structure, developmental expression, and immunolocalization of the murine laminin alpha4 chain. J Biol Chem. 1997 Oct 31;272(44):27862-8.

Jaeger A. Charakterisierung von Apoptoseprozessen während der Differenzierung von humanen neuralen VM197-Progenitorzellen *in vitro*. April 2010. Dissertation. University of Rostock.

Jiang Y, de Bruin A, Caldas H, Fangusaro J, Hayes J, Conway EM, Robinson ML, Altura RA. Essential role for Survivin in early brain development. J Neurosci. 2005 Jul 27;25(30):6962-70.

Jongpaiboonkit L, King WJ, Lyons GE, Paguirigan AL, Warrick JW, Beebe DJ, Murphy WL. An adaptable hydrogel array format for 3-dimensional cell culture and analysis. Biomaterials. 2008 Aug;29(23):3346-56.

Jori FP, Napolitano MA, Melone MA, Cipollaro M, Cascino A, Altucci L, Peluso G, Giordano A, Galderisi U. Molecular pathways involved in neural *in vitro* differentiation of marrow stromal stem cells. J Cell Biochem. 2005 Mar 1;94(4):645-55.

Kabos P, Ehtesham M, Kabosova A, Black KL, Yu JS. Generation of neural progenitor cells from whole adult bone marrow. Exp Neurol. 2002 Dec;178(2):288-93.

Kallunki P, Sainio K, Eddy R, Byers M, Kallunki T, Sariola H, Beck K, Hirvonen H, Shows TB, Tryggvason K. A truncated laminin chain homologous to the B2 chain: structure, spatial expression, and chromosomal assignment. J Cell Biol. 1992 Nov;119(3):679-93.

Kam L, Shain W, Turner JN, Bizios R. Selective adhesion of astrocytes to surfaces modified with immobilized peptides. Biomaterials. 2002 Jan;23(2):511-5.

Khor E, Lim LY. Implantable applications of chitin and chitosan. Biomaterials. 2003 Jun;24(13):2339-49.

Kihlmark M, Imreh G, Hallberg E. Sequential degradation of proteins from the nuclear envelope during apoptosis. J Cell Sci. 2001 Oct;114(Pt 20):3643-53.

Kim DS, Kim JY, Kang M, Cho MS, Kim DW. Derivation of functional dopamine neurons from embryonic stem cells. Cell Transplant. 2007;16(2):117-23.

Kim KK, Adelstein RS, Kawamoto S. Identification of neuronal nuclei (NeuN) as Fox-3, a

new member of the Fox-1 gene family of splicing factors. J Biol Chem. 2009 Nov 6;284(45):31052-61.
Kiss JZ, Troncoso E, Djebbara Z, Vutskits L, Muller D.The role of neural cell adhesion molecules in plasticity and repair. Brain Res Brain Res Rev. 2001 Oct;36(2-3):175-84.

Kleinman HK, McGarvey ML, Hassell JR, Star VL, Cannon FB, Laurie GW, Martin GR. Basement membrane complexes with biological activity. Biochemistry. 1986 Jan 28;25(2):312-8.

Koh HS, Yong T, Chan CK, Ramakrishna S. Enhancement of neurite outgrowth using nano-structured scaffolds coupled with laminin. Biomaterials. 2008 Sep;29(26):3574-82.

Koopman G, Reutelingsperger CP, Kuijten GA, Keehnen RM, Pals ST, van Oers MH. Annexin V for flow cytometric detection of phosphatidylserine expression on B cells undergoing apoptosis. Blood. 1994 Sep 1;84(5):1415-20.

Kranenburg O, van der Eb AJ, Zantema A. Cyclin D1 is an essential mediator of apoptotic neuronal cell death. EMBO J. 1996 Jan 2;15(1):46-54.

Labrador RO, Butí M, Navarro X. Influence of collagen and laminin gels concentration on nerve regeneration after resection and tube repair. Exp Neurol. 1998 Jan;149(1):243-52.

Lagenaur C, Lemmon V. An L1-like molecule, the 8D9 antigen, is a potent substrate for neurite extension. Proc Natl Acad Sci U S A. 1987 Nov;84(21):7753-7.

Landshamer S, Hoehn M, Barth N, Duvezin-Caubet S, Schwake G, Tobaben S, Kazhdan I, Becattini B, Zahler S, Vollmar A, Pellecchia M, Reichert A, Plesnila N, Wagner E, Culmsee C. Bid-induced release of AIF from mitochondria causes immediate neuronal cell death. Cell Death Differ. 2008 Oct;15(10):1553-63.

Lange C, Mix E, Rateitschak K, Rolfs A. Wnt signal pathways and neural stem cell differentiation. Neurodegener Dis. 2006;3(1-2):76-86.

Lange C, Mix E, Frahm J, Glass A, Müller J, Schmitt O, Schmöle AC, Klemm K, Ortinau S, Hübner R, Frech MJ, Wree A, Rolfs A. Small molecule GSK-3 inhibitors increase neurogenesis of human neural progenitor cells. Neurosci Lett. 2011 Jan 13;488(1):36-40.

Langer R, Tirrell DA. Designing materials for biology and medicine. Nature. 2004 Apr 1;428(6982):487-92.

Lankiewicz S, Marc Luetjens C, Truc Bui N, Krohn AJ, Poppe M, Cole GM, Saido TC, Prehn JH. Activation of calpain I converts excitotoxic neuron death into a caspase-independent cell death. J Biol Chem. 2000 Jun 2;275(22):17064-71.

Lecoeur H. Nuclear apoptosis detection by flow cytometry: influence of endogenous endonucleases. Exp Cell Res. 2002 Jul 1;277(1):1-14.

Lee J, Kuroda S, Shichinohe H, Ikeda J, Seki T, Hida K, Tada M, Sawada K, Iwasaki Y. Migration and differentiation of nuclear fluorescence-labeled bone marrow stromal cells after transplantation into cerebral infarct and spinal cord injury in mice. Neuropathology. 2003 Sep;23(3):169-80.

Lee J, Cuddihy MJ, Kotov NA. Three-dimensional cell culture matrices: state of the art. Tissue Eng Part B Rev. 2008 Mar;14(1):61-86.

Lelièvre SA, Weaver VM, Nickerson JA, Larabell CA, Bhaumik A, Petersen OW, Bissell

MJ. Tissue phenotype depends on reciprocal interactions between the extracellular matrix and the structural organization of the nucleus. Proc Natl Acad Sci U S A. 1998 Dec 8;95(25):14711-6.

Lemmon V, Burden SM, Payne HR, Elmslie GJ, Hlavin ML. Neurite growth on different substrates: permissive versus instructive influences and the role of adhesive strength. J Neurosci. 1992 Mar;12(3):818-26.

Levenberg S, Burdick JA, Kraehenbuehl T, Langer R. Neurotrophin-induced differentiation of human embryonic stem cells on three-dimensional polymeric scaffolds. Tissue Eng. 2005 Mar-Apr;11(3-4):506-12.

Levenberg S, Huang NF, Lavik E, Rogers AB, Itskovitz-Eldor J, Langer R. Differentiation of human embryonic stem cells on three-dimensional polymer scaffolds. Proc Natl Acad Sci U S A. 2003 Oct 28;100(22):12741-6.

Li M, Wang X, Meintzer MK, Laessig T, Birnbaum MJ, Heidenreich KA. Cyclic AMP promotes neuronal survival by phosphorylation of glycogen synthase kinase 3beta. Mol Cell Biol. 2000 Dec;20(24):9356-63.

Li MO, Sarkisian MR, Mehal WZ, Rakic P, Flavell RA. Phosphatidylserine receptor is required for clearance of apoptotic cells. Science. 2003 Nov 28;302(5650):1560-3.

Li J, Spletter ML, Johnson DA, Wright LS, Svendsen CN, Johnson JA. Rotenone-induced caspase 9/3-independent and -dependent cell death in undifferentiated and differentiated human neural stem cells. J Neurochem. 2005 Feb;92(3):462-76.

Li YJ, Chung EH, Rodriguez RT, Firpo MT, Healy KE. Hydrogels as artificial matrices for human embryonic stem cell self-renewal. J Biomed Mater Res A. 2006 Oct;79(1):1-5.

Li GN, Livi LL, Gourd CM, Deweerd ES, Hoffman-Kim D. Genomic and morphological changes of neuroblastoma cells in response to three-dimensional matrices. Tissue Eng. 2007 May;13(5):1035-47.

Li Q, Chau Y. Neural differentiation directed by self-assembling peptide scaffolds presenting laminin-derived epitopes. J Biomed Mater Res A. 2010 Sep 1;94(3):688-99.

Liebmann T, Rydholm S, Akpe V, Brismar H. Self-assembling Fmoc dipeptide hydrogel for in situ 3D cell culturing. BMC Biotechnol. 2007 Dec 10;7:88.

Liedmann A, Rolfs A, Frech MJ. Cultivation of human neural progenitor cells in a 3-dimensional self-assembling peptide hydrogel. J Vis Exp. 2012 Jan 11;(59):e3830. doi: 10.3791/3830.

Liedmann A, Frech S, **Morgan PJ,** Rolfs A, Frech MJ. Differentiation of human neural progenitor cells in functionalized hydrogel matrices. Bioresearch Open Access. 2012; 1(1):16-24.

Liesi P, Närvänen A, Soos J, Sariola H, Snounou G. Identification of a neurite outgrowth-promoting domain of laminin using synthetic peptides. FEBS Lett. 1989 Feb 13;244(1):141-8.

Liesi P, Seppälä I, Trenkner E. Neuronal migration in cerebellar microcultures is inhibited by antibodies against a neurite outgrowth domain of laminin. J Neurosci Res. 1992 Sep;33(1):170-6.

Lindholm D, Arumäe U. Cell differentiation: reciprocal regulation of Apaf-1 and the

inhibitor of apoptosis proteins. J Cell Biol. 2004 Oct 25;167(2):193-5.

Lindsten T, Golden JA, Zong WX, Minarcik J, Harris MH, Thompson CB. The proapoptotic activities of Bax and Bak limit the size of the neural stem cell pool. J Neurosci. 2003 Dec 3;23(35):11112-9.

Ling ZD, Potter ED, Lipton JW, Carvey PM. Differentiation of mesencephalic progenitor cells into dopaminergic neurons by cytokines. Exp Neurol. 1998 Feb;149(2):411-23.

Linseman DA, Butts BD, Precht TA, Phelps RA, Le SS, Laessig TA, Bouchard RJ, Florez-McClure ML, Heidenreich KA. Glycogen synthase kinase-3beta phosphorylates Bax and promotes its mitochondrial localization during neuronal apoptosis. J Neurosci. 2004 Nov 3;24(44):9993-10002.

Liu JC, Heilshorn SC, Tirrell DA. Comparative cell response to artificial extracellular matrix proteins containing the RGD and CS5 cell-binding domains. Biomacromolecules. 2004 Mar-Apr;5(2):497-504.

Ljungberg C, Johansson-Ruden G, Boström KJ, Novikov L, Wiberg M. Neuronal survival using a resorbable synthetic conduit as an alternative to primary nerve repair. Microsurgery. 1999;19(6):259-64.

Loebel DA, Watson CM, De Young RA, Tam PP. Lineage choice and differentiation in mouse embryos and embryonic stem cells. Dev Biol. 2003 Dec 1;264(1):1-14.

Lonze BE, Ginty DD. Function and regulation of CREB family transcription factors in the nervous system. Neuron. 2002 Aug 15;35(4):605-23.

Luckenbill-Edds L. Laminin and the mechanism of neuronal outgrowth. Brain Res Brain Res Rev. 1997 Feb;23(1-2):1-27.

Ma W, Fitzgerald W, Liu QY, O'Shaughnessy TJ, Maric D, Lin HJ, Alkon DL, Barker JL. CNS stem and progenitor cell differentiation into functional neuronal circuits in three-dimensional collagen gels. Exp Neurol. 2004 Dec;190(2):276-88.

Madihally SV, Matthew HW. Porous chitosan scaffolds for tissue engineering. Biomaterials. 1999 Jun;20(12):1133-42.

Mahmood A, Lu D, Lu M, Chopp M. Treatment of traumatic brain injury in adult rats with intravenous administration of human bone marrow stromal cells. Neurosurgery. 2003 Sep;53(3):697-702; discussion 702-3.

Mahmood A, Lu D, Qu C, Goussev A, Chopp M. Long-term recovery after bone marrow stromal cell treatment of traumatic brain injury in rats. J Neurosurg. 2006 Feb;104(2):272-7.

Mahoney MJ, Anseth KS. Three-dimensional growth and function of neural tissue in degradable polyethylene glycol hydrogels. Biomaterials. 2006 Apr;27(10):2265-74.

Malanga M, Pleschke JM, Kleczkowska HE, Althaus FR. Poly(ADP-ribose) binds to specific domains of p53 and alters its DNA binding functions. J Biol Chem. 1998 May 8;273(19):11839-43.

Malinda KM, Nomizu M, Chung M, Delgado M, Kuratomi Y, Yamada Y, Kleinman HK, Ponce ML. Identification of laminin alpha1 and beta1 chain peptides active for endothelial cell adhesion, tube formation, and aortic sprouting. FASEB J. 1999 Jan;13(1):53-62.

Maniotis AJ, Chen CS, Ingber DE. Demonstration of mechanical connections between integrins, cytoskeletal filaments, and nucleoplasm that stabilize nuclear structure. Proc Natl Acad Sci U S A. 1997 Feb 4;94(3):849-54.

Marchand R, Woerly S. Transected spinal cords grafted with in situ self-assembled collagen matrices. Neuroscience. 1990;36(1):45-60.

Martin SJ, Reutelingsperger CP, McGahon AJ, Rader JA, van Schie RC, LaFace DM, Green DR. Early redistribution of plasma membrane phosphatidylserine is a general feature of apoptosis regardless of the initiating stimulus: inhibition by overexpression of Bcl-2 and Abl. J Exp Med. 1995 Nov 1;182(5):1545-56.

Martin BC, Minner EJ, Wiseman SL, Klank RL, Gilbert RJ. Agarose and methylcellulose hydrogel blends for nerve regeneration applications. J Neural Eng. 2008 Jun;5(2):221-31.

Martinou JC, Dubois-Dauphin M, Staple JK, Rodriguez I, Frankowski H, Missotten M, Albertini P, Talabot D, Catsicas S, Pietra C, et al. Overexpression of BCL-2 in transgenic mice protects neurons from naturally occurring cell death and experimental ischemia. Neuron. 1994 Oct;13(4):1017-30.

Martins A, Araújo JV, Reis RL, Neves NM. Electrospun nanostructured scaffolds for tissue engineering applications. Nanomedicine (Lond). 2007 Dec;2(6):929-42.

Mattson MP, Chan SL. Calcium orchestrates apoptosis. Nat Cell Biol. 2003 Dec;5(12):1041-3.

Mayer-Proschel M, Kalyani AJ, Mujtaba T, Rao MS. Isolation of lineage-restricted neuronal precursors from multipotent neuroepithelial stem cells. Neuron. 1997 Oct;19(4):773-85.

Mazel S, Burtrum D, Petrie HT. Regulation of cell division cycle progression by bcl-2 expression: a potential mechanism for inhibition of programmed cell death. J Exp Med. 1996 May 1;183(5):2219-26.

Mazemondet O, Hubner R, Frahm J, Koczan D, Bader BM, Weiss DG, Uhrmacher AM, Frech MJ, Rolfs A, Luo J. Quantitative and kinetic profile of Wnt/β-catenin signaling components during human neural progenitor cell differentiation. Cell Mol Biol Lett. 2011 Dec;16(4):515-38.

McMahon HT, Bolshakov VY, Janz R, Hammer RE, Siegelbaum SA, Südhof TC. Synaptophysin, a major synaptic vesicle protein, is not essential for neurotransmitter release. Proc Natl Acad Sci U S A. 1996 May 14;93(10):4760-4.

Middleton G, Piñón LG, Wyatt S, Davies AM. Bcl-2 accelerates the maturation of early sensory neurons. J Neurosci. 1998 May 1;18(9):3344-50.

Midorikawa R, Takei Y, Hirokawa N. KIF4 motor regulates activity-dependent neuronal survival by suppressing PARP-1 enzymatic activity. Cell. 2006 Apr 21;125(2):371-83.

Miho Y, Kouroku Y, Fujita E, Mukasa T, Urase K, Kasahara T, Isoai A, Momoi MY, Momoi T. bFGF inhibits the activation of caspase-3 and apoptosis of P19 embryonal carcinoma cells during neuronal differentiation. Cell Death Differ. 1999 May;6(5):463-70.

Miner JH, Lewis RM, Sanes JR. Molecular cloning of a novel laminin chain, alpha 5, and widespread expression in adult mouse tissues. J Biol Chem. 1995 Dec 1;270(48):28523-6.

Miner JH, Yurchenco PD. Laminin functions in tissue morphogenesis. Annu Rev Cell Dev

Biol. 2004;20:255-84.

Mitalipov S, Wolf D. Totipotency, pluripotency and nuclear reprogramming. Adv Biochem Eng Biotechnol. 2009;114:185-99.

Mooney DJ, Hansen LK, Langer R, Vacanti JP, Ingber DE. Extracellular matrix controls tubulin monomer levels in hepatocytes by regulating protein turnover. Mol Biol Cell. 1994 Dec;5(12):1281-8.

Moore A, Donahue CJ, Bauer KD, Mather JP. Simultaneous measurement of cell cycle and apoptotic cell death. Methods Cell Biol. 1998;57:265-78.

Morgan PJ, Ortinau S, Frahm J, Krüger N, Rolfs A, Frech MJ. Protection of neurons derived from human neural progenitor cells by veratridine. Neuroreport. 2009 Aug 26;20(13):1225-9.

Morgan PJ. Characterisation of calcium signalling and functional development in an immortalised human neural progenitor cell line. 2011. Dissertation. University of Rostock.

Morgan PJ, Liedmann A, Hübner R, Hovakimyan M, Rolfs A, Frech MJ. Human Neural Progenitor Cells Show Functional Neuronal Differentiation and Regional Preference After Engraftment onto Hippocampal Slice Cultures. Stem Cells Dev. 2011 Dec 23.

Mosahebi A, Wiberg M, Terenghi G. Addition of fibronectin to alginate matrix improves peripheral nerve regeneration in tissue-engineered conduits. Tissue Eng. 2003 Apr;9(2):209-18.

Moxham G. Organic nanostructures: Nanofibres cut down to size. Nature Nanotechnology. 2008 February. doi:10.1038/nnano.2008.56

Muller D, Wang C, Skibo G, Toni N, Cremer H, Calaora V, Rougon G, Kiss JZ. PSA-NCAM is required for activity-induced synaptic plasticity. Neuron. 1996 Sep;17(3):413-22.

Muller D, Djebbara-Hannas Z, Jourdain P, Vutskits L, Durbec P, Rougon G, Kiss JZ. Brain-derived neurotrophic factor restores long-term potentiation in polysialic acid-neural cell adhesion molecule-deficient hippocampus. Proc Natl Acad Sci U S A. 2000 Apr 11;97(8):4315-20.

Munisamy S, Vaidyanathan TK, Vaidyanathan J. A bone-like precoating strategy for implants: collagen immobilization and mineralization on pure titanium implant surface. J Oral Implantol. 2008;34(2):67-75.

Munoz JR, Stoutenger BR, Robinson AP, Spees JL, Prockop DJ. Human stem/progenitor cells from bone marrow promote neurogenesis of endogenous neural stem cells in the hippocampus of mice. Proc Natl Acad Sci U S A. 2005 Dec 13;102(50):18171-6.

Nagata S. Apoptotic DNA fragmentation. Exp Cell Res. 2000 Apr 10;256(1):12-8

Namba T, Mochizuki H, Onodera M, Namiki H, Seki T. Postnatal neurogenesis in hippocampal slice cultures: early *in vitro* labeling of neural precursor cells leads to efficient neuronal production. J Neurosci Res. 2007 Jun;85(8):1704-12.

Negoescu A, Lorimier P, Labat-Moleur F, Drouet C, Robert C, Guillermet C, Brambilla C, Brambilla E. In situ apoptotic cell labeling by the TUNEL method: improvement and evaluation on cell preparations. J Histochem Cytochem. 1996 Sep;44(9):959-68.

Nomizu M, Weeks BS, Weston CA, Kim WH, Kleinman HK, Yamada Y. Structure-activity

study of a laminin alpha 1 chain active peptide segment Ile-Lys-Val-Ala-Val (IKVAV). FEBS Lett. 1995 May 29;365(2-3):227-31.
Nomizu M, Song SY, Kuratomi Y, Tanaka M, Kim WH, Kleinman HK, Yamada Y. Active peptides from the carboxyl-terminal globular domain of laminin alpha2 and Drosophila alpha chains. FEBS Lett. 1996 Oct 28;396(1):37-42.

Nomizu M, Kuratomi Y, Song SY, Ponce ML, Hoffman MP, Powell SK, Miyoshi K, Otaka A, Kleinman HK, Yamada Y. Identification of cell binding sequences in mouse laminin gamma1 chain by systematic peptide screening. J Biol Chem. 1997 Dec 19;272(51):32198-205.

Novikov LN, Novikova LN, Mosahebi A, Wiberg M, Terenghi G, Kellerth JO. A novel biodegradable implant for neuronal rescue and regeneration after spinal cord injury. Biomaterials. 2002 Aug;23(16):3369-76.

Novikova LN, Mosahebi A, Wiberg M, Terenghi G, Kellerth JO, Novikov LN. Alginate hydrogel and matrigel as potential cell carriers for neurotransplantation. J Biomed Mater Res A. 2006 May; 77(2):242-52.

Nowakowski GS, Dooner MS, Valinski HM, Mihaliak AM, Quesenberry PJ, Becker PS. A specific heptapeptide from a phage display peptide library homes to bone marrow and binds to primitive hematopoietic stem cells. Stem Cells. 2004;22(6):1030-8.

O'Connor SM, Stenger DA, Shaffer KM, Maric D, Barker JL, Ma W. Primary neural precursor cell expansion, differentiation and cytosolic Ca(2+) response in three-dimensional collagen gel. J Neurosci Methods. 2000 Oct 30;102(2):187-95.

Olie RA, Simões-Wüst AP, Baumann B, Leech SH, Fabbro D, Stahel RA, Zangemeister-Wittke U. A novel antisense oligonucleotide targeting Survivin expression induces apoptosis and sensitizes lung cancer cells to chemotherapy. Cancer Res. 2000 Jun 1;60(11):2805-9.

Olson HE, Rooney GE, Gross L, Nesbitt JJ, Galvin KE, Knight A, Chen B, Yaszemski MJ, Windebank AJ. Neural stem cell- and Schwann cell-loaded biodegradable polymer scaffolds support axonal regeneration in the transected spinal cord. Tissue Eng Part A. 2009 Jul;15(7):1797-805.

Orive G, Anitua E, Pedraz JL, Emerich DF. Biomaterials for promoting brain protection, repair and regeneration. Nat Rev Neurosci. 2009 Sep;10(9):682-92. Epub 2009 Aug 5.

Ortinau S, Schmich J, Block S, Liedmann A, Jonas L, Weiss DG, Helm CA, Rolfs A, Frech MJ. Effect of 3D-scaffold formation on differentiation and survival in human neural progenitor cells. Biomed Eng Online. 2010 Nov 11; 9(1):70.

Oudega M, Gautier SE, Chapon P, Fragoso M, Bates ML, Parel JM, Bunge MB. Axonal regeneration into Schwann cell grafts within resorbable poly(alpha-hydroxyacid) guidance channels in the adult rat spinal cord. Biomaterials. 2001 May;22(10):1125-36.

Pan L, Ren Y, Cui F, Xu Q. Viability and differentiation of neural precursors on hyaluronic acid hydrogel scaffold. J Neurosci Res. 2009 Nov 1; 87(14):3207-20.

Patino MG, Neiders ME, Andreana S, Noble B, Cohen RE. Collagen as an implantable material in medicine and dentistry. J Oral Implantol. 2002;28(5):220-5.

Patist CM, Mulder MB, Gautier SE, Maquet V, Jérôme R, Oudega M. Freeze-dried poly(D,L-lactic acid) macroporous guidance scaffolds impregnated with brain-derived

neurotrophic factor in the transected adult rat thoracic spinal cord. Biomaterials. 2004 Apr;25(9):1569-82.

Paulsson M. The role of laminin in attachment, growth, and differentiation of cultured cells: a brief review. Cytotechnology. 1992;9(1-3):99-106.

Peattie RA, Nayate AP, Firpo MA, Shelby J, Fisher RJ, Prestwich GD. Stimulation of *in vivo* angiogenesis by cytokine-loaded hyaluronic acid hydrogel implants. Biomaterials. 2004 Jun;25(14):2789-98.

Peixoto PM, Ryu SY, Bombrun A, Antonsson B, Kinnally KW. MAC inhibitors suppress mitochondrial apoptosis. Biochem J. 2009 Oct 12;423(3):381-7.

Pelham RJ Jr, Wang Y. Cell locomotion and focal adhesions are regulated by substrate flexibility. Proc Natl Acad Sci U S A. 1997 Dec 9;94(25):13661-5.

Pennartz S, Belvindrah R, Tomiuk S, Zimmer C, Hofmann K, Conradt M, Bosio A, Cremer H. Purification of neuronal precursors from the adult mouse brain: comprehensive gene expression analysis provides new insights into the control of cell migration, differentiation, and homeostasis. Mol Cell Neurosci. 2004 Apr;25(4):692-706.

Perale G, Giordano C, Bianco F, Rossi F, Tunesi M, Daniele F, Crivelli F, Matteoli M, Masi M. Hydrogel for cell housing in the brain and in the spinal cord. Int J Artif Organs. 2011 Mar;34(3):295-303.

Petka WA, Harden JL, McGrath KP, Wirtz D, Tirrell DA. Reversible hydrogels from self-assembling artificial proteins. Science. 1998 Jul 17;281(5375):389-92.

Pettmann B, Henderson CE. Neuronal cell death. Neuron. 1998 Apr;20(4):633-47.

Plas DR, Thompson CB. Cell metabolism in the regulation of programmed cell death. Trends Endocrinol Metab. 2002 Mar;13(2):75-8.

Ponce ML, Nomizu M, Delgado MC, Kuratomi Y, Hoffman MP, Powell S, Yamada Y, Kleinman HK, Malinda KM. Identification of endothelial cell binding sites on the laminin gamma 1 chain. Circ Res. 1999 Apr 2;84(6):688-94.

Popov SG, Villasmil R, Bernardi J, Grene E, Cardwell J, Wu A, Alibek D, Bailey C, Alibek K. Lethal toxin of Bacillus anthracis causes apoptosis of macrophages. Biochem Biophys Res Commun. 2002 Apr 26;293(1):349-55.

Powell SK, Rao J, Roque E, Nomizu M, Kuratomi Y, Yamada Y, Kleinman HK. Neural cell response to multiple novel sites on laminin-1. J Neurosci Res. 2000 Aug 1;61(3):302-12.

Prang P, Müller R, Eljaouhari A, Heckmann K, Kunz W, Weber T, Faber C, Vroemen M, Bogdahn U, Weidner N. The promotion of oriented axonal regrowth in the injured spinal cord by alginate-based anisotropic capillary hydrogels. Biomaterials. 2006 Jul;27(19):3560-9.

Putcha GV, Harris CA, Moulder KL, Easton RM, Thompson CB, Johnson EM Jr. Intrinsic and extrinsic pathway signaling during neuronal apoptosis: lessons from the analysis of mutant mice. J Cell Biol. 2002 Apr 29;157(3):441-53.

Rahmanzadeh R, Hüttmann G, Gerdes J, Scholzen T. Chromophore-assisted light inactivation of pKi-67 leads to inhibition of ribosomal RNA synthesis. Cell Prolif. 2007 Jun;40(3):422-30.

Rangappa N, Romero A, Nelson KD, Eberhart RC, Smith GM. Laminin-coated poly(L-lactide) filaments induce robust neurite growth while providing directional orientation. J Biomed Mater Res. 2000 Sep 15;51(4):625-34.
Ratner BD, Bryant SJ. Biomaterials: where we have been and where we are going. Annu Rev Biomed Eng. 2004;6:41-75.

Reichert JC, Heymer A, Berner A, Eulert J, Nöth U.Fabrication of polycaprolactone collagen hydrogel constructs seeded with mesenchymal stem cells for bone regeneration. Biomed Mater. 2009 Dec;4(6):065001.

Reynolds BA, Weiss S. Generation of neurons and astrocytes from isolated cells of the adult mammalian central nervous system. Science. 1992 Mar 27;255(5052):1707-10.

Richard BL, Nomizu M, Yamada Y, Kleinman HK. Identification of synthetic peptides derived from laminin alpha1 and alpha2 chains with cell type specificity for neurite outgrowth. Exp Cell Res. 1996 Oct 10;228(1):98-105.

Rideout HJ, Stefanis L. Caspase inhibition: a potential therapeutic strategy in neurological diseases. Histol Histopathol. 2001 Jul;16(3):895-908.

Rodin S, Domogatskaya A, Ström S, Hansson EM, Chien KR, Inzunza J, Hovatta O, Tryggvason K. Long-term self-renewal of human pluripotent stem cells on human recombinant laminin-511. Nat Biotechnol. 2010 Jun;28(6):611-5.

Sah NK, Khan Z, Khan GJ, Bisen PS. Structural, functional and therapeutic biology of Survivin. Cancer Lett. 2006 Dec 8;244(2):164-71.

Saha K, Keung AJ, Irwin EF, Li Y, Little L, Schaffer DV, Healy KE. Substrate modulus directs neural stem cell behavior. Biophys J. 2008 Nov 1;95(9):4426-38.

Sakiyama SE, Schense JC, Hubbell JA. Incorporation of heparin-binding peptides into fibrin gels enhances neurite extension: an example of designer matrices in tissue engineering. FASEB J. 1999 Dec;13(15):2214-24.

Salinas CN, Anseth KS. The influence of the RGD peptide motif and its contextual presentation in PEG gels on human mesenchymal stem cell viability. J Tissue Eng Regen Med. 2008 Jul;2(5):296-304.

Sangsanoh P, Waleetorncheepsawat S, Suwantong O, Wutticharoenmongkol P, Weeranantanapan O, Chuenjitbuntaworn B, Cheepsunthorn P, Pavasant P, Supaphol P. *In vitro* biocompatibility of schwann cells on surfaces of biocompatible polymeric electrospun fibrous and solution-cast film scaffolds. Biomacromolecules. 2007 May;8(5):1587-94.

Santini MT, Rainaldi G, Indovina PL. Apoptosis, cell adhesion and the extracellular matrix in the three-dimensional growth of multicellular tumor spheroids. Crit Rev Oncol Hematol. 2000 Nov-Dec;36(2-3):75-87.

Savill J, Gregory C, Haslett C. Cell biology. Eat me or die. Science. 2003 Nov 28;302(5650):1516-7.

Scheffler B, Schmandt T, Schröder W, Steinfarz B, Husseini L, Wellmer J, Seifert G, Karram K, Beck H, Blümcke I, Wiestler OD, Steinhäuser C, Brüstle O. Functional network integration of embryonic stem cell-derived astrocytes in hippocampal slice cultures. Development. 2003 Nov;130(22):5533-41.

Schmöle AC, Brennführer A, Karapetyan G, Jaster R, Pews-Davtyan A, Hübner R, Ortinau S, Beller M, Rolfs A, Frech MJ. Novel indolylmaleimide acts as GSK-3beta inhibitor in human neural progenitor cells. Bioorg Med Chem. 2010 Sep 15;18(18):6785-95.

Schneider A, Garlick JA, Egles C. Self-assembling peptide nanofiber scaffolds accelerate wound healing. PLoS One. 2008 Jan 9;3(1):e1410.

Schnell E, Klinkhammer K, Balzer S, Brook G, Klee D, Dalton P, Mey J. Guidance of glial cell migration and axonal growth on electrospun nanofibers of poly-epsilon-caprolactone and a collagen/poly-epsilon-caprolactone blend. Biomaterials. 2007 Jul;28(19):3012-25.

Schöler HR (2007). "The Potential of Stem Cells: An Inventory". ISBN 9780754657552.

Scholzen T, Gerdes J. The Ki-67 protein: from the known and the unknown. J Cell Physiol. 2000 Mar;182(3):311-22.

Schwartz CM, Spivak CE, Baker SC, McDaniel TK, Loring JF, Nguyen C, Chrest FJ, Wersto R, Arenas E, Zeng X, Freed WJ, Rao MS. NTera2: a model system to study dopaminergic differentiation of human embryonic stem cells. Stem Cells Dev. 2005 Oct;14(5):517-34.

Semino CE, Kasahara J, Hayashi Y, Zhang S. Entrapment of migrating hippocampal neural cells in three-dimensional peptide nanofiber scaffold. Tissue Eng. 2004 Mar-Apr; 10(3-4):643-55.

Semino CE. Self-assembling peptides: from bio-inspired materials to bone regeneration. J. Dent Res. 2008 Jul;87(7):606-16.

Shain KH, Landowski TH, Dalton WS. Adhesion-mediated intracellular redistribution of c-Fas-associated death domain-like IL-1-converting enzyme-like inhibitory protein-long confers resistance to CD95-induced apoptosis in hematopoietic cancer cell lines. J Immunol. 2002 Mar 1;168(5):2544-53.

Shankar SL, Mani S, O'Guin KN, Kandimalla ER, Agrawal S, Shafit-Zagardo B. Survivin inhibition induces human neural tumor cell death through caspase-independent and -dependent pathways. J Neurochem. 2001 Oct;79(2):426-36.

Shichinohe H, Kuroda S, Lee JB, Nishimura G, Yano S, Seki T, Ikeda J, Tamura M, Iwasaki Y. *In vivo* tracking of bone marrow stromal cells transplanted into mice cerebral infarct by fluorescence optical imaging. Brain Res Brain Res Protoc. 2004 Aug;13(3):166-75.

Shikinami Y, Okuno M. Bioresorbable devices made of forged composites of hydroxyapatite (HA) particles and poly-L-lactide (PLLA): Part I. Basic characteristics. Biomaterials. 1999 May;20(9):859-77.

Shin H, Quinten Ruhé P, Mikos AG, Jansen JA. *In vivo* bone and soft tissue response to injectable, biodegradable oligo(poly(ethylene glycol) fumarate) hydrogels. Biomaterials. 2003 Aug;24(19):3201-11.

Shyu WC, Lin SZ, Yen PS, Su CY, Chen DC, Wang HJ, Li H. Stromal cell-derived factor-1 alpha promotes neuroprotection, angiogenesis, and mobilization/homing of bone marrow-derived cells in stroke rats. J Pharmacol Exp Ther. 2008 Feb;324(2):834-49.

Silva GA, Czeisler C, Niece KL, Beniash E, Harrington DA, Kessler JA, Stupp SI. Selective differentiation of neural progenitor cells by high-epitope density nanofibers. Science. 2004

Feb 27;303(5662):1352-5.

Skaper SD. Poly(ADP-Ribose) polymerase-1 in acute neuronal death and inflammation: a strategy for neuroprotection. Ann N Y Acad Sci. 2003 May;993:217-28; discussion 287-8.

Skubitz AP, Letourneau PC, Wayner E, Furcht LT. Synthetic peptides from the carboxy-terminal globular domain of the A chain of laminin: their ability to promote cell adhesion and neurite outgrowth, and interact with heparin and the beta 1 integrin subunit. J Cell Biol. 1991 Nov;115(4):1137-48.

Somervaille TC, Linch DC, Khwaja A. Growth factor withdrawal from primary human erythroid progenitors induces apoptosis through a pathway involving glycogen synthase kinase-3 and Bax. Blood. 2001 Sep 1;98(5):1374-81.

Song Z, Yao X, Wu M. Direct interaction between Survivin and Smac/DIABLO is essential for the anti-apoptotic activity of Survivin during taxol-induced apoptosis. J Biol Chem. 2003 Jun 20;278(25):23130-40.

Sreejalekshmi KG, Nair PD. Biomimeticity in tissue engineering scaffolds through synthetic peptide modifications-altering chemistry for enhanced biological response. J Biomed Mater Res A. 2011 Feb;96(2):477-91. doi: 10.1002/jbm.a.32980.

Stacpoole SR, Bilican B, Webber DJ, Luzhynskaya A, He XL, Compston A, Karadottir R, Franklin RJ, Chandran S. Derivation of neural precursor cells from human ES cells at 3% O(2) is efficient, enhances survival and presents no barrier to regional specification and functional differentiation. Cell Death Differ. 2011 Jun;18(6):1016-23.

Stokols S, Tuszynski MH. The fabrication and characterization of linearly oriented nerve guidance scaffolds for spinal cord injury. Biomaterials. 2004 Dec;25(27):5839-46.

Stokols S, Sakamoto J, Breckon C, Holt T, Weiss J, Tuszynski MH. Templated agarose scaffolds support linear axonal regeneration. Tissue Eng. 2006 Oct;12(10):2777-87.

Susin SA, Lorenzo HK, Zamzami N, Marzo I, Snow BE, Brothers GM, Mangion J, Jacotot E, Costantini P, Loeffler M, Larochette N, Goodlett DR, Aebersold R, Siderovski DP, Penninger JM, Kroemer G. Molecular characterization of mitochondrial apoptosis-inducing factor. Nature. 1999 Feb 4;397(6718):441-6.

Susin SA, Daugas E, Ravagnan L, Samejima K, Zamzami N, Loeffler M, Costantini P, Ferri KF, Irinopoulou T, Prévost MC, Brothers G, Mak TW, Penninger J, Earnshaw WC, Kroemer G. Two distinct pathways leading to nuclear apoptosis. J Exp Med. 2000 Aug 21;192(4):571-80.

Suzuki K, Suzuki Y, Ohnishi K, Endo K, Tanihara M, Nishimura Y.Regeneration of transected spinal cord in young adult rats using freeze-dried alginate gel. Neuroreport. 1999 Sep 29;10(14):2891-4.

Suzuki K, Suzuki Y, Tanihara M, Ohnishi K, Hashimoto T, Endo K, Nishimura Y. Reconstruction of rat peripheral nerve gap without sutures using freeze-dried alginate gel. J Biomed Mater Res. 2000 Mar 15;49(4):528-33.

Tabesh H, Amoabediny G, Nik NS, Heydari M, Yosefifard M, Siadat SO, Mottaghy K. The role of biodegradable engineered scaffolds seeded with Schwann cells for spinal cord regeneration. Neurochem Int. 2009 Feb;54(2):73-83.

Tamm I, Wang Y, Sausville E, Scudiero DA, Vigna N, Oltersdorf T, Reed JC. IAP-family protein Survivin inhibits caspase activity and apoptosis induced by Fas (CD95), Bax, caspases, and anticancer drugs. Cancer Res. 1998 Dec 1;58(23):5315-20.

Taraballi F, Natalello A, Campione M, Villa O, Doglia SM, Paleari A, Gelain F. Glycinee-spacers influence functional motifs exposure and self-assembling propensity of functionalized substrates tailored for neural stem cell cultures. Front Neuroengineering. 2010 Feb 8; 3:1.

Tashiro K, Sephel GC, Weeks B, Sasaki M, Martin GR, Kleinman HK, Yamada Y. A synthetic peptide containing the IKVAV sequence from the A chain of laminin mediates cell attachment, migration, and neurite outgrowth. J Biol Chem. 1989 Sep 25;264(27):16174-82.

Tashiro K, Nagata I, Yamashita N, Okazaki K, Ogomori K, Tashiro N, Anai M. A synthetic peptide deduced from the sequence in the cross-region of laminin A chain mediates neurite outgrowth, cell attachment and heparin binding. Biochem J. 1994 Aug 15;302 (Pt 1):73-9.

Temple S, Alvarez-Buylla A. Stem cells in the adult mammalian central nervous system. Curr Opin Neurobiol. 1999 Feb;9(1):135-41.

Theodosis DT, Bonfanti L, Olive S, Rougon G, Poulain DA. Adhesion molecules and structural plasticity of the adult hypothalamo-neurohypophysial system. Psychoneuroendocrinology. 1994;19(5-7):455-62.

Thonhoff JR, Lou DI, Jordan PM, Zhao X, Wu P. Compatibility of human fetal neural stem cells with hydrogel biomaterials *in vitro*. Brain Res. 2008 Jan 2; 1187:42-51.

Tong YW, Shoichet MS. Enhancing the neuronal interaction on fluoropolymer surfaces with mixed peptides or spacer group linkers. Biomaterials. 2001 May; 22(10):1029-34.

Tonge DA, Golding JP, Edbladh M, Kroon M, Ekström PE, Edström A. Effects of extracellular matrix components on axonal outgrowth from peripheral nerves of adult animals *in vitro*. Exp Neurol. 1997 Jul;146(1):81-90.

Tysseling VM, Sahni V, Pashuck ET, Birch D, Hebert A, Czeisler C, Stupp SI, Kessler JA. Self-assembling peptide amphiphile promotes plasticity of serotonergic fibers following spinal cord injury. J Neurosci Res. 2010 Nov 1;88(14):3161-70.

Uemura M, Refaat MM, Shinoyama M, Hayashi H, Hashimoto N, Takahashi J. Matrigel supports survival and neuronal differentiation of grafted embryonic stem cell-derived neural precursor cells. J Neurosci Res. 2010 Feb 15; 88(3):542-51.

van Engeland M, Ramaekers FC, Schutte B, Reutelingsperger CP. A novel assay to measure loss of plasma membrane asymmetry during apoptosis of adherent cells in culture. Cytometry. 1996 Jun 1;24(2):131-9.

Vandivier RW, Henson PM, Douglas IS. Burying the dead: the impact of failed apoptotic cell removal (efferocytosis) on chronic inflammatory lung disease. Chest. 2006 Jun;129(6):1673-82.

Vekrellis K, McCarthy MJ, Watson A, Whitfield J, Rubin LL, Ham J. Bax promotes neuronal cell death and is downregulated during the development of the nervous system. Development. 1997 Mar;124(6):1239-49.

Venugopal J, Ramakrishna S. Biocompatible nanofiber matrices for the engineering of a

dermal substitute for skin regeneration. Tissue Eng. 2005 May-Jun;11(5-6):847-54.

Venugopal J, Zhang YZ, Ramakrishna S. Fabrication of modified and functionalized polycaprolactone nanofibre scaffolds for vascular tissue engineering. Nanotechnology. 2005 Oct;16(10):2138-42.

Vermes I, Haanen C, Steffens-Nakken H, Reutelingsperger C. A novel assay for apoptosis. Flow cytometric detection of phosphatidylserine expression on early apoptotic cells using fluorescein labelled Annexin V. J Immunol Methods. 1995 Jul 17;184(1):39-51.

Wajant H. The Fas signaling pathway: more than a paradigm. Science. 2002 May 31;296(5573):1635-6.

Waleh NS, Gallo J, Grant TD, Murphy BJ, Kramer RH, Sutherland RM. Selective down-regulation of integrin receptors in spheroids of squamous cell carcinoma. Cancer Res. 1994 Feb 1;54(3):838-43.

Wang K, Yin XM, Chao DT, Milliman CL, Korsmeyer SJ. BID: a novel BH3 domain-only death agonist. Genes Dev. 1996 Nov 15;10(22):2859-69.

Wang X, Wu YC, Fadok VA, Lee MC, Gengyo-Ando K, Cheng LC, Ledwich D, Hsu PK, Chen JY, Chou BK, Henson P, Mitani S, Xue D. Cell corpse engulfment mediated by C. elegans phosphatidylserine receptor through CED-5 and CED-12. Science. 2003 Nov 28;302(5650):1563-6.

Wang CX, Song JH, Song DK, Yong VW, Shuaib A, Hao C. Cyclin-dependent kinase-5 prevents neuronal apoptosis through ERK-mediated upregulation of Bcl-2. Cell Death Differ. 2006 Jul;13(7):1203-12.

Wang LS, Chung JE, Chan PP, Kurisawa M. Injectable biodegradable hydrogels with tunable mechanical properties for the stimulation of neurogenesic differentiation of human mesenchymal stem cells in 3D culture. Biomaterials. 2010 Feb; 31(6):1148-57.

Weaver VM, Petersen OW, Wang F, Larabell CA, Briand P, Damsky C, Bissell MJ. Reversion of the malignant phenotype of human breast cells in three-dimensional culture and *in vivo* by integrin blocking antibodies. J Cell Biol. 1997 Apr 7;137(1):231-45.

Weaver VM, Lelièvre S, Lakins JN, Chrenek MA, Jones JC, Giancotti F, Werb Z, Bissell MJ. beta4 integrin-dependent formation of polarized three-dimensional architecture confers resistance to apoptosis in normal and malignant mammary epithelium. Cancer Cell. 2002 Sep;2(3):205-16.

Wei YT, Tian WM, Yu X, Cui FZ, Hou SP, Xu QY, Lee IS. Hyaluronic acid hydrogels with IKVAV peptides for tissue repair and axonal regeneration in an injured rat brain. Biomed Mater. 2007 Sep;2(3):S142-6.

Weinand C, Gupta R, Huang AY, Weinberg E, Madisch I, Qudsi RA, Neville CM, Pomerantseva I, Vacanti JP. Comparison of hydrogels in the *in vivo* formation of tissue-engineered bone using mesenchymal stem cells and beta-tricalcium phosphate. Tissue Eng. 2007 Apr;13(4):757-65.

Weyer A, Schilling K. Developmental and cell type-specific expression of the neuronal marker NeuN in the murine cerebellum. J Neurosci Res. 2003 Aug 1;73(3):400-9.

Willerth SM, Arendas KJ, Gottlieb DI, Sakiyama-Elbert SE. Optimization of fibrin scaffolds

for differentiation of murine embryonic stem cells into neural lineage cells. Biomaterials. 2006 Dec;27(36):5990-6003.

Willerth SM, Sakiyama-Elbert SE. Approaches to neural tissue engineering using scaffolds for drug delivery. Adv Drug Deliv Rev. 2007 May 30;59(4-5):325-38.

Willits RK, Skornia SL. Effect of collagen gel stiffness on neurite extension. J Biomater Sci Polym Ed. 2004;15(12):1521-31.

Woerly S, Plant GW, Harvey AR. Cultured rat neuronal and glial cells entrapped within hydrogel polymer matrices: a potential tool for neural tissue replacement. Neurosci Lett. 1996 Mar 1;205(3):197-201.

Woerly S, Fort S, Pignot-Paintrand I, Cottet C, Carcenac C, Savasta M. Development of a sialic acid-containing hydrogel of poly[N-(2-hydroxypropyl) methacrylamide]: characterization and implantation study. Biomacromolecules. 2008 Sep;9(9):2329-37. Epub 2008 Aug 21.

Wright KO, Messing EM, Reeder JE. DBCCR1 mediates death in cultured bladder tumor cells. Oncogene. 2004 Jan 8;23(1):82-90.

Xie Y, Yang Y, Kang X, Li R, Volakis LI, Zhang X, Lee LJ, Kniss DA. Bioassembly of three-dimensional embryonic stem cell-scaffold complexes using compressed gases. Biotechnol Prog. 2009 Mar-Apr;25(2):535-42.

Xu XY, Li XT, Peng SW, Xiao JF, Liu C, Fang G, Chen KC, Chen GQ. The behaviour of neural stem cells on polyhydroxyalkanoate nanofiber scaffolds. Biomaterials. 2010 May; 31(14):3967-75.

Yang J, Liu X, Bhalla K, Kim CN, Ibrado AM, Cai J, Peng TI, Jones DP, Wang X. Prevention of apoptosis by Bcl-2: release of cytochrome c from mitochondria blocked. Science. 1997 Feb 21;275(5303):1129-32.

Yang F, Murugan R, Ramakrishna S, Wang X, Ma YX, Wang S. Fabrication of nano-structured porous PLLA scaffold intended for nerve tissue engineering. Biomaterials. 2004 May;25(10):1891-900.

Yano S, Kuroda S, Lee JB, Shichinohe H, Seki T, Ikeda J, Nishimura G, Hida K, Tamura M, Iwasaki Y. *In vivo* fluorescence tracking of bone marrow stromal cells transplanted into a pneumatic injury model of rat spinal cord. J Neurotrauma. 2005 Aug;22(8):907-18.

Yano S, Kuroda S, Shichinohe H, Hida K, Iwasaki Y. Do bone marrow stromal cells proliferate after transplantation into mice cerebral infarct?--a double labeling study. Brain Res. 2005 Dec 14;1065(1-2):60-7.

Ye Z, Zhang H, Luo H, Wang S, Zhou Q, DU X, Tang C, Chen L, Liu J, Shi YK, Zhang EY, Ellis-Behnke R, Zhao X. Temperature and pH effects on biophysical and morphological properties of self-assembling peptide RADA16-I. J Pept Sci. 2008 Feb;14(2):152-62.

Yin XM, Oltvai ZN, Korsmeyer SJ. BH1 and BH2 domains of Bcl-2 are required for inhibition of apoptosis and heterodimerization with Bax. Nature. 1994 May 26;369(6478):321-3.

Youle RJ. (2007) Cell biology. Cellular demolition and the rules of angagement. Science. Feb.9; 315(5813):776-7.

Yu X, Dillon GP, Bellamkonda RB. A laminin and nerve growth factor-laden three-dimensional scaffold for enhanced neurite extension. Tissue Eng. 1999 Aug;5(4):291-304.

Yu JL, Coomber BL, Kerbel RS. A paradigm for therapy-induced microenvironmental changes in solid tumors leading to drug resistance. Differentiation. 2002 Dec;70(9-10):599-609.

Yu HS, Jin GZ, Won JE, Wall I, Kim HW. Macrochanneled bioactive ceramic scaffolds in combination with collagen hydrogel: A new tool for bone tissue engineering. J Biomed Mater Res A. 2012 May 5. doi: 10.1002/jbm.a.34163.

Zahir N, Weaver VM. Death in the third dimension: apoptosis regulation and tissue architecture. Curr Opin Genet Dev. 2004 Feb;14(1):71-80.

Zakeri Z, Lockshin RA. Cell death during development. J Immunol Methods. 2002 Jul 1;265(1-2):3-20.

Zhang KZ, Westberg JA, Hölttä E, Andersson LC. BCL2 regulates neural differentiation. Proc Natl Acad Sci U S A. 1996 Apr 30;93(9):4504-8.

Zhang Z, Galileo DS. Retroviral transfer of antisense integrin alpha6 or alpha8 sequences results in laminar redistribution or clonal cell death in developing brain. J Neurosci. 1998 Sep 1;18(17):6928-38.

Zhang S. Emerging biological materials through molecular self-assembly. Biotechnol Adv. 2002 Dec;20(5-6):321-39.

Zhang S. Fabrication of novel biomaterials through molecular self-assembly. Nat Biotechnol. 2003 Oct;21(10):1171-8.

Zhang S, Ellis-Behnke R, Zhao X, Spirio L. PuraMatrix: Self-assembling peptide nanofiber scaffolds. Scaffolding in Tissue Engineering. 2004. www.puramatrix.com

Zhang F, Shi GS, Ren LF, Hu FQ, Li SL, Xie ZJ. Designer self-assembling peptide scaffold stimulates pre-osteoblast attachment, spreading and proliferation. J Mater Sci Mater Med. 2009 Jul;20(7):1475-81.

Zhao M, Momma S, Delfani K, Carlen M, Cassidy RM, Johansson CB, Brismar H, Shupliakov O, Frisen J, Janson AM. Evidence for neurogenesis in the adult mammalian substantia nigra. Proc Natl Acad Sci U S A. 2003 Jun 24;100(13):7925-30.

Zhao L, He C, Gao Y, Cen L, Cui L, Cao Y. Preparation and cytocompatibility of PLGA scaffolds with controllable fiber morphology and diameter using electrospinning method. J Biomed Mater Res B Appl Biomater. 2008 Oct;87(1):26-34.

Zhu H, Schulz J, Schliephake H. Human bone marrow stroma stem cell distribution in calcium carbonate scaffolds using two different seeding methods. Clin Oral Implants Res. 2010 Feb;21(2):182-8.

Zinkel S, Gross A, Yang E. BCL2 family in DNA damage and cell cycle control. Cell Death Differ. 2006 Aug;13(8):1351-9.

Zou H, Li Y, Liu X, Wang X. An APAF-1.cytochrome c multimeric complex is a functional apoptosome that activates procaspase-9. J Biol Chem. 1999 Apr 23;274(17):11549-56.

8. Appendix

Abbreviations

AIF	Apoptosis-inducing-factor
aNSC	Adult neural stem cells
Apaf-1	Apoptotic protease activating factor - 1
ATP	Adenosine triphosphate
B27	Media supplement
Bax	Bcl-2-associated X protein
Bcl-2	B-cell lymphoma 2
BDNF	Brain derived neurotrophic factor
bFGF	Basic fibroblast growth factor
Bid	BH3-interacting domain death agonist
BMHP	Bone marrow homing peptide
BSA	Bovin serum albumin
CARD	Caspase recruiting domain
CBB	Coomassie-Brilliant-Blue
CCD	Colloidal Commassie dye
c-jun	Jun proto-oncogen
CNS	Central nervous system
DAPI	4’,6-Diamidin-2’-phenylindoldihydrochlorid
dd	Days differentiated
DED	Death effector domain
DISC	Death-inducing signalling complex
DMEM / F12	Dulbecco’s modified eagle medium
DMSO	Dimethyl sulfoxid
DNA	Desoxyribonuclein acid
dp	Days proliferated
DRG	Dorsal root ganglion
ECM	Extracellular matrix
EDTA	Ethylenediaminetetraacetic acid
EGF	Epidermal growth factor

EGTA	Ethylene glycol tetraacetic acid
ERK	Mitogen-activated protein kinase
ES cells	Embryonic stem cells
FADD	Fas-associated death domain protein
FasL	Fas ligand
FCS	Fetal calf serum
FDA	Food and Drug Administration
FGF-2	Fibroblast growth factor
GAPDH	Glyceraldehyde 3-phosphate dehydrogenase
GF	Growth factor
GFAP	Glial fibrillary acidic protein
GSK-3	Glycogen synthase kinase-3
HA	Hyaluronic acid
HBSS	Hank's bananced salt solution
HEMA	Hydroxyethyl methacrylate
hESCs	Human embryonic stem cells
hNPCs	Human neural progenitor cells
hNSCs	Human neural stem cells
HuC/D	Human neuronal protein HuC/HuD
IAPs	Inhibitor of apoptosis proteins
IF	Immunofluorescence
IGF-1	Insulin-like growth factor-1
IKVAV	Isolucine-lysine-valine-alanine-valine sequence
IM-12	Indolylmaleimide
iPS cells	Induced pluripotent cells
L1	Neural adhesion molecule
LCT	C-terminal 23 amino acid sequence
LEF1	Transcription factor
LRAP	Leucine-rich amelogenin peptide
MAC	Mitochondrial apoptosis-induced channel
MAGUK	Membrane-associated guanylate kinase
MAP kinase	Mitogen-activated protein kinase
MEK-ERK	Ras-Raf-MEK-ERK pathway or MAP kinase pathway
MHC-receptor	Major histocompartibility complex - receptor

NCAM	Neural cell adhesion molecule
NeuN	Neuronal nuclar antigen
NFkB	Kappa-light-chain-enhancer
NGF	Nerve growth factor
NGS	Normal goat serum
NPCs	Neural progenitor cells
NSCs	Neuronal stem cells
NT3	Neurotrophin-3
p53	Transcription factor / tumour suppressor
PA	Peptide amphiphile
PAA	Poly(acrylic acid)
PAN-MA	Poly(acrylonitrile-co-methylacrylate)
PARP-1	Poly(ADP-ribose)-Polymerase-1
PBS	Phosphate buffered saline
pc	Post coitum
PCD	Programmed cell death
PCL	Poly(e-carpolactone)
PDGF	Platelet-derived growth factor
PDL	Poly-d-lysine
PDS	Polydioxanone
PEG	Poly(ethylene glycol)
PEGDA	Poly(ethylene glycol) diglycidyl-co-poly(ethylene glycol diacrylate
PFA	Paraformaldehyde
PFS	-PFSSTKT- peptide sequence
PGA	Poly(glycolic acid)
PHB	Poly(3-hydroxybutyrate)
pHEMA	Poly(2-hydroxylethyl methacrylate)
PI	Propidium iodide
PI3-K	Phosphinositide 3-kinase
PLA	Poly(lactic acid)
PLGA	Poly(lactic-co-glycolic acid)
PLLA	Poly(L-lactic acid)
PM	PuraMatrix 3D scaffold

PML	PuraMatrix 3D scaffold with laminin
PM-PFS	PuraMatrix 3D scaffold modified with PFS-peptide
PM-SDP	PuraMatrix 3D scaffold modified with SDP-peptide
PNVP	Poly(N-vinyl 2-pyrrolidone)
PPF	Poly(propylene fumarate)
Ppy	Polypyrrole polymers
PS	Phosphatidylserine
PSA-NCAM	Polysialic acid-Ncam
PSD95	Postsynaptic density protein 95
PVA	Poly(vinylalchol)
PVDF	Polyvinylidene fluoride
RADA-16-I	Peptide Ac-RADARADARADARADA-$COHN_2$ = PuraMatrix
REM	Scanning electron microscopy
ReNcell VM	Neural progenitor cell line
RER	Rough endoplasmatic reticulum
RGD sequence	Adhesion peptide, Arg-Gly-Asp
RT	Room temperature
RT-PCR	Real-time reverse transcriptase polymerase chain reactio
SAP-90	Synapse-associated protein 90
SCs	Stem cells
SDP	-SDPGYIGSR- peptide sequence
SDS	Sodium dodecyl sulphate
SEM	Standard error of the mean
SMACs	Second mitochondria-derived activator of caspases
src	Tyrosinkinase
ST14A	Rat striatal progenitor cells
TBS	Tris buffered saline
TCF	Transcription factor
TCT	C-terminal 12 amino acid sequence
TGF-ß	Tumour growth factor-ß
TH	Tyrosine hydroxylase
TNF	Tumor necrosis factor
TNF-R1	Tumor necrosis factor receptor 1

TRADD	TNF receptor-associated death domain
TRAP	Tyrosine-rich amelogenin peptide
TTBS	Tris buffered saline with Tween 20
TUNEL	Terminal deoxynucleotidyl transferase dUTP nick end labelling
vmIPNs	Variable moduli interpenetrating polymer networks
WB	Western blot
XIAP	X-linked inhibitor of apoptosis protein

Abstracts und posterpresentation

- Poster and talk for 5th International Stem Cell School in Regenerative Medicine / Berlin / Germany / 2008
  "Growth and differentiation of human neural progenitor cells in functionalized 3D scaffolds"
  A.Liedmann, S. Block, L. Jonas, C.A. Helm; A. Rolfs and S. Ortinau

- Poster for 6th International Stem Cell School in Regenerative Medicine / Odense / Denmark / 2009
  "Differentiation and Survival of Human Neural Progenitor Cells in Functionalized 3D Scaffolds"
  A. Liedmann, L. Jonas, M. Frech, A. Rolfs and S. Ortinau

- Poster for 7th International Stem Cell School in Regenerative Medicine / Prag / Czech Republic / 2009
  "Differentiation and Survival of Human Neural Progenitor Cells in Functionalized 3D Scaffolds compared to 2D"
  A. Liedmann, M.J. Frech, A. Rolfs and S. Ortinau

- Poster for 8th International Stem Cell School in Regenerative Medicine / Stockholm / Sweden / 2010
  "Differentiation and Survival of Human Neural Progenitor Cells in Functionalized 3D Scaffolds"
  A. Liedmann, L. Jonas, M. Frech, A. Rolfs and S. Ortinau

- Poster for 9th Göttingen Meeting of the German Neuroscience Society / Göttingen / Germany / 2011
  "Differentiation and Survival of Human Neural Progenitor Cells in self-assembling peptide hydrogel 3D Scaffolds"
  A. Liedmann, P. Morgan, A. Rolfs and M.J. Frech

Publication list:

- **Differentiation of human neural progenitor cells regulated by Wnt-3a**
  Rayk Hübner, Anne-Caroline Schmöle, Andrea Liedmann, Moritz J. Frech, Arndt Rolfs, Jiankai Luo
  Biochem Biophys Res Commun. 2010 Sep 24;400(3):358-62.; PMID: 20735988

- **Effect of 3D-scaffold formation on differentiation and survival in human neural progenitor cells**
  Stefanie Ortinau, Jürgen Schmich, Stephan Block, Andrea Liedmann, Ludwig Jonas, Dieter G Weiss, Christiane A Helm, Arndt Rolfs, Moritz J. Frech
  Biomed Eng Online. 2010 Nov 11;9(1):70.; PMID: 21070668

- **Human neural progenitor cells show functional neuronal differentiation and regional preference in rat hippocampal co-cultures**
  Peter J Morgan, Andrea Liedmann, Rayk Hübner, Marine Hovakimyan, Arndt Rolfs, Moritz J Frech
  Stem Cells Dev. 2011 Dec 23.; PMID: 21867424

- **Cultivation of human neural progenitor cells in a 3-dimensional self-assembling peptide hydro gel**
  Andrea Liedmann, Arndt Rolfs, Moritz J Frech
  J Vis Exp. 2012 Jan 11; PMID: 22258286

- **Neuronal Differentiation of Neural Human Neural Progenitor Cells in Functionalised Hydrogel Matrices**
  Andrea Liedmann, Peter J Morgan, Stefanie Ortinau, Arndt Rolfs, Moritz J Frech
  Bioresearch Open Access. 2012; 1(1):16-24.

Acknowledgements

At this point I would like to thank all people made a contribution through their motivation, appreciation, great assistance and patience to the success of this work.

Especially I would like to thank Prof. Arndt Rolfs for giving me the opportunity to work in his institute on the interesting theme and his interest in my work.

I want to thank all members of the work group for the good teamwork and all the good little advices and assistance.

A special thank goes to Dr. Moritz Frech for his help and support.

For the providing of cells and all many little assistance I thank Ellen Ewald and Norman Krüger.

Many thanks to Jan Lukas for helpful discussions and suggestions and for being a good friend during this time.

Thanks to my best friend Steffi her understanding in hard times and for her outstanding mental support.

At last I want to thank my boyfriend Jens. Additional I want to thank my parents and my stist for their great support and patience during all periods of my life.

Thank you !